UNIVERSITÀ DEGLI STUDI DI SALERNO
Dipartimento di Farmacia

Dottorato di ricerca
in Biologia dei Sistemi
Ciclo XIV

Role of Annexin A1 in tumor progression

Dottoranda	**Dott.ssa** *Raffaella Belvedere*
Tutor	**Chiar.mo Prof.** *Antonello Petrella*
Coordinatore	**Chiar.ma Prof.ssa** *Antonella Leone*

Chapter IV. ANNEXIN A1

Chapter V. FORMYL PEPTIDE RECEPTORS

AIM OF THE WORK

Chapter VI. MATERIAL AND METHODS

Chapter VII. RESULTS

DISCUSSION

APPENDIX. COMPUTATIONAL DESIGN OF PROTEIC INHIBITORS OF ANXA1

BIBLIOGRAPHY

ACKNOWLEDGEMENTS

The present PhD project belongs to the general theme of scientific investigation relative to the study of biological functions of Annexin A1 both in physiological and in pathological processes. The aim of this work has been to identify and characterize in details the biological mechanisms underlying the protein involvement in tumor progression, with particular attention to pancreatic cancer. Few scientific works have reported information about the correlation of Annexin A1 with pancreatic cancer progression. The study of patients' biopsies had shown that protein expression was associated to the increase of metastatization degree, a minor cell differentiation and a minor time of survival of patients. To better define the role of Annexin A1 in this model, we analyzed four cell lines of human pancreatic cancer: MIA PaCa-2, PANC-1, BxPC-3 and CAPAN-2. All of them presented very similar levels of Annexin A1 expression but only MIA PaCa-2 and PANC-1 showed a mesenchymal phenotype, as demonstrated by the high levels of vimentin, a typical mesenchymal marker, so only these ones are described as more aggressive cells. For this reason, we continued the investigation of Annexin A1 in MIA PaCa-2 and PANC-1 cells. By immunofluorescence assay we showed that Annexin A1 co-localized with Focal Adhesion Kinases and F-actin, two proteins typically involved in cell migration, so we postulated the hypothesis that Annexin A1 could be involved in cell motility. To identify the functional role of Annexin A1 in these cell lines, a down-modulation of protein expression was performed by transient transfection of specific siRNAs. Through the assays of Wound healing and invasion through a coating of matrigel, we showed that MIA PaCa-2 and PANC-1 with lower Annexin A1 levels migrated and invaded slower than control cells.

Several functions of Annexin A1 are carried out by its extracellular form which interacts with the Formyl Peptide Receptors (FPR) in both autocrine and paracrine manner. The expression of the receptor isoforms FPR-1 and FPR-2 was analyzed by cytofluorimetric assay and PCR. Receptor activation was studied in presence of either agonists such as fMLP and Ac2-26, a mimetic peptide of Annexin A1, or antagonists like Boc-1. To verify if the pathways triggered by the activation of Formyl Peptide Receptors were involved in the processes of cell migration and invasion, we performed the assays of Woung healing and invasion with MIA PaCa-2 and PANC-1 in presence of receptor agonists and antagonists: fMLP and Ac2-26 stimulated migration and invasion in either cell line, while antagonist Boc-1 reverted this effect. Through compartimentalized protein extractions, MIA PaCa-2 cell line, but not PANC-1 cells showed, in addition to the full length form of 37kDa, a shorter form of 33kDa relative to the C-terminal portion, the likely result of a proteolytic cleavage that the protein undergoes when it is phosphorylated.

Moreover only MIA PaCa-2 externalized Annexin A1 in the 37, 33 and 3kDa forms; this last one corresponded to the N-terminal portion which is considered as the sequence with the main biological functions. So we focused our attention on the extracellular form of Annexin A1: following the administration of a specific blocking antibody, MIA PaCa-2 cells lost their capability of migration and invasion. On the other hand, PANC-1 were not affected by the antibody, confirming the absence of the protein in their supernatant. Furthermore, after the addition of the supernatant of MIA PaCa-2, the PANC-1 cell line acquired a greater migration rate, confirming the importance of the protein in the processes of migration and invasion.

To better characterize the role of Annexin A1 *in vitro* and, above all, *in vivo,* we generated Annexin A1 knock-out clones of MIA PaCa-2 cells. We chose the technique of Gene-CRISPR/Cas9 with which we created the genomic delection of Annexin A1, compared with wild type cells and cells transfected with PGS, a scrambled vector used as technical control. By the proteomic analysis of the obtained clones, 36 proteins appeared up-regulated and 26 down-modulated in absence of Annexin A1, these proteins could be involved in several cell pathways like cell proliferation and trafficking, metabolism, cytoskeletal organization and others. Based on the previous data, we preferred to better characterize the aspect of the cytoskeletal organization. We confirmed the variation of some proteins that seemed particularly interesting: for example we validated the down-modulation of vimentin and lamin A/C; on the other hand up-regulation of CD44 and cytokeratin 18 was observed. By immunofluorescence analysis, a strong depolimerization of F-actin in MIA PaCa-2 knock-out for Annexin A1 was detected. So we analyzed the processes of migration and invasion showing that MIA PaCa-2 without Annexin A1 migrated and invaded in a significant slower manner compared with MIA PaCa-2 wild type and transfected with PGS. Furthermore, no modifications were observed in the expression of proteins involved in the pathways triggered by Formyl Peptide Receptors. In fact MIA PaCa-2 knock-out for Annexin A1 showed very similar levels of the receptor isoforms 1 and 2. These receptors appeared active since the migration and invasion rate of the MIA PaCa-2 cells knock-out for Annexin A1 increased in the presence of agonist Ac2-26 and decreased with antagonist Boc-1. Moreover, to complete the characterization of clones, we analyzed the cell proliferation, showing that these cells proliferated more rapidly, had higher S/G2 phases and higher levels of proteins as Cyclin A1, phospho-ERK and ALDH7A1.

Finally, MIA PaCa-2 wild type, PGS and Annexin A1 knock-out have been used to create orthotopic xenografts in the pancreas of SCID female

mice. In the absence of Annexin A1, the tumor mass appeared not affected and retained a volume very similar to the tumor generated by MIA PaCa-2 wild type and PGS but the metastatization degree strongly decreased. This phenomenon was analyzed in mice livers which represent the first organ mainly affected by pancreatic cancer metastasis.

Annexin 1 (ANXA1) is a multifunctional protein of 37 kDa, and represents the first characterized member of the annexin superfamily, so called since their main property is to bind (i.e. to annex) cell membranes in Ca^{2+}-dependent manner. ANXA1 is over-expressed in tissues from patients affected by pancreatic carcinoma (PC), where the protein seems to be associated with the malignant transformation and the poor prognosis. In this PhD project, experiments were performed to understand the role of ANXA1 in human PC development with particular attention to migration and invasion processes. We observed in all the analyzed PC cell lines, a huge expression and a localization of ANXA1 mostly on the motility sub-structures. Interestingly, in MIA PaCa-2 cells we found also two cleaved forms of ANXA1 (33 and 3 kDa) that localize at cellular membranes and are secreted outside the cells, as confirmed by MS analysis. MIA PaCa-2 and PANC-1 cell lines express Formyl Peptide Receptors (FPRs) 1 and 2: the treatment of this cells with the ANXA1 mimetic peptide, Ac2-26, induced intracellular calcium release, consistent with nFPR activation, and significantly increased cell migration/invasion rate. ANXA1 effects on MIA PaCa-2 and PANC-1 migration and invasiveness were observed both by down-modulating its expression through siRNAs and by treatment with a blocking antibody. The importance of the secreted form of ANXA1 in cellular motility was confirmed when MIA PaCa-2 were compared with PANC-1 cells that lack both the cleaved and the externalized forms. Moreover, the treatment of PANC-1 cells with MIA PaCa-2 supernatants, significantly increased the migration rate of these cells. To better characterize the functional role of the protein in PC progression, ANXA1 Knock-Out (KO) clones from MIA PaCa-2 cells were obtained. The expression of several proteins was affected by the absence of ANXA1, particularly the cytoskeletal organization was negatively conditioned. In fact, MIA PaCa-2 ANXA1 KO lost their migratory and invasive capabilities, proliferated more rapidly and seemed to acquire a less aggressive phenotype. To confirm this aspect the MIA PaCa-2 wild type, PGS (the scrambled vector) and ANXA1 KO were implanted to create orthotopic xenograft *in vivo*. The PC mass of ANXA1 KO MIA PaCa-2 was not significantly smaller than the other experimental points, but the metastatization degree appeared particularly reduced as showed on livers of mice with MIA PaCa-2 wild type and PGS which showed a higher degree of metastatic lesions compared to MIA PaCa-2 ANXA1 KO.

This project provides new insights on the role of ANXA1 in PC progression. In *in vitro* models, the intracellular ANXA1 is involved in the maintenance of the cytoskeleton integrity. When secreted, the protein stimulates PC cells migration and invasion through FPR activation. This is

confirmed by in vivo xenograft experiments where ANXA1 appears to stimulate the metastatization process.

5-FU: 5-Fluoruracil
αSMA: α Smooth Muscle Actin
ABC: ATP-Binding Cassette
Ac2-26: NH_2-terminal mimetic peptide
Ach: Acetylcholine
ADM: Acinar-Ductal Metaplasia
ALDH: Aldehyde Dehydrogenase
ALX: lipoxin A_4 receptor
AMP: Adenosine Monophosphate
ANXA1: Annexin A1
ARF: Alternate Reading Frame
ATP: Adenosine Triphosphate
BC: Breast Cancer
bHLH: basic Helix-Loop-Helix
BMP: Bone Morphogenetic Protein
Boc1: *t*-Boc-Met-Leu-Phe
Boc2: *t*-Boc-Met-D-Leu-D-Phe
bp: base pair
CA: Carbohydrate Antigen
CAII: Carbonic Anhydrase II
CAF:Cancer-Associated Fibroblasts
Cas9: CRISPR associated protein 9
CCK: Cholecytokinin
CD: Cluster of Differentiation
CFTR: Cystic Fibrosis Transmembrane Receptor
Cdc42: Cell division control protein 42
CDK: Cyclin-Dependent Kinase
CDKN2A: Cyclin-Dependent Kinase inhibitor 2A
CK: Cytokeratin
COX-2: Cyclooxygenase-2
cPLA2: cytosolic Phospholipase A2
CRC: Colon Rectal Cancer
CRISPR: Clustered, Regularly Interspaced, Short Palindromic Repeat
CSC: Cancer Stem Cell
CsH: Cyclosporin H
CT: Computer Tomography
CysLT1: Cysteinyl Leukotriene receptor 1
DAPK: Death Associated Protein Kinase
DC: Dendritic Cell
DDR2: Discoidin Domain Receptor tyrosine kinase 2
DPC4: Deleted in Pancreatic Carcinoma 4 gene

DSB: DNA Double-Strand Break
DTT: Dithiothreitol
ECM: Extracellular Matrix
EGF: Epidermal Growth Factor
EGFR: Epidermal Growth Factor Receptor
EMT: Epithelial to Mesenchymal Transition
ErbB2: Epidermal growth factor receptor tyrosine kinase
ERK: Extracellular signal-Regulated Protein
FAK: Focal Adhesion Kinase
FBS: Fetal Bovine Serum
FGF: Fibroblast Growth Factor
fMLP: formylMethionilLeucilPhenylalanine
FoxD3: Forkhead box D3
FPR: Formil Peptide Receptor
FPRL1: FPR-like 1
FPRL2: FPR-like 2
FSP1: Fibroblast-Specific Protein 1
GEF: Guanine-nucleotide Exchange Factor
GLP-1: Glucagon-Like Peptide-1
GO: Gene Ontology
GPCR: G Protein Coupled Receptor
GR: Glucocorticoid Receptor
GRE: Glucocorticoid Responsive Element
GRK: G protein coupled kinase
GRP: Gastric Releasing Peptide
GTP: Guanosine Triphosphate
HD: Homozygous Deletion
HDR: Homology-Directed Repair
HGF: Hepatocyte Growht Factor
HIF1α: Hypoxia Induced Factor 1 α
HL-60: Human promyelocyitc Leukemia
HNF1β: Hepatocyte Nuclear Factor 1 β
HNF6: Hepatocyte Nuclear Factor
HS: Horse Serum
ID: Inhibitor of DNA binding protein
IFN: Interferon
IL: Interleukin
INK4A: Inhibitors of CDK4
iNOS: inducible Nitric Oxide Synthase
IP3: Inositol triphosphate

IPMN: Intraductal Papillary Mucinous Neoplasm

JNK: Jun N-terminal Kinase

KO: Knock Out

KRAS: Kirsten Rat Sarcoma Oncogene

LC-FFA: Long Chain-Free Fatty acid

LC/MS: Liquid Chromatography-Mass Spectrometry

LL37: Leucine Leucine 37

LPS: Lipopolysaccharide

LXA_4: Lipoxin A_4

MAPK: Mitogen Activated Protein Kinase

MCH: Melanin Concentrating Hormone

MCN: Mucinous Cystic Neoplasm

MDM2: Mouse Double Minute 2 homolog

MEK: Mitogen-activated ERK Kinase

MET: Mesenchymal to Epithelial Transition

MMP: Membrane Metallo-Proteases

MRI: Magnetic Resonance Imaging

MT1-MMP: Membrane-Ttethered poteases – Membrane Metallo-Protease

MVB: Multivesicular Bodie

nab: albumin nanoparticles

NF-kB: Nuclear Factor kappa-light-chain-enhancer of activated B cells

NHEJ: Non-Homologous End Joining

OCN: Ostecalcin

PAM: Protospacer-Adjacent Motif

PanIN: Pancreatic Intraepithelial Neoplasia

PBMC: Peripheral Blood leucocytes

PBS: Phosphate Buffer Saline

PC: Pancreatic Cancer

PDAC: Pancreatic Ductal Adenocarcinoma

PDGF: Platelet Derived Growth Factor

Pdx1: Pancreatic and duodenal homeobox 1

PI3K: Phosphoinositide 3-Kinase

PIP2: Phosphatidylinositol 4,5-bisphosphate

PKA/C: Protein Kinase A/C

PLCb: Phospholipase C b

PRL: Prolactin

PMN: Polymorphonuclear leukocyte

RER: Rough Endoplasmic Reticulum

Rho: Ras homologue

SAA: Serum Amyloid A

SBEs: SMAD Binding Elements
SCID: Severe Combined Immunodeficiency
SDF: Stroma-Derived Factor
sgRNA: single-guide RNA
shRNA: short hairpin RNA
siRNA: small interference RNA
SKCO-15: Human colonic ephitelial cells
SPARC: Secreted Protein Acidic and Rich in Cystein
SUMO-1:Small Ubiquitin-related Modifier-1
TALEN: Transcription Activator-Like Effector Nuclease
TCF: T Cell Factor
TG: Triglyceride
TGF: Trasforming Growth Factor
TNF: Tumor Necrosis Factor
uPAR: uroknase Plasminogen Activator Receptor
VEFG: Vascular Endothelial Growth Factor
WT: Wild Type
WASP: Wiskott–Aldrich Syndrome Protein
Zeb: Zinc finger E-box binding homeobox
ZFN: Zinc-Finger Nuclease
ZG: Zymogen Granule
ZO-1: Zona Occludens 1

CHAPTER 1

PANCREAS

1.1 Pancreatic anatomy

The pancreas is a soft, elongated, flattened gland of 12-20 cm in length and a weight of about 100 grams. The name pancreas derives from the Greek roots '*pan*' meaning 'all' and '*creas*' meaning 'flesh' [1]. It is composed by four parts as head, neck, body and tail in a manner represented in figure 1.1. Furthermore, about its physiological role, it is divided in a exocrine and endocrine portions.
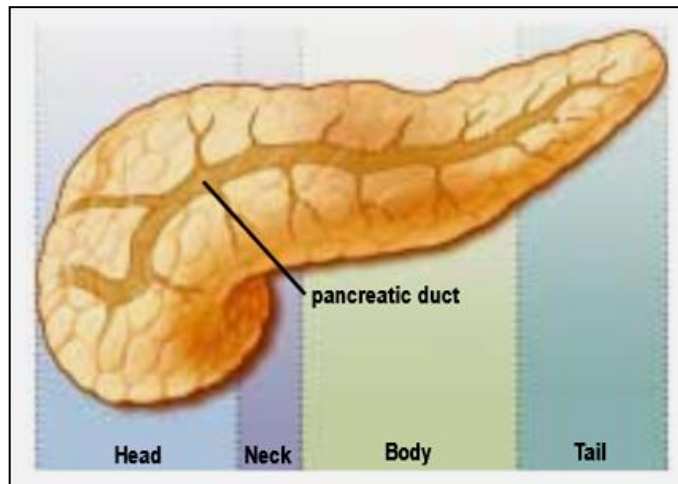
Figure 1.1: Pancreas sections [2]

The tail of the pancreas and the spleen are in the left upper quadrant of the abdomen, instead the head of the pancreas is in the right upper quadrant just to the right of the midline (Fig. 1.2):

- The head of the pancreas lies in the loop of the duodenum;
- The tail of the pancreas lies near the hilum of the spleen;
- The body of the pancreas lies posterior to the distal portion of the stomach between the tail and the neck;
- The portion of the pancreas that lies anterior to the aorta is thinner than the adjacent portions of the head and body of the pancreas. This

region is sometimes designated as the neck of the pancreas and marks the junction of the head and body;

- The close proximity of the neck of the pancreas to major blood vessels posteriorly including the superior mesenteric artery, superior mesenteric-portal vein, inferior *vena cava*, and aorta limits the option for a wide surgical margin when pancreatectomy is done;
- The common bile duct passes through the head of the pancreas to join the main duct of the gland near the duodenum. The portion nearest the liver lies in a groove on the dorsal aspect of the head;
- The *minor papilla* where the accessory pancreatic duct drains into the duodenum and the *major papilla* (ampulla of Vater) where the main pancreatic duct enters the duodenum are depicted.[3; 4].
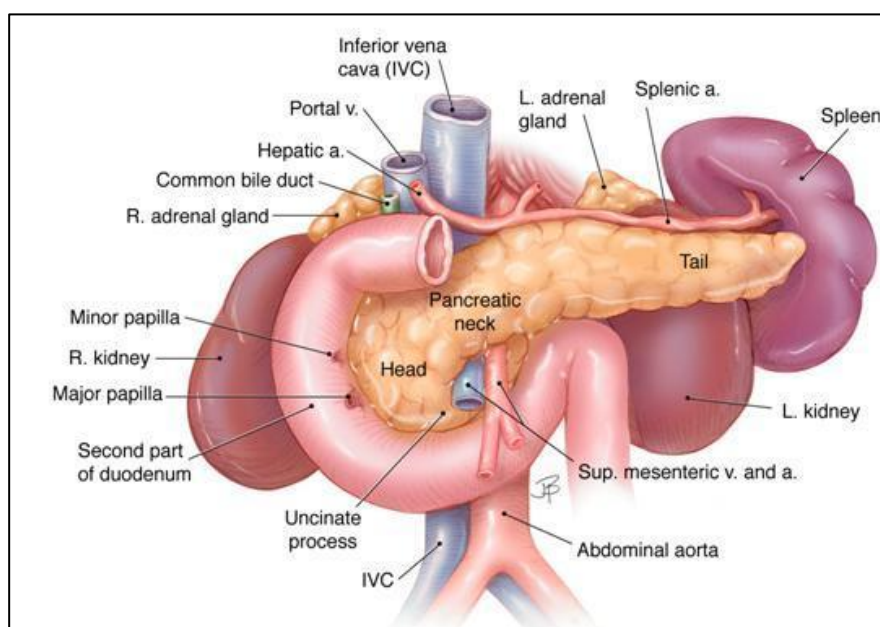
Figure 1.2: Anatomic relationships of the pancreas with surrounding organs and structures

The celiac trunk and the superior mesenteric artery both arise from the abdominal aorta and have multiple branches that supply several organs including the pancreas. The anastomosis of their branches around the pancreas provides collateral circulation that generally assures a secure arterial supply to the organ. Most of the arteries are accompanied by veins that drain into the portal and splenic veins as they pass behind the pancreas.

The superior mesenteric vein becomes the portal vein when it joins the splenic vein [3].

1.1.2 The exocrine portion

The exocrine cells are packed with membrane-bound secretory granules which contain digestive enzymes that are exocytosed into the lumen of the acinus. The pancreatic acini are arranged in clusters like grapes at the ends of a branching duct system. Centroacinar cells are typically located at the junction of an acinus or acinar tubule with a small ductule, but they may be interspersed within an acinar tubule.
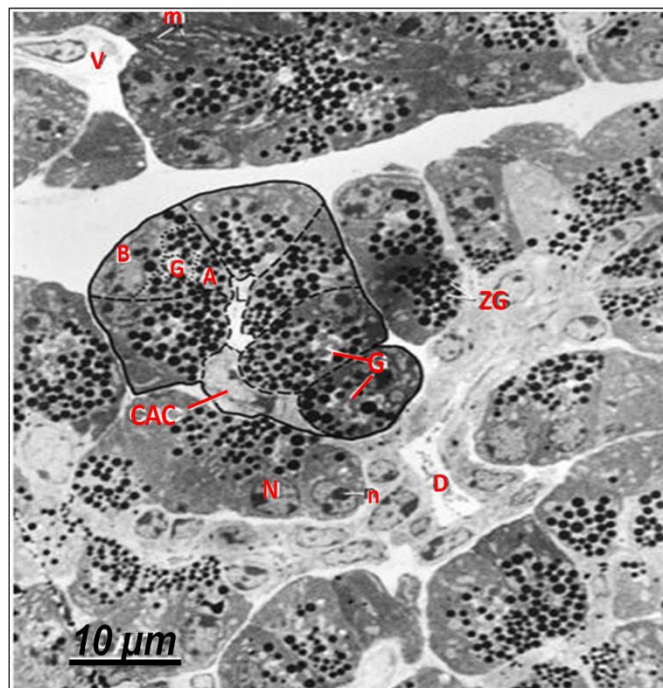
Figure 1.3: Pancreatic tissue with acinar, centroacinar and ductal cells [5]

The acinar cells have several short, slender microvilli about 0.2 µm in length and extend into the lumen of the acinus. The lumen typically contains flocculent electron-dense material, which is the secreted digestive enzymes. Thin filaments form the axis of the microvilli as well as a network beneath the apical plasmalemma. These microfilaments apparently play a structural role because their disruption causes expansion of the acinar lumen and loss of microvilli. In figure 1.3 are shown the acinar cells which are larger than

centroacinar cells and are easily identified because of the darkly stained the zymogen granules (ZG). The basal portion (B), in the opposite site of the luminal one (A), of the canard cells lies next to the interstitial space that contains vessels (V), nerves and connective tissue. Nuclei (N) with nucleoli (n) are in the basal portion of the acinar cells: the nucleus usually is spherical, about 6 µm in diameter, with one or more nucleoli in the interior. Mitochondria (m) appear elongate, cylindrical structures that may appear oval in cross-section and may contain well-developed cristae and many matrix granules and they occur throughout the cytoplasm, among the granular endoplasmic reticulum or zymogen granules and adjacent to the basolateral cell border. The cytoplasmic matrix occupies about 45% of the cell volume. Tight junctions form a belt-like band around the apical end of the cell and are produced by the apposition of the external membrane leaflets of neighboring cells. These junctions prevent the reflux of secreted substances from the duct into the intercellular space. Gap junctions are distributed on the lateral cellular membranes and are formed by the apposition of larger, disk-shaped membrane plaques, they allow communication between cells. Rough endoplasmic reticulum (RER) occupies about 20% of the cell volume and fills most of the basal region of the acinar cells, although small amounts also occur in the apical region adjacent to and among the zymogen granules. This reticulum is composed of numerous parallel cisternal membranes covered with closely spaced attached ribosomes, giving the structures a granular appearance. The Golgi complex (G) is located between the nucleus and the mass of zymogen granules present in the resting gland, it consists of flattened, membranous saccules as well as small vesicles or vacuoles that contain flocculent electron-dense material. The Golgi complex is believed to play an important role in the transport of secretory proteins and the formation of zymogen granules, in fact the precursors of zymogen granules that formed starting from Golgi complex are membrane-bound vesicles slightly larger than zymogen granules and much less numerous, occupying only about 2% of the cytoplasm. Studies of the chemical composition of the zymogen granules, that appear as spherical, membrane-bound vesicles and slightly less than 1 mm in diameter, have shown that they contain about 12 to 15 different digestive enzymes, which make up about 90% of the granule protein. [6; 7].

About the ductal system, the duct of Wirsung is the main pancreatic one from which originates the accessory duct of Santorini, other connections are the interlobular ducts, that drain into the main duct throughout the pancreas and the intralobular ducts (sometimes called intercalated ductules) that link acinar tubules to the interlobular ducts. Enzymes from acinar cells are released into a bicarbonate-rich solution that is secreted by the

centroacinar and ductal cells and flows from the acini and acinar tubules to the intralobular ducts, then into the interlobular ducts and main duct and, finally, into the duodenum at the major or minor papillae. The integrity of the duct system is of key importance in preventing entry of the exocrine enzymes into the interstitial space where they may be activated and cause tissue damage manifest as pancreatitis. The main and interlobular ducts have thick dense collagenous walls. The connective tissue component of the duct wall becomes progressively thinner as the ducts branch and become narrower. Intercellular tight junctions, also called *zonula occludens*, between duct cells, centroacinar cells and acinar cells play a major role in preventing leakage of the duct system [6].

Ductal cells express markers such as cytokeratin 19 (K19), cystic fibrosis transmembrane receptor (CFTR), carbonic anhydrase II (CAII), DBA lectin and transcriptional factors as HNF1β (Hepatocyte Nuclear Factor 1 β), HNF6 (Hepatocyte Nuclear Factor) and Sox9 [8].

1.1.3 The endocrine portion

The bulk of the pancreas is composed of pancreatic exocrine cells and their associated ducts, but embedded within this exocrine tissue, there is roughly one million small clusters of cells called the *Islets of Langerhans*, which are the endocrine cells of the pancreas and secrete insulin, glucagon and several other hormones. Islets vary greatly in size, ~70% are in the size range of 50-250 μm in diameter in humans with an average in the range of 100-150 μm [9]. Smaller islets are dispersed throughout the acinar lobules and most larger islets lie along the main and interlobular ducts of the pancreas. Most islets are spherical or ellipsoid, but they can be irregular in shape, reflecting sometimes the pressure of an adjacent structure, often a duct. In the tail of the pancreas there is a higher population density of islets than in the head and body [10; 11; 12; 13]. In adult humans the number of islets is calculated to be 500000-1 million whereas, they comprise 1-2% of the pancreas in adults of most mammalian species. In addition to the islets, isolated islet cells may be found dispersed in the acinar lobules or in association with ducts [14; 15]. The differences among the islets are detectable through electron microscopy (Fig.1.4).
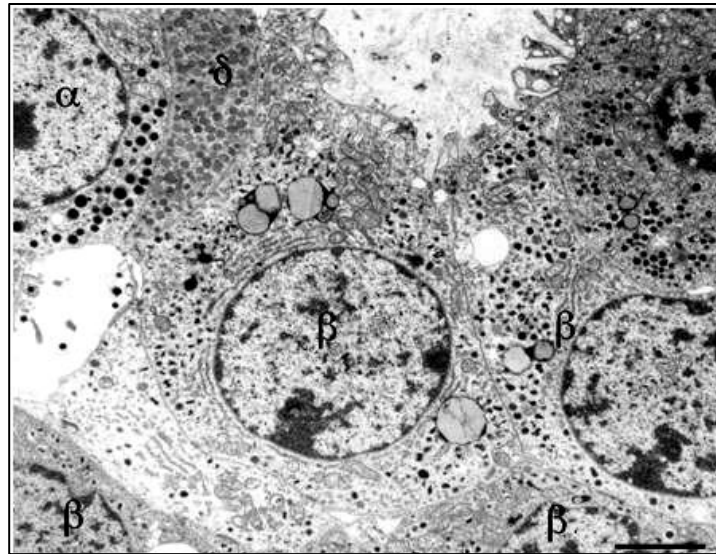
Figure 1.4: The α-, β-, and δ-cells are labeled. At the ultrastructural level, the cell types are distinguished primarily by differences in their granules. The α-cell granules are typically slightly larger than β-cell granules. δ-cell granules are typically less densely stained than the granules in α- and β-cells. Scale bar = 4 μm [5]

Each islet is surrounded and penetrated by a rich network of capillaries lined by a fenestrated endothelium, these capillaries are arranged in a portal system that conveys blood from the islets to acinar cells. This insula-acinar portal system consists of afferent arterioles that enter the islet, form a capillary glomerulus and leave the islet as efferent capillaries passing into the exocrine tissue. A parallel arterial system supplies blood directly to the exocrine pancreas and permits the local action of islet hormones on the exocrine pancreas. Acinar cells surrounding islets of Langerhans, termed peri-insular acini, are morphologically and biochemically different from acini situated farther away (tele-insular acini): they appear as have larger cells, with different ratios of specific digestive enzymes [16]. β cells, the most numerous (50% to 80%), secrete insulin, α cells (5% to 20%) secrete glucagon, PP cells (10% to 35%) secrete pancreatic polypeptide, δ cells (5%) secrete somatostatin. Other rare cell types, like ε ones, occur in the islets. In humans, the islets are subdivided into units, each of which exhibits a central aggregation of β cells surrounded by varying numbers of peripherally located cells that secrete the other hormones (Fig.1.5).
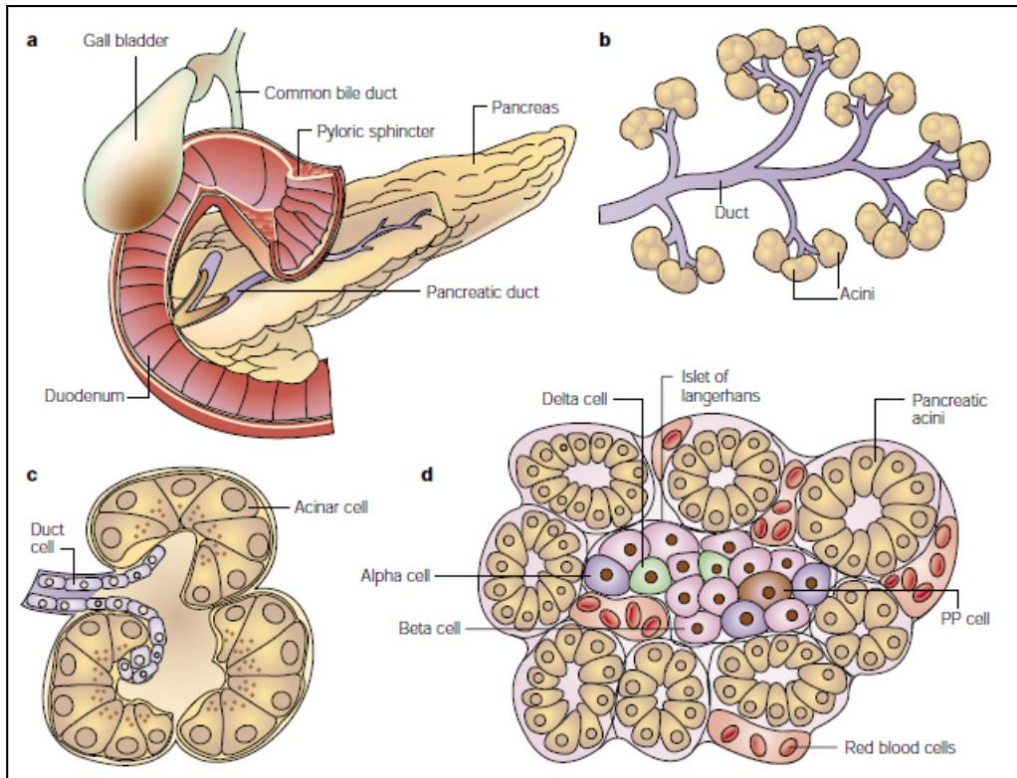
Figure 1.5: *a.* Gross anatomy of the pancreas; *b.* The exocrine pancreas; *c.* a single acinus; *d.* A pancreatic islet embedded in exocrine tissue [17].

1.2 Pancreatic development

The pancreas appears as a complex organ comprised of three critical cell lineages: islet, acinar and ductal. As is the case for other endodermal organs, the development of the pancreas is thought to result from interactions between the epithelium and its associated mesenchyme. The pancreas is first discernible as the dorsal bud that emerges from the proximal duodenum at four weeks of gestation. Particularly, the pancreatobiliary system appears at gestation week 5 in the human; then the fusion of the dorsal and ventral anlagen occurs during week 7. Full development of acinar tissue extends into the postnatal period. In mice, pancreatic development begins at embryonic day 8.5 (e8.5) and is largely complete by day e14.5 [18; 19]. Its embryological origin has two buds developing on the dorsal and the ventral side of the duodenum. Pancreatic development is a tightly regulated process, with the endocrine and exocrine compartments emerging from a common progenitor population; this process involves the interplay of Hedgehog and Notch

signaling and other cues from the mesenchyme. Notably, Pdx1 is required for the specification of pancreatic lineages [20].

The pancreas develops from two outgrowths of the distal part to the stomach. The ventral diverticulum gives rise to the common bile duct, gallbladder, liver and the ventral pancreatic portion that becomes a part of the head of the pancreas with its duct system including the uncinate portion of this organ. The dorsal pancreatic anlagen gives rise to a portion of the head, the body and tail of the pancreas including a major duct that is continuous through the three regions. Fusion of the duct systems results in the formation of the main pancreatic duct from the ducts of both dorsal and ventral anlagen. The caudal portion of the head of the pancreas (uncinate) and the *major papilla* (ampulla of Vater) are derived from the ventral anlagen. It becomes apparent that the duct of Santorini is derived from the dorsal part, whereas the duct of Wirsung is derived from the fusion of duct systems of both dorsal and ventral anlagen and drains into the duodenum at the ampulla of Vater. Furthermore, "common channel" refers to the fused portion of the bile and pancreatic ducts proximal to entry into the duodenum. The common channel has received much attention because stones in the biliary tract (gallstones) may lodge in the common channel causing obstruction of both pancreatic and biliary duct systems which is frequently the cause of acute pancreatitis [21].

Of intense interest in the study of ductal cells has been their potential capacity to give rise to islet cells, following the model reported in figure 1.6. If possible, this would be another vehicle to generate islet cells for transplantation as well as a potential treatment of diabetes mellitus, furthermore One study concluded that β cell progenitors can be activated in the injured adult mouse pancreas and are located in the ductal lining [22; 23]. Generally, metaplasia is the word used to define the conversion or replacement of one differentiated cell type with another in the context of a given tissue. In some tissues, metaplasia is associated with an increased risk of cancer.
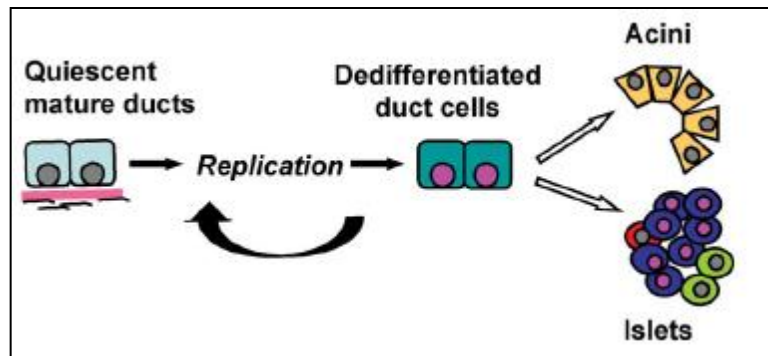
Figure 1.6: Mature duct cells regress to a less differentiated phenotype and then act as pancreatic progenitors to form new acini, islets and ducts [24].

1.3 Pancreatic functions

1.3.1 The exocrine portion

The pancreas can be considered as two glands that are intimately mixed together into one organ. The exocrine portion of the pancreas plays a major role in the digestion of food. The stomach slowly releases partially digested food into the duodenum as a thick and acidic liquid called chyme. The acini, the major functional units of the pancreas, secrete pancreatic juice to complete the digestion of chyme in the duodenum. They respond to several intracellular messengers as acetylcholine (Ach), cholecytokinin (CCK), bombesin (GRP –gastric releasing peptide-) and substance P. Pancreatic juice is a mixture of water, salts, bicarbonate and many different digestive enzymes. The pancreatic enzymes are specialize in digesting specific compounds found in chime and it is possible to recognize:

- *Pancreatic amylase: it* breaks large polysaccharides like starches and glycogen into smaller sugars such as maltose, maltotriose and glucose. Maltase, secreted by the small intestine**,** then breaks maltose into the monosaccharide glucose, which the intestines can directly absorb.
- *Trypsin*, *chymotrypsin (endopeptidases)* and *carboxypeptidase* (esopeptidase): they are protein-digesting enzymes that break proteins down into their aminoacid subunits. These aminoacids can then be absorbed by the intestines.
- *Pancreatic lipase*: it is a lipid-digesting enzyme that breaks large triglyceride molecules into fatty acids and monoglycerides. Bile released by the gallbladder emulsifies fats to increase the surface

area of triglycerides that pancreatic lipase can react with. The fatty acids and monoglycerides produced by pancreatic lipase can be absorbed by the intestines.

- *Ribonuclease* and *deoxyribonuclease*: they digest nucleic acids. Ribonuclease breaks down molecules of RNA into the sugar ribose and the nitrogenous bases adenine, cytosine, guanine and uracil. Deoxyribonuclease digests DNA molecules into the sugar deoxyribose and the nitrogenous bases adenine, cytosine, guanine, and thymine.

The mechanism by which proteins are exported is well characterized: they are first synthesized on polysomes, later they cross the RER (thanks to the SRP –signal-peptide recognition particle– a cytosolic protein which facilitates the binding of mRNA-ribosomal complex to RER) and the Golgi apparatus. Starting from this one, the secretory granules then move by an undefined mechanism to the apical portion of the acinar cells, fuse with it and discharge their contents into the luminal space by an exocytosis process.

If these proteins are secreted inside the pancreatic parenchyma, the consequences can be potentially disastrous with a strong autodigestion. For this reason the enzymes are produced like proenzymes and are packaged in the zymogen granules. They remain inactive until their reach to the duodenal lumen. For example, once in the duodenum, trypsinogen, the major proteolytic enzyme is converted to active trypsin by an enzyme called enterokinase, a brush border enzyme expressed in the duodenal mucosa. The same active trypsin is essential for the activation of other proteolytic and lipolytic pancreatic enzymes. Finally, acinar cells product also the trypsin inhibitor, which is packaged in zymogen granules together with trypsinogen and activates small amounts of trypsin that may form inside the cells or the body of pancreas [25; 26].

The basal volume of pancreatic secretion is estimated to be 0.2/0.3 ml/min, although, when stimulated, pancreatic secretion clan reach 4.0/4.5 ml/min; compressively, the daily output of pancreatic juice is approximatively of 2.5 L [27].

Duct cells secrete a bicarbonate-rich fluid at a considerable variable flow rate of 0.4 ml/min depending of the state of pancreas stimulation. The purpose of alkaline secretion is to neutralize gastric acid that enters the duodenum, an essential process for achieving optimal conditions for pancreatic enzyme activity. In fact, inadequate bicarbonate secretion with failure to reach a neutral pH, as occurs in chronic pancreatitis, contributes to severe maldigestions. As it is elucidated in figure 1.7, carbonic anhydrase catalyzes the production of HCO_3^- and H^+ from carbonic acid. HCO_3^- is then

transported across the luminal plasma membrane by a HCO_3^-/Cl^- exchanger. The major source of luminal Cl^- is now believed to be from the concomitant secretion of the anion via a luminal membrane Cl^- channel. This channel is regulated by cAMP-dependent protein kinase or CFTR protein, which is defective just in cystic fibrosis. The recycling of Cl^- is, therefore, a major factor in determining HCO_3^- secretion: the inhibition of Cl^- channel activity will decrease HCO_3^- secretion. This may explain why pancreatic insufficiency develops in some cystic fibrosis patients, as it results from defective ductal secretion. In this condition, proteinaceous acinar secretions become concentrated and their precipitation can cause blockage and destruction of pancreatic ducts. Proton generated during the production of HCO_3^- must be rapidly transported out of the cells or cell pH would drop precipitously. This occurs at the basolateral membrane through two different mechanisms. One involves Na^+/K^+ ATPase (proton pump), different from the one found in parietal cells of the stomach, in the basolateral membrane and may provide an alternative and perhaps primary mechanism for rapid proton extrusion. Na^+/K^+ ATPase is also present in the basolateral membrane, it is necessary for producing favorable electrochemical gradients for Cl^- secretion. Na^+, some K^+ and water accompany HCO_3^- secretion, mostly entering the duct lumen by passive paracellular diffusion, their rate of transport is determined by prevailing electrochemical and osmotic forces [28].
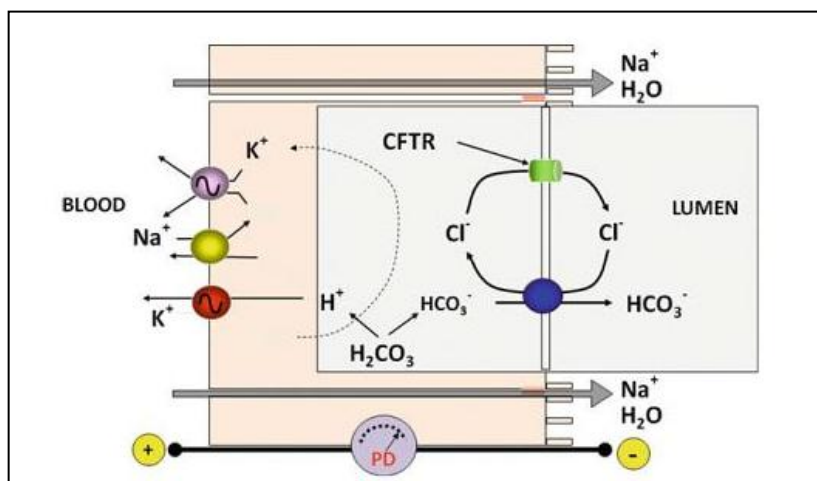
Figure 1.7: Mechanism of active bicarbonate secretion by pancreatic ductal cells [27].

Therefore, ductal cells of the pancreas have recently been under scrutiny as they may be pancreatic stem cells. When the pancreas is

damaged by duct ligation, cellophane wrapping, pancreatectomy, genetically targeted destruction by IFNγ or when cells are specifically destroyed by streptozotocin, there is some increase in the mitotic activity in the ducts and limited regeneration of the organ. This led to the hypothesis that, during regeneration, duct cells act as progenitors for the generation of new pancreatic cells, however, only cell tracing experiments would make the link between the cells observed in the ducts and new islets [28].

1.3.2 The endocrine portion

The endocrine portion of the pancreas controls the homeostasis of glucose in the bloodstream. In general, the islet is composed of 5 cell types: α, β, δ, ε, and PP that produce glucagon, insulin, somatostatin, ghrelin and pancreatic polypeptide, respectively. Of these hormones, insulin is the primary hormone whose actions on a variety of cell types shifts, on balance, the metabolic flux of nutrients (primarily glucose) toward storage forms of energy (glycogen, protein and fat) and is therefore considered an anabolic hormone. By contrast, glucagon, acting typically in an antagonistic fashion to insulin, functions as a catabolic hormone, causing breakdown of glycogen, protein and fat. The other hormones of the islet appear to have either a secondary or uncertain physiologic role in metabolism: somatostatin functions in the inhibition of insulin and glucagon secretion, whereas the significance of pancreatic polypeptide and ghrelin are unclear [29; 30].

Nutrients in the form of glucose, aminoacids and long chain-free fatty acids (LC-FFAs) are absorbed from the gastrointestinal tract into the portal circulation, where they are detected by β cells via an integrated biochemical-based sensing mechanism (in the case of aminoacids, the β cell primarily responds to valine and arginine). This sensing mechanism is tightly coupled to the production and release of insulin into the blood stream.

Two phases of insulin release are observed: an acute or first phase and a more chronic or second one. First, insulin release is reflective of membrane-docked of insulin granules that are engaged immediately upon stimulus coupling. In the second phase, insulin release represents pre-formed or newly-formed granules recruited to the membrane after the immediate stimulus response. Studies have shown that a positive autocrine/paracrine response of insulin (via its receptor signaling) is important in the maintenance of insulin synthesis in the β cell; the secretion mechanism is described in figure 1.8.
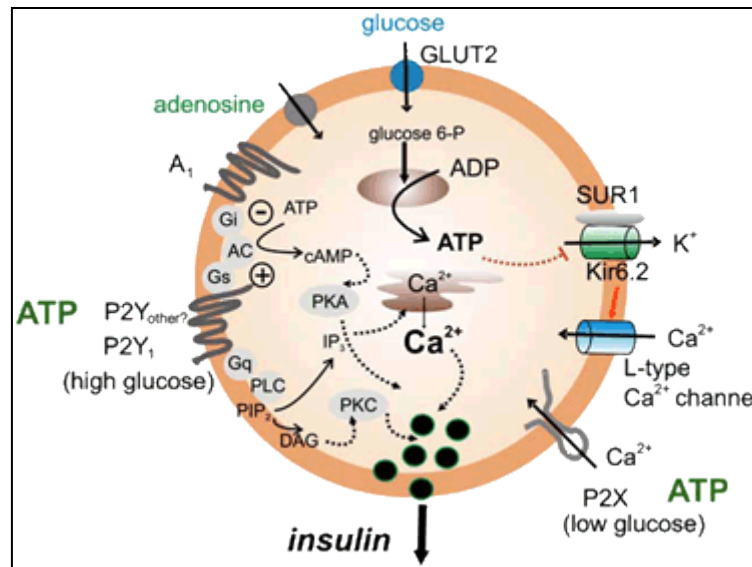
Figure 1.8: The insulin secretion mechanism in detail [31].

Although the insulin receptor is present in a host of key metabolically active organs (for example, liver, muscle, fat and brain) and cells (α cells and β cells of the pancreatic islet). Its actions in each of these organs and cells differ: in the liver, insulin promotes glycolysis, inhibits gluconeogenesis, promotes synthesis of glycogen (glycogenesis) and inhibits the breakdown of glycogen (glycogenolysis); in adipose tissue, insulin promotes glucose uptake and glycolysis, the synthesis and storage of triglycerides (TGs) and the inhibition of lipid breakdown; in skeletal muscle, insulin promotes glucose uptake and glycolysis, the synthesis and storage protein and the inhibition of protein breakdown; in bone, finally, insulin acts primarily on osteoblasts to promote osteoclast activity and enhance production and release of osteocalcin (OCN), a hormone that supports insulin release by the β cell. Insulin actions in the brain are now better appreciated and include the regulation of female fertility, appetite, and overall glucose homeostasis. Within the β cell, paracrine/autocrine effects of insulin sustain β cell growth, survival and function. Taken together, the actions of insulin in these tissues support anabolic pathways that lead to the generation of ATP and the conversion of ingested nutrients into the major storage forms of energy (glycogen, protein and fat) [30].

In contrast, α cells of the pancreatic islets secrete the hormone glucagon, which serves to counterbalance the actions of insulin. Glucagon promotes glycogenolysis and inhibits glycogenesis in liver and skeletal muscle, enhances lipolysis and inhibits triglyceride synthesis in adipose

tissue. α cells also express cell surface insulin receptor and respond locally to secreted insulin by suppressing glucagon release.

The liver is thought to secrete an yet unidentified factor(s) that appears to feed back to support β cell mass. The gut secretes incretin hormones (glucagon-like peptide-1 or GLP-1 and glucose-dependent insulinotropic peptide or GIP), which support glucose-dependent insulin secretion and β cell replication. Both GLP-1 and GIP are proteolytic products of the larger pro-glucagon peptide, which is also produced by α cells of the islet. However, it is unclear whether α cell-derived incretins are a major contributor to β cell function/replication, although at least one study using human tissue has suggested that it may contribute.

In addition, a healthy gut microbiota profile is thought to be essential to maintain leanness and normal β cell function. Furthermore, the cells of the central nervous system are known to secrete multiple peptides (melanin concentrating hormone –MCH-, serotonin and prolactin –PRL- and others) that have been shown both *in vitro* and *in vivo* to support β cell function and proliferation. Likewise, bone-derived OCN has been shown to support β cell replication and insulin secretion [32; 33].

CHAPTER 2

PANCREATIC CARCINOMA

2.1 Introduction: epidemiology, etiology and symptoms

Pancreatic cancer (PC) is the fourth leading cause of cancer death in the West World countries. It accounts for 277.000 new cases diagnosed each year in the world, among which approximately 49.000 occur in the USA and Europe [34]. With a 5-year survival rate of only 3% and a median survival of less than 6 months, a diagnosis of PC represents now the true problem for this tumor. Due to a lack of specific symptoms and limitations in diagnostic methods, the disease often eludes detection during its formative stages. Whipple and colleagues reported the first pancreaticoduodenectomy in 1935 and surgery since offers the only possibility of cure, although surgical intervention alone rarely achieves a curative end point but, for the 15/20% of patients who undergo potentially curative resection, the 5-year survival is only 20% [35; 36].

The etiology of PC remains poorly defined, although important clues of disease pathogenesis have emerged from epidemiological and genetic studies. PC is generally associated with advancing age: rare before the age of 40, it gradually culminates in a 40-fold increased risk by the age of 80. The incidence of PC is declining slowly in white men, but it is increasing in other groups, possibly because of changes in smoking patterns. Women account for 57% of new cases. Smoking, diabetes and obesity increase risk, instead a link between alcohol or coffee consumption and PC has not been verified [37; 38; 39; 40]. Physical activity, high fruit and vegetable intake and, possibly, nonsteroidal anti-inflammatory drugs reduce the risk [41]. On the genetic level, numerous studies have documented an increased risk (approximately threefold) in relatives of PC patients, it is estimated that 10% of PCs are due to an inherited predisposition, even if it has a lower penetrance unlike familial cancer syndromes for breast, colon and melanoma [42; 43; 44; 45].

PC often develops without clear early signs or symptoms and the eventual manifestations depends on the tumor location within the gland. Up to 50% of patients presents jaundice, which is more common with patients whose cancers are located in the head of the pancreas where tumors can cause obstruction of the adjacent biliary system [46]. Other common manifestations are vague abdominal discomfort, nausea and weight loss. Large tumors that advance beyond the pancreas can also cause duodenal

obstruction or gastrointestinal bleeding. Steatorrhea can also result from obstruction of the pancreatic duct, whereas hyperglycemia and diabetes have been associated with early manifestation of disease. Patients with advanced disease can also present abdominal and back pain, anorexia, dyspepsia, gallbladder enlargement, migratory thrombosis (Trousseaux syndrome), subcutaneous fat necrosis (panniculitis), hyperglycemia, ascites and depression [45; 47; 48].

Based on the information about the physiologic development of pancreas, it has been found in some tissues that metaplasia can be associated with the increased risk of cancer. Pancreatic acinar cells have the capacity to undergo metaplasia to a ductal cell phenotype in the setting of acute or chronic inflammation, representing an important link to pancreatic ductal adenocarcinoma (PDAC). Acinar-ductal metaplasia (ADM) might represent reprogramming of a progenitor population, direct transdifferentiation of acinar cells to ductal cells, or transdifferentiation via an intermediate cell type (potentially a progenitor cell) [49]. Metaplastic acinar structures are highly proliferative, express Notch target genes, and exhibit mosaic expression patterns for EGFR, ErbB2, and pErk, reminiscent of the PDAC precursors [50; 51; 52]. Spontaneous ADM has been described *in vitro*, accompanied by the induction of Pdx1 expression during culture of acinar cells [53]. Another relevant transcription factor is Mist1. Mist1 functions as a homodimer, and its loss results in ADM *in vitro*, with accompanying induction of cytokeratins K19 and K20. Transgenic mice expressing a dominant-negative Mist1 undergo ADM in vivo [54]. Collectively, these studies suggest that loss of Mist1 initiates metaplasia and that Pdx1 expression fosters ADM.

2.2 The genomic landscape of PC

2.2.1 KRAS (Kirsten Rat Sarcoma Oncogene)

The better characterized forms of PC almost universally carries one or more of four genetic defects. Particularly, ninety percent of tumors have activating mutations in the KRAS oncogene. KRAS encodes a small guanine nucleotide transferase, GTPase, that in its active GTP-bound form promotes a wide range of cellular responses including proliferation, survival, migration and metabolism through several effector pathways including the Raf/MEK/ERK (MAPK) and PI3K/AKT kinase cascades (Fig. 2.1) [55]. Transcription of the mutant KRAS gene produces an abnormal Ras protein that is 'locked' in its activated form, resulting in the aberrant activation of

proliferative and survival signaling pathways. Furthermore, there is evidences for an important contribution of autocrine epidermal growth factor (EGF)-family signalling. This autocrine loop and resulting stimulation of the phosphatidylinositol 3-kinase (PI3K) pathway is required for transformation of several cell lineages by *RAS*-family oncogenes. Consistent with the existence of such an autocrine loop, pancreatic ductal adenocarcinomas (PDAC), the more frequent kind of PC, overexpress EGF-family ligands (such as transforming growth factor-α -TGF-α- and EGF) and receptors (EGFR, ERBB2, also known as HER2/neu, and ERBB3) [56; 57; 58]. The main mutation of this gene is KRAS ^{G12D} and in several cases it is used also in *in vivo* models, for example engineered mice in which KRAS is activated develop spontaneous PanINs and later PDAC, above all if they are subjected to pancreatic constant inflammatory insults (patients suffering from chronic pancreatitis have a 16-fold increased risk of developing PC) [59; 60; 61; 62]. Even *in vitro* fibroblast expressing KRAS^{G12D} exhibit elevated Ras-GTP levels with the association of enhanced proliferative properties and escape from premature senescence [63]. The activated mutation of Kras^{G12D} could be one of the earliest genetic abnormalities of pancreatic neoplasia and is sufficient to initiate the transformation of pancreatic ductal cells to PanINs, but, to guarantee tumor development *in vivo*, it is usual to induce chronic pancreatitis [64]. Several reports show that the most efficient method to induce pancreatitis is the use of caerulein, a CCK analog that binds and activates the CCK receptor. There are two distinct CCK receptor subtypes, namely CCK1 (previously named CCKA) and CCK2 (previously named CCKB) receptors. CCK receptors are G-protein-coupled receptors initiating transient Ca^{2+} oscillations by activating phospholipase C and induction of inositol triphosphate (IP3)-dependent Ca^{2+} release from endoplasmic reticulum in pancreatic acinar cells. CCK1R mediates for example the secretion of pancreatic digestive enzymes and may also be involved in the regulation of satiety and feeding behavior, while CCK2R stimulate gastric acid production. CCK1R has a role in the exocrine effects of cerulein such as amylase secretion. However, CCK2R is now recognized to mediate the mitogenic and anti-apoptotic effects of gastrin on gastrointestinal and pancreatic cells. In a pancreatic tumor cell line expressing the endogenous CCK2R, the proliferative effects of the CCK2R have been shown to be induced by the activation of the Jak2/Stat3 pathway by this receptor [65]. Caerulein-induced acute pancreatitis is a well-studied animal model in which this substance causes an edematous pancreatitis. Initiation of acute inflammation is mediated through premature intracellular activation of zymogens in the acinar cells, leading to acinar death and an inflammatory response associated with

mild pancreatic edema [66; 67]. Interestingly, oncogenic K-Ras activation is rarely observed in human endocrine tumors and this may in part explain the concept that tumor mainly arises from the acinar cell compartment of the exocrine pancreas [68].
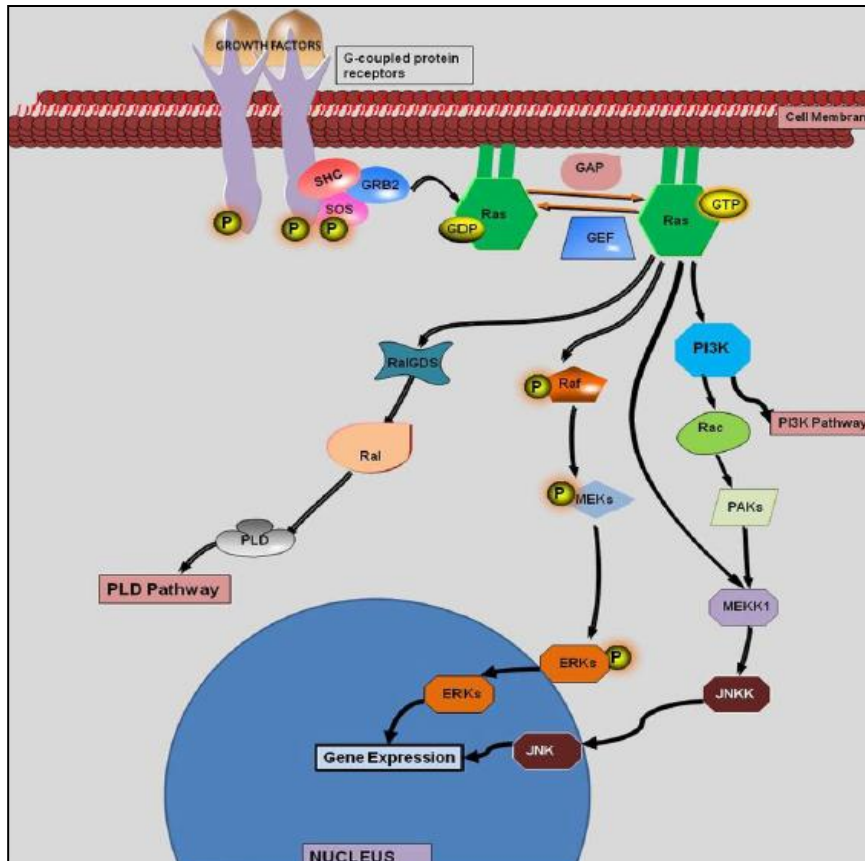
Figure 2.1: The Ras activation cascade [69].

2.2.2 CDKN2A (Cyclin-Dependent Kinase inhibitor 2A)

Activation of KRAS alone in the pancreatic epithelium led to the development of PanINs, highlighting the need for additional cooperating events to promote tumor progression to the malignant PDAC stage. In a number of studies, additional genetic alterations have been combined with activation of KRAS to identify cooperating events context of KRAS-dependent pancreatic tumorigenesis [70]. The inactivation of the CDKN2A gene is the resultant loss of the p16 protein, a regulator of the G1-S transition of the cell cycle, and a corresponding increase in cell proliferation. The inheritance of

mutant *CDKN2A* alleles confers a 13-fold increased risk of pancreatic cancer. Loss of *CDKN2A* function is brought by mutation, deletion or promoter hypermethylation and occurs in 80/95% of sporadic pancreatic adenocarcinomas. *CDKN2A* loss is generally seen in moderately advanced lesions that show features of dysplasia. The locus 9q21 encodes two tumour suppressors: INK4A (INhibitors of CDK4) and ARF (the Alternate Reading Frame protein product of the CDKN2A locus), via distinct first exons and alternative reading frames [71; 72; 73]. INK4A inhibits CDK4/CDK6-mediated phosphorylation of RB (retinoblastoma), thereby blocking entry into the S phase of the cell cycle; ARF stabilizes p53 by inhibiting its MDM2 (Mouse double minute 2 homolog)-dependent proteolysis. INK4A seems to be the more important PC suppressor, as germline and sporadic mutations have been identified that target this protein. When primary cells are placed into culture, *INK4A*-transcript expression is induced and this can be considered a stress response to the inappropriate growth environment that is associated with *in vitro* culture [74; 75]. This induction by environmental stress and aberrant proliferative signals provides a plausible basis for the tumour-suppression function of INK4A, although the relationship of this phenomenon to cancer suppression *in vivo* is not established. Other studies have implicated INK4A in the cellular response to DNA damage *in vivo*, so the absence of INK4A might also contribute to the chemoresistance of pancreatic adenocarcinoma [76]. Notably, while *KRAS* mutations are often detected in non-neoplastic states, such as chronic pancreatitis and, possibly, in normal pancreas, loss of *INK4A* usually occurs only in later stages of pancreatic neoplasia [77; 78; 79]. Although loss of INK4A probably facilitates the oncogenicity of activated *RAS* alleles, as shown in animal models, its occurrence later in pancreatic tumour progression indicates that the intersection of these pathways might require other events, such as disrupted contacts with the extracellular matrix or elevations in the level of activated *KRAS* [80].

2.2.3 TP53

The *TP53* tumor-suppressor gene is mutated, generally by missense alterations of the DNA binding domain, in 50%–75% of tumors. In general, TP53 functions as a heterotetrameric complex that transactivates key target genes in response to a variety of cellular insults, resulting in cell cycle arrest or apoptosis. *TP53* mutations arise in later-stage PanINs that have acquired significant features of dysplasia, reflecting the function of *TP53* in preventing

malignant progression, permitting, in this way, cells to bypass DNA damage control checkpoints and apoptotic signals and contributing to genomic instability [81]. In contrast to many other cancer types, in PC there does not seem to be a reciprocal relationship in the loss of *CDKN2A* and *TP53*. The initiation of pancreatic tumorigenesis by endogenous KRAS[G12D] expression in the context of *Trp53[R172H]* greatly hastens the development of locally invasive and widely metastatic PDAC that faithfully recapitulates all of the extant features of the human disease [82]. Cytogenetic studies have provided evidence that telomere dynamics might contribute to this genomic instability [83]. Although reactivation of telomerase is crucial to the emergence of immortal cancer cells, a preceding and transient period of telomere shortening and dysfunction might also contribute to carcinogenesis by leading to the formation of chromosomal rearrangements through breakage–fusion–bridge cycles. The survival of cells with critically short telomeres (crisis), which continue to go through breakage–fusion–bridge events, is enhanced by inactivation of the p53-dependent DNA-damage response, allowing the acquisition of oncogenic chromosomal alterations. Studies in the telomerase-knockout mouse support this model, as telomere dysfunction and p53 loss cooperate to promote the development of carcinomas in multiple tissues. An analysis of a large series of human pancreatic cancer cell lines revealed that telomeres were frequently lost from chromosome ends and that anaphase bridging occurred, indicating that persistent genomic instability is associated with critically short telomeres. Telomere dysfunction was an early step in the pathogenic process. Moreover, studies of PDAC revealed that tumors have shortened telomere length and that the activation of telomerase is a late event [84; 85; 86; 87].

2.2.4 SMAD4

The deleted in pancreatic carcinoma 4 gene (DPC4, also known as SMAD4/MADH4 - mothers against decapentaplegic homolog 4 -) is lost in about 50% of pancreatic cancers, resulting in aberrant signaling by the transforming growth factor-β (TGFβ) cell surface receptor. This gene maps to chromosome 18q21 [88]. The pathogenic role of SMAD4 inactivation is strongly supported by the identification of inactivating intragenic lesions of *SMAD4* in a subset of tumors. *SMAD4* seems to be a progression allele for pancreatic adenocarcinoma, as its loss occurs only in later-stage PanINs and it has become a predictor of decreased survival in pancreatic adenocarcinoma [89; 90; 91]. In a study using human pancreatic cancer

samples from primary and metastatic lesion, mutations in the DPC4 gene have been associated with higher metastatic potential [92]. The mechanism by which *SMAD4* loss contributes to tumorigenesis is likely to involve its role in TFG-β mediated growth inhibition. TGF-β can behave as both a tumor suppressor and a tumor promoter. Its tumor suppressor function can be explained largely by its ability to inhibit proliferation of normal epithelial and lymphoid cells by either blocking the G1–S cell cycle transition (from which most human cancers originate) and to induce apoptosis [93]. However, late-stage human carcinomas often become resistant to TGF-β growth inhibition and, in addition, secrete elevated levels of this growth factor [94]. But, by now, the roles of TGF-β signaling in pancreatic adenocarcinoma pathogenesis are not well defined: its role can be well illustrated as a tumor suppressor pathway by the presence of chromosomal deletions and mutations in DPC4 in 55% of pancreatic tumors, a tumor suppressor that has been implicated in mediating the growth inhibitory and antiangiogenic effects of TGF-β [88; 95; 96]. This cytokine shows inconsistent effects on cultured cell lines with respect to cell proliferation rates and dependency on SMAD4 status for TGF-β responsiveness. Furthermore *SMAD4* loss is also likely to contribute to tumor progression through effects on the interaction of tumor with stroma [97; 98; 99; 100]. Particularly, heterotypic microenvironmental cellular interactions seem to be important in the pathogenesis of pancreatic adenocarcinoma. Notably, these tumors show a marked proliferation of stromal fibroblasts and deposition of extracellular matrix components such as matrix metalloproteinases and collagens (desmoplasia) [101].The role of this process in cancer pathogenesis remains uncertain, as it is not well established whether the response is part of the tumorigenic programme or whether it represents a form of host defence against the tumor. Recent evidence indicates that the carcinoma cells direct the desmoplastic response and that TGF-β contributes to this process [102]. There are suggestions that *SMAD4* loss might be permissive for these effects, notably, *Smad4*-deficient tumors show increased growth and invasiveness in this model. Another role for SMAD4 in regulating heterotypic interactions is indicated by experiments in which Smad4 is reintroduced into some pancreatic adenocarcinoma cell lines. In these experiments, Smad4 blocks tumorigenic growth in immunodeficient mice by inhibiting angiogenesis, but does not affect cell sensitivity to TGF-β [96]. These concepts are consistent with recent studies showing that cancers 'programme' an oncogenic stroma that, in turn, contributes to tumor growth through paracrine signaling, angiogenesis and protection from immune attack [103; 104].

Generally, transgenic mouse models which are commonly used are reported in the table 2.1:

Genotype (reference)	Time of expression	Time to tumor development (mo)	Pancreatic cancer phenotype	Survival (mo)
PDX-1-Cre; LSL-Kras^{G12D}[36]	E8.5	6	PDAC; penetrant PanIN; age dependent increase severity; occasionally PDAC with long latency	16
P48$^{+/-Cre}$; LSL-Kras^{G12D}[36]	E9.5	8	PDAC; penetrant PanIN; age dependent increase severity; occasionally PDAC with long latency	16
PDX-1-Cre; LSL-Kras^{G12D}; LSL-Trp53$^{R172H/-}$[24]	E8.5	2-3	PDAC Accelerated PanIN; well differentiated PDCA	5-6
Mist1$^{KrasG12D/+}$[25]	E10.5	2	Accelerated development of acinar-derived PanIN; mixed subtypes pancreatic cancer	10.8
KPCB$^{wt/wt}$[42]	E8.5	2-3	PDAC	5.6
KPCB$^{Tr/wt}$[42]	E8.5	3	PDAC	4.8
KPCB$^{Tr/\Delta 11}$[42]	E8.5	1.5	PDAC; mixed	2.8
CKB$^{wt/\Delta 11}$[41]	E8.5	6	PDAC	12
CKB$^{wt/wt}$[41]	E8.5	6	PDAC	13.5
CPB$^{\Delta 11/\Delta 11}$[41]	E8.5	3-5	PDAC; mixed	10
Pdx1-Cre; Kras^{G12D} Ink4a/Arf^{flox}[25]	E8.5	2	PDAC; accelerated development of PanIN; poorly differentiated PDAC	2-3
Pdx1-Cre; Kras^{G12D} Smad4$^{flox/flox}$[55]	E8.5	2-3	IPMN; PDAC	2-6
Ptf1a$^{cre/+}$; LSL-Kras$^{G12D/+}$; Tgfbr2$^{flox/flox}$[27]	E9.5	1	PDAC; accelerated PanIN; PDAC development	2

Table 2.1: Mouse models of pancreatic carcinoma [105]

2.3 Staging of PC

In 1905, S.P.L. Hulst described for the first time small microscopic lesions in the pancreas which are now described as "pancreatic intraepithelial neoplasia (PanIN)". PanIN lesions are noninvasive epithelial proliferation within the smaller pancreatic ducts and they are graded histologically as PanIN-1 (low-grade), PanIN-2 (intermediate-grade) or PanIN-3 (high-grade) characterized by columnar to cuboidal cells with varying amunts of mucins and based on the degree of architectural and cellular atypia present in the lesion (Fig. 2.2) [106].
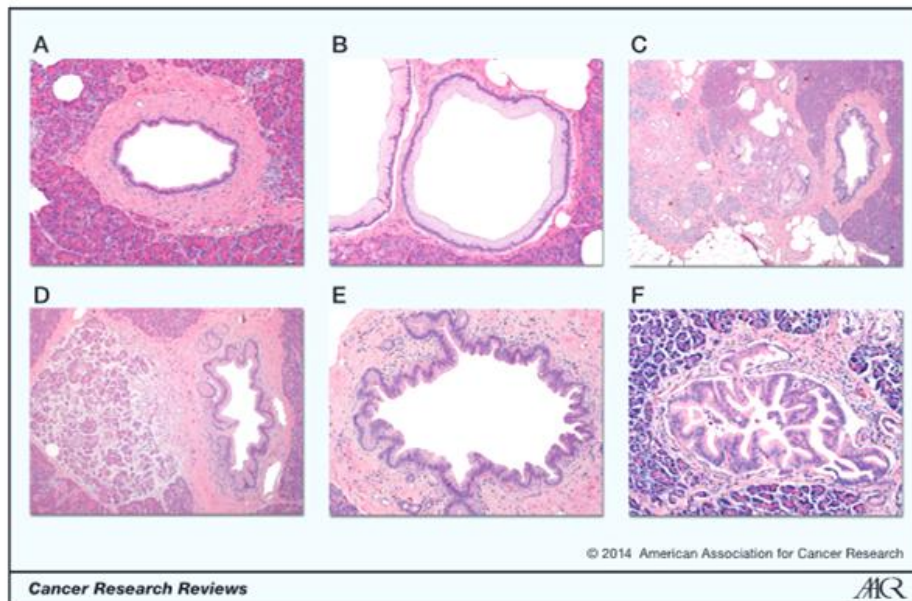
Figure 2.2: A normal pancreatic duct (A) and multiple PanIN lesions (B-F). PanIN-1 (B), PanIN with associated lobulocentric atrophy (B and C), PanIN-2 (E), and PanIN-3 (F), all hematoxylin and eosin images [107].

Generally PanIN lesions are not detected macroscopically and are clinically silent. PanIN-1 is characterized by two early stages: PanIN-1A and PanIN-1B which show minimal cytological and architectural atypia. PanIN-2 lesions show mild to moderate cytological atypia with frequent papillary formation and also nuclear abnormalities for example enlargement, some loss of polarity, crowding. PanIN-3 is the most severe lesion with abnormal cell mitosis and budding into lumen [108]. Paralleling this histologic progression is a genetic progression. PanIN-1 and PanIN-2 often harbor genetic alterations in the KRAS and p16/CDKN2A genes, whereas PanIN-3 lesions and invasive adenocarcinomas, in addition to genetic alterations in KRAS and p16/CDKN2A, also often harbor mutations in TP53 and SMAD4 (Fig. 2.3) [109; 110]. High-grade PanINs, however, are rarely found, unless there is an associated invasive pancreatic cancer or the patient which has a strong family history of PC; these observations support the hypothesis that PanIN lesions are precursors to invasive adenocarcinoma [111; 112; 113].
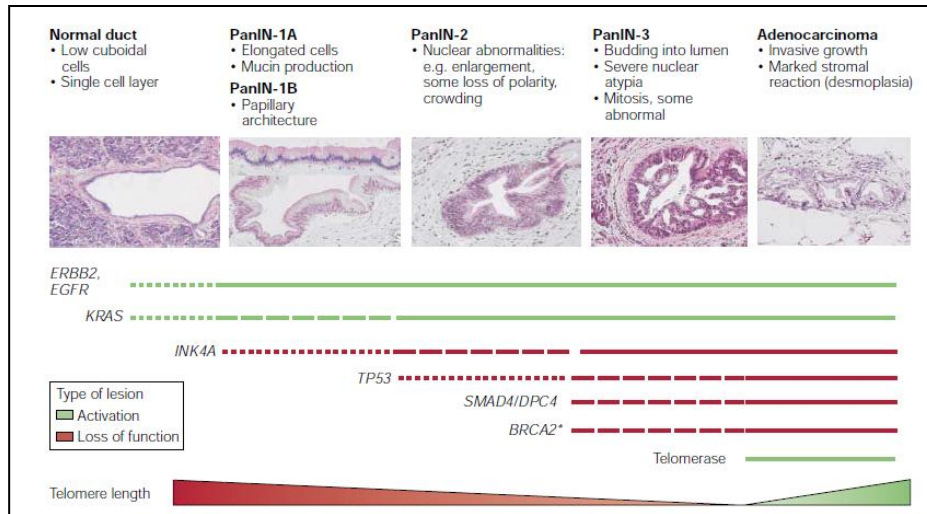
Figure 2.3: Genetic progression model of pancreatic adenocarcinoma [17]

The second major precursor lesion to be identified in the pancreas was the intraductal papillary mucinous neoplasm (IPMN). IPMNs arise in the larger pancreatic ducts and, as the name suggests, they are typically papillary and often produce copious amounts of mucins. IPMNs are, by definition, larger than PanINs (>1.0 cm, with respect to <0.5 cm for PanINs) [3]. As is observed with PanINs, low-grade IPMNs often harbor KRAS and p16/CDKN2A gene mutations, high-grade IPMNs harbor further mutations in TP53 and SMAD4. When an adenocarcinoma arises in association with an IPMN, the IPMN and the invasive carcinoma almost always harbor the samegenetic alterations, supporting the hypothesis that IPMNs are a precursor to invasive adenocarcinomas [114]. Far less common than IPMNs, are the Mucinous cystic neoplasms (MCNs), they are large mucin-producing precancerous lesions of the pancreas that almost always arise in the body of tail of the gland and commonly arise in women. In contrast to IPMNs, MCNs do not significantly involve the pancreatic duct system. However, like IPMNs, MCNs can progress to adenocarcinoma. The KRAS, p16/CDKN2A, RNF43, TP53 and SMAD4 genes have all been reported to be mutated in MCNs [3; 114]. Finally, it can be mentioned some small cancer lesions, rarely encountered outside of screening trials. There have been several reports of long-term survival of patients with surgically resected small, lymph node negative, pancreatic cancers [115].

2.4 Biomarkers for detection of PC

One of the main difficulties about PC detection is just the lack of reliable screening tests, either molecular or imaging based. Commonly used imaging studies as abdominal CT (computer tomography) or MRI (Magnetic Resonance Imaging) are still inadequate for diagnosing PC at an early stage since they do not reliably detect tumors smaller than 1-2 cm [116]. The mucin-associated carbohydrate antigen CA 19–9 is a biomarker of PDAC with limited clinical utility in the screening setting. CA 19–9 has demonstrated modest effectiveness in the screening of symptomatic individuals with a range of 70–90% of cases. But the principal limitations of CA 19–9 include its frequent elevation associated with nonmalignant conditions such as pancreatitis and obstructive jaundice and its inability to detect many early stage malignancies [117; 118]. These limitations of CA 19–9 have led investigators to search for alternative biomarkers for use in screening for PDAC. For example, a panel of 7 proteins (ALCAM, ICAM-1, LCN2, TIMP-1, REG1A, REG3 and IGFBP-4) with or without the addition of CA 19–9, selected based on findings in a mouse model, was able to discriminate human PC cases from matched controls in a small group of presymptomatic and prediagnostic blood samples [119]. Biomarker profiles indicative of a specific cancer include not only those factors produced by the tumor itself but also represent the systemic response to the growing tumor including acute phase reactants, inflammatory cytokines, growth and angiogenic factors, etc. An accurate panel of circulating levels of significant biomarkers in patients diagnosed with PC, benign pancreatic disease and healthy control individuals is reported in table 2.2:

Class	Biomarker	Units	Healthy Mean	Benign Mean	PDAC Mean	PDAC vs. Healthy[1] p-value	PDAC vs. Benign[1] p-value
Tumor Markers	CA 19–9	U/ml	5.42	2.61	56.04	< 0.001	< 0.001
	CA-125	U/ml	27.4	26.9	1073.1	< 0.001	< 0.001
Hormones	GH	ng/ml	1.93	1.17	2.40	< 0.001	< 0.001
	Prolactin	ng/ml	6.18	23.66	14.10	< 0.001	< 0.001
	PTH	pg/ml	27.2	43.5	38.6	< 0.001	ns
Apoptosis Markers	Cytokeratin 19 (Cyfra 21–1)	pg/ml	20.16	122.8	7579.0	< 0.01	ns
	sFas	ng/ml	8.88	9.27	13.62	< 0.001	< 0.05
	sFasL	pg/ml	50.0	47.5	40.3	< 0.001	< 0.05
Invasion/Adhesion Mediators	MMP-2	ng/ml	178.4	192.7	198.3	< 0.01	ns
	MMP-3	ng/ml	11.8	22.2	49.8	< 0.001	ns
	MMP-9	ng/ml	116.9	164.1	164.7	< 0.01	ns
	ICAM-1	ng/ml	177.1	535.4	1011.3	< 0.001	< 0.05
	TIMP-1	ng/ml	116.2	184.0	331.5	< 0.001	< 0.001
	TIMP-2	ng/ml	102.5	101.9	113.8	< 0.01	< 0.01
	TIMP-3	ng/ml	13.8	11.1	21.6	< 0.001	< 0.01
	TIMP-4	ng/ml	1.54	1.75	2.13	< 0.001	< 0.001
Cytokines/Chemokines/ Receptors	IL-2R	pg/ml	561.8	969.2	1607.1	< 0.001	< 0.05
	IL-8	pg/ml	10.5	16.7	37.7	< 0.001	ns
	IL-6	pg/ml	17.5	18.5	21.5	< 0.01	ns
	IP-10	pg/ml	93.8	94.7	115.5	< 0.001	< 0.001
	MPO	ng/ml	72.2	120.4	125.4	< 0.001	ns
	TNF-α	pg/ml	6.14	7.60	7.14	< 0.05	ns
	TNF-RI	ng/ml	6.09	8.10	10.60	< 0.001	< 0.01
	TNF-RII	ng/ml	4.26	5.31	9.02	< 0.001	ns
Growth/Angiogenesis Factors	Angiostatin	µg/ml	6.60	6.00	6.04	< 0.01	ns
	EGFR	ng/ml	10.4	10.0	8.9	< 0.001	< 0.05
	Endostatin	ng/ml	146.5	169.3	195.4	< 0.001	< 0.05
	ErbB2	ng/ml	1.10	1.21	1.65	< 0.001	ns
	IGFBP-1	ng/ml	16.04	39.06	50.73	< 0.001	ns
	Thrombospondin	µg/ml	16.05	16.73	14.07	< 0.01	ns
Adipokines	Adiponectin	µg/ml	26.3	24.3	33.3	< 0.001	< 0.01
	Leptin	ng/ml	5.47	3.80	3.10	< 0.05	ns
Apolipoproteins	ApoAI	µg/ml	226.9	211.8	103.6	< 0.001	< 0.001
	ApoAII	ng/ml	3.23	2.60	2.10	< 0.001	< 0.01
	ApoCIII	ng/ml	231.3	223.3	195.6	< 0.001	ns
	ApoE	ng/ml	63.0	66.5	95.9	< 0.001	< 0.05
Other	OC	ng/ml	5.62	7.37	4.87	< 0.001	< 0.001
	OPG	pg/ml	441.7	719.5	824.1	< 0.001	< 0.01
	OPN	ng/ml	1.48	6.52	16.15	< 0.001	< 0.001
	CRP	mg/ml	16.45	67.87	120.50	< 0.001	< 0.001
	GLP-1 (active)	pg/ml	18.59	17.91	24.07	< 0.05	ns
	HE4	ng/ml	3.63	2.07	5.11	< 0.001	< 0.05
	SAA	µg/ml	100.2	1012.4	2769.2	< 0.001	< 0.001
	Transglutaminase II	ng/ml	24.67	48.18	62.52	< 0.05	ns

[1]p-value representing significance determined by 1-way ANOVA with Tukey's multiple comparison test; ns – not significant.

Table 2.2: Biomarkers, their concentration and significance in healthy individuals and patients with benign lesions or PDAC [120].

Other markers not expressed in normal ductal cells but observed in low-grade to high-grade PanIN are tumor-associated glycoproteins as CEA and CA125. Conventional PDACs show also at least focal mucin positivity:

the MUC protein are variously expressed in all types of ductal neoplasms. MUC1 is expressed in the 86% of cases, MUC3, 4, 5AC in the 71%, MUC6 (a pyloric gland mucin) in 20% and MUC2 in 6% [3; 121].

2.5 Treatment of PC

The progress in the development of systemic treatment of advanced PC has been slow. The antinucleoside gemcitabine is the standard of care: when it is combined with either cisplatin or oxaliplatin in individual trials, no benefits over single gemcitabine could be shown [122; 123; 124; 125]. Other data showed that gemcitabine combined with 5-fluoruracil (5-FU) might provide a therapeutic advantage over gemcitabine alone [126]. But if gemcitabine still represents the first-line chemotherapeutic agent for the advanced and also metastatic pancreatic cancer, with marginal survival advantage and amelioration of disease-related symptoms, resistance phenomena have been increasing in recent years and its effectiveness has been reduced to <20% [127; 128]. Resistance to gemcitabine treatment is mainly attributed to an altered apoptotic threshold in PC cells [129]. Several experimental reports showed that one of the proteins involved in the acquisition of resistance is MUC4, a member of the mucin family. This family comprises the secreted and membrane-bound forms of protein with a high-molecular weight and heavy O-glycosilation sites that participate in the lubrification of luminal epithelial surface and protection against external insults. Among them MUC4, which is constituted by the extracellular and transmembrane domains and a short cytoplasmic carboxyl-tail, is considered as mediator of intracellular signals involved in cancer development. MUC4, together with other mucins, can play a role for the sustained growth, survival and metastasis of cancer cells at distant tissues and organs and drug resistance [130; 131]. MUC4 is normally absent in the pancreas but an aberrant expression is detected both in PanIN and in its relative advanced cancer [132; 133]. The mechanism by which MUC4 can reduce the apoptotic grade is based on its contribution to enhanced cellular proliferation through its interaction with the epidermal growth factor receptor tyrosine kinase (ErbB2) with subsequent activation of Erk and Akt signaling pathways [134]. Particularly, using MUC4 knockdown and overexpression cancer cell models, this protein has been shown to modify tumorigenity and metastasis by altering the behavior properties of tumor cells [135; 136; 137].

2.5.1 The importance of the PC microenvironment in therapy

The microenvironment of pancreatic adenocarcinoma has a complex role in tumor growth and therapeutic response [138].These cancers are characterized by a dense stroma consisting of proliferating myofibroblasts (pancreatic stellate cells) and deposition of type I collagen, hyaluronic acid and other extracellular matrix components, as well as multiple types of inflammatory cells, including macrophages, mast cells, lymphocytes and plasma cells. Factors that are produced in the stroma, such as connective-tissue growth factor, may directly contribute to the survival of tumor cells [139].The fibrous stroma may contribute to this reduced blood flow and its high interstitial pressure may impair drug delivery [140]. The stroma is not only a mechanical barrier but also constitutes a dynamic compartment critically involved in the process of tumor formation, progression, invasion and metastasis; stromal cells express multiple proteins such as Cox-2 (Cyclooxygenase-2), PDGF (Platelet Derived Growth Factor) receptor, VEGF (Vascular Endothelial Growth Factor), SDF (stroma-derived factor), chemokines, integrins, SPARC (secreted protein acidic and rich in cystein) and hedgehod pathway elements, among others, that have been associated with a worse prognosis and resistance to treatment [141]. Encapsulation of therapeutic agents using albumin nanoparticles (nab) overcomes biological, physical and chemical obstacles, such as the stroma [142]. This allows the administration of insoluble lipophilic agents, as nab- paclitaxel which is an amorphous and crystalline form of paclitaxel bound to albumin (at a concentration of 3–4%). The biological activity of nab-paclitaxel is solely based on its affinity for the mitotic spindle; albumin confers tropism to cancer tissue, while paclitaxel binding stabilizes microtubules and prevents the assembly that is necessary for mitosis, transport and intracellular motility [143]. Nab-paclitaxel therapy caused more cases of complete regression, increased survival and delayed recurrence. This result may be explained by the ability of nab-paclitaxel to achieve higher intratumoral concentrations (up to a 33% increase) compared to conventional paclitaxel. These results could also be explained by of the absence of conventional solvents (which inhibit the albumin dependent pathway), decrease in the generation of micelles, and/or the retention of nab-paclitaxel in tumor microvessels [144; 145]. Several studies suggest that SPARC functions as a stromal chaperon playing a critical role in collagen turnover in PC, it is the target of nab-paclitaxe [141]. Moreover, data obtained from genetically engineered mouse models indicate that nab-paclitaxel antitumour effects were dose-dependent but SPARC independent, thereby inducing apoptotic cell death in the tumor rather than

stromal cells. On the other hand, as inhibitors of the hedgehog pathway stop the desmoplastic reaction, the stroma involution observed after nab-paclitaxel treatment in PDAC may resemble regression of fibrotic matrix found with this drug in others settings. As reactive stromal cells convert extracellular matrix (ECM) into inert tissue with deficient non-angiogenic vasculature and taxanes suppress breast cancer metastasis through abrogation of stromal cells (α-smooth muscle), it would be tempting to speculate that there could be a functional interaction between nab-paclitaxel and stromal cells in neoplastic diseases. However, the molecular mechanisms governing this hypothetical link have not been clarified yet [146].

In conclusion, it is possible to summarize the current therapeutic regimens as it follows:

FOLFIRINOX (5-FU, irinotecan, and oxaliplatin),
FOLFOX (5-FU and oxaliplatin),
Gem-nab (gemcitabine and nab-paclitaxel),
Gem-Ox (gemcitabine and oxaliplatin),
Gem-Cap (gemcitabine and capecitabine),
GTX (gemcitabine, docetaxel, and capecitabine) [147].

CHAPTER 3

THE EPITHELIAL TO MESENCHYMAL TRANSITION

3.1 Introduction

The epithelial to mesenchymal transition (EMT) is a key process in the embryonic development, when, to provide the organ formation, the first epithelial cells change their own phenotype to generate the mesoderm. The EMT has been characterized starting from '80 years, but in the 1995 Elizabeth Hay was continuing to describe it as "epithelial to mesenchymal transformation", only later the term "transformation" was replaced with "transition", by consent to the reversible features of the process (MET), when the cells of the mesoderm are subjected to a new transformation to create epithelial organs, like kidney or ovary. But the EMT is still less characterized [148; 149]. Epithelial cells form layers that are closely adjoined by specialized membrane structures, such as desmosomes, tight, gap and adherens junctions. They are polarized cells with adhesion molecules as cadherins and certain integrins in specific apical-basolateral zones. These molecules are involved in the organization of cell-cell junctions as a lateral belt, the polarized organization of actin cytosckeleton and the presence of the basal lamina at the basal surface. Epithelial cells have not motility, they can move only within the epithelial layer. On the other hand, mesenchymal cells, characterized by a strong migratory ability, do not form as organized cell layer, are not polarized, have not adhesion molecules and they show spindle-shape, named fibroblast-like morphology [150].

During EMT different phenomenon participate like the activation of several transcriptional factors, the production of enzymes of (ECM degradation and cytoskeleton proteins; it changes the expression of microRNA. Beyond the physiological elements, EMT conducts an important role also in the tissue reparation and in pathological stresses like inflammation and advanced tumor state. For these reasons, it is possible, by now, to classify 3 types of EMT (Fig. 3.1).
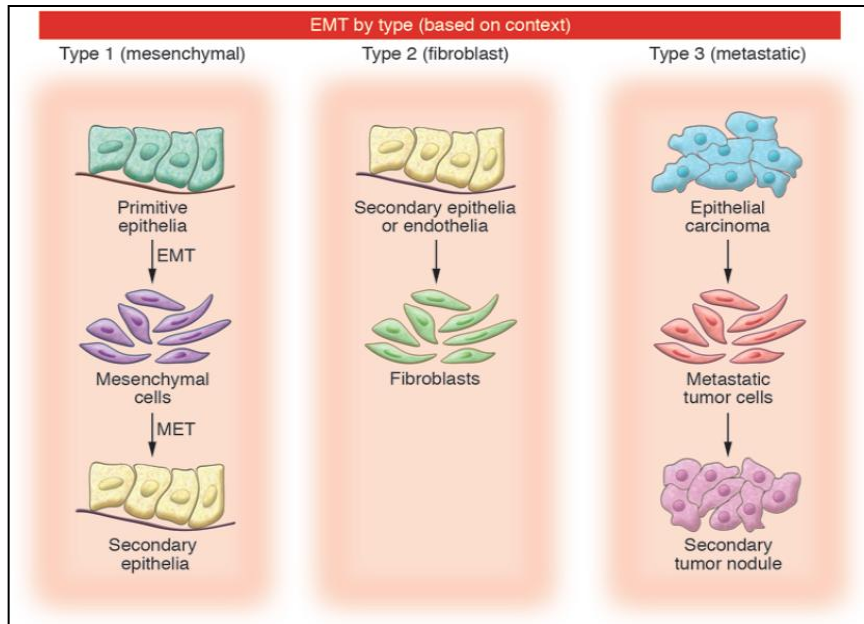
Figure 3.1: Three types of EMT are identifiable depending on the phenotype of generated cells.

3.1.2 Type 1 EMT: mesenchymal

During the embryonic implantation, EMT enhances the invasion of the endometrial cells, which can, in this way, anchor to the placenta. Then, during the gastrulation, the epithelial cells begin to differentiate to form mesoderm and ectoderm. Epithelial cells answer to the Wnt pathway which is activated by the TGFβ; the other important transcriptional factors are Snail that, for example, represses the E-cadherin, a cell-cell adhesion molecule [151]. The other genes which are involved above all in the neural crest formation starting from primary neuroepithelial cells are *Sox*, *Slug*, *FoxD3* (*Forkhead box D3*) but also FGF, BMP and c-Myb [152].

3.1.3 Type 2 EMT: epithelial-fibroblast transition (EFT)

Fibrosis is mediated by inflammatory cells and by fibroblast which product the components of the ECM like collagene, laminine, elastine, tenacine, above all in organs like intestin, kindney and liver EMT is associated to the fibrosis. In these phases the proteins that are considered markers of the fibrotic EMT are FSP1 (*Fibroblast-specific protein 1*, also named S100A4),

αSMA (*α Smooth muscle actin*), collagene I, the other markers like desimne and vimentine are utilized like sensors of chronic inflammation in the cited organs [153]. In the microvascular endothelial cells the EMT, defined as EndEMT, appears in a post-ischemic situation; in this inflammatory contest, cells lose the expression of CD31 and the integrin αVβ3, following the effect of the TGFβ [154; 155]. Other examples of EMT are reported also in patients with kidney fibrosis and Crohn disease where cells first epithelial expressed cytokeratines, αSMA, vimentine and ZO-1 (*Zona Occludens 1*) [156; 157].

3.1.4 Type 3 EMT: metastatic

The characteristic elements of EMT with the relative loss of epithelial markers has been observed in different pathological states, including the epithelial tumor progression. The analysis of the molecular mechanisms at the base of the plasticity of the epithelial cells suggested that the inappropriate expression of mesenchymal markers enhances migration and invasion. Therefore, the development of EMT in cancer progression correlates with advanced states and poor prognosis [158].
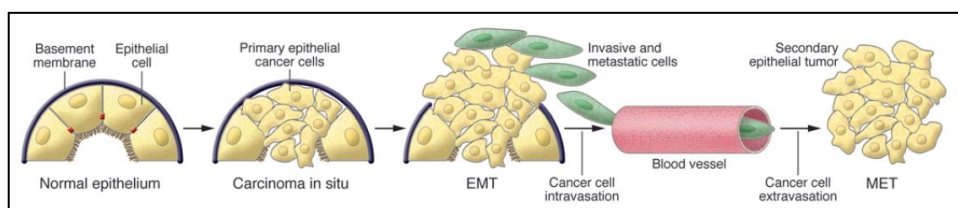
Figure 3.2: Contribution of EMT in tumor progression [151].

Like summarized in figure 3.2, the progression from normal epithelium to the invasive carcinoma proceeds through several passages which include the loss of cell polarity, the detachment from basal membrane; the composition of this membrane changes with respect to the cell-ECM junctions. The following step concerns the input in the blood stream with the intravasation and they dissemination, the attachment in a secondary site and the formation of micro- and macrometastases. In this phase cells become again epithelial thanks to MET [159; 160].

3.2 The effectors of EMT

Among the components which are regulated during EMT there are epithelial adhesion proteins such as E-cadherin, α- and γ-catenin, about the last one, both transcriptional and transductional expression is repressed. There are three groups of transcriptional factors activated during EMT. The first one includes Snail 1 and 2, zinc finger proteins which are capable to directly regulate the E-box domain of E-cadherin promoter by metilation. Recently, it has been shown that Snail 1, in human breast cancer cells, MCF-7 and MDA-MB-231 contributes to the activation of the protein MT1-MMP (*Membrane-tethered poteases – Membrane metallo-proteases*), MT2-MMP and MMP9, on the contrary Snail 2 directly acts on MT4-MMP e MMP2 [161; 162].

The second group is formed by Zeb (*Zinc Finger E-box binding homeobox*) 1 and 2, which equally repress E-cadherin, not directly but through a negative feedback, involving also the action of miRNA200. Both groups act also in down-modulation of ZO-1 and claudin. Through trandendothelial migration assay, it has been shown that the expression of Zeb1 enhances human prostate cancer cells PC3 to leave the extracellular barrier and enter the blood stream [163; 164].

Finally, the third group is composed by the bHLH (*basic Helix-Loop-Helix*) factors as Twist 1 and 2, E12/E47; particularly Twist1 suppresses E-cadherin activating Snail but acts also alone like mediator of cell invasion [159]. Generally, Twist1 is a mediator of proteases like MT-MMPs, ADAMs, MMPs which organized in the invadopodia, subcellular structures rich of actin, assigned to the invasion process, above all if it is linked to the tumor progression. The invadopodia formation is mediated also by a autocrine loop of PDGF (*Platelet Derived Growth Factor*), just induced by Twist, on the own receptor PDGFRα [165].

3.3 Markers of EMT

A variety of biomarkers have been used to demonstrate all three subtypes of EMT. In recent years, changes in the level of expression of different cadherins, so-called cadherin switches, have been increasingly used to monitor EMT. Indeed, the cadherin switch from E-cadherin to N-cadherin, which is expressed in mesenchymal cells, fibroblasts, cancer cells, and neural tissue, has often been used to monitor the progress of EMT during embryonic development and cancer progression. In addition, because OB-cadherin is a

more definitive marker for activated fibroblasts, an E-cadherin–OB-cadherin switch is of interest for type 2 EMT associated with fibrogenesis [166; 167].

An integrin switch also reflects alterations in cell-ECM interactions, facilitating EMT. For example, in colon carcinoma, only cancer cells that have undergone type 3 EMT to a metastatic phenotype express high levels of β6 integrin, the normal epithelial and noninvasive cancer cells have low-level expression of this protein [168]. Increased expression of α5 integrin also correlates with the metastatic potential of B16F10 melanoma cells and EMT suggesting that also this integrin plays a role in each subtype of EMT [169].

Another EMT marker that reflects adaptation to the altered ECM microenvironment associated with EMT is the collagen-specific receptor tyrosine kinase DDR2 (discoidin domain receptor tyrosine kinase 2). Upon binding to type I or type X collagen, DDR2 mediates upregulation of MMP1 and cell motility [170; 171].

A controversial marker of EMT is vimentin, the protein of intermediate filaments, which is expressed in various cells, including fibroblasts, endothelial cells, cells of the hematopoietic lineages, and glial cells. However, because adult epithelial cells transiently express vimentin in response to various insults, it is not considered a marker of type 2 EMT. By contrast, vimentin is commonly used to identify cells undergoing type 3 EMT in cancers. This information is based on a positive correlation of vimentin expression with increased invasiveness and metastasis [172].

β-catenin is another component of the adherence junctions. It forms a bridge between the cytoplasmic domain of the cadherins and the actin cytoskeleton. The level of β-catenin in the cytoplasm are regulated through its recruitment to cadherin-binding partners or ubiquitination and subsequent degradation. Particularly, the interaction between β-catenin and E-cadherin are regulated by tyrosine phosphorylation in the carboxyl terminal of the first protein. These reactions destabilize the cadherin- β-catenin bond and promote loss of intracellular adhesion. Conversely, dephosphorylation of β-catenin residues increases the activity of E-cadherin and β-catenin and α-catenin reassembly. After tyrosine phosphorylation of β-catenin, its cytosolic pool is increased and may increase the transcriptional activity of the β-catenin-TCF (*T Cell Factor*) complex. So, β-catenin has been used as a marker of EMT in various studies of embryonic development, cancer, and fibrosis, in particular in cells that undergo EMT [153; 173; 174; 175].

Fibronectin is a high-molecular weight glycoprotein that serves as a scaffold for fibrillar ECM [176]. Because it is one of the first molecules to appear when the fibrillar ECM is formed, it has been used as an indicator of type 1 EMT associated with gastrulation, palate fusion, and neurulation [177].

Even though fibronectin is an integral constituent of the fibrotic ECM associated with tissue fibrosis and the desmoplastic stroma in tumors, the utility of fibronectin as a type 2 and type 3 EMT biomarker is limited, in part, because it is produced by various cell types, including fibroblasts, mononuclear cells, and epithelial cells. Both type 2 and type 3 EMT, however, are associated with increased fibronectin expression *in vitro* [178].

Of the principal basement membrane constituents (type IV collagens, laminin, nidogen, and sulfated proteoglycans) that are downregulated during EMT, laminin is best established as a biomarker of the process. Laminins are heterotrimeric glycoproteins composed of one α chain, one β chain, and one γ chain, 15 different heterotrimers are known [179]. Both type 1 and type 2 EMT are associated with downregulation of laminin1 *in vitro* and disruption and loss of laminin1 *in vivo* [180; 181]. By contrast, upregulation of laminin 5 (α3β3γ2) is associated with type 3 EMT in cancer and type 2 EMT in tissue fibrosis [182].

The main EMT markers are listed in table 3.1.

Markers of EMT			
Acquired markers		**Attenuated markers**	
Name	**EMT type**	**Name**	**EMT type**
Cell-surface proteins			
N-cadherin	1, 2	E-cadherin	1, 2, 3
OB-cadherin	3	ZO-1	1, 2, 3
$\alpha5\beta1$ integrin	1, 3		
$\alpha V\beta6$ integrin	1, 3		
Syndecan-1	1, 3		
Cytoskeletal markers			
FSP1	1, 2, 3	Cytokeratin	1, 2, 3
α-SMA	2, 3		
Vimentin	1, 2		
β-Catenin	1, 2, 3		
ECM proteins			
$\alpha1(I)$ collagen	1, 3	$\alpha1(IV)$ collagen	1, 2, 3
$\alpha1(III)$ collagen	1, 3	Laminin 1	1, 2, 3
Fibronectin	1, 2		
Laminin 5	1, 2		
Transcription factors			
Snail1 (Snail)	1, 2, 3		
Snail2 (Slug)	1, 2, 3		
ZEB1	1, 2, 3		
CBF-A/KAP-1 complex	2, 3		
Twist	1, 2, 3		
LEF-1	1, 2, 3		
Ets-1	1, 2, 3		
FOXC2	1, 2		
Goosecoid	1, 2		
MicroRNAs			
miR10b	2	Mir-200 family	2
miR-21	2, 3		

Table 3.1: The main markers for EMT [159]

3.4 The inducers of EMT

There are multiple signals from the microenvironment which act on the EMT and they can be both cell- and tissue-specific. Beyond the pathways of Wnt and Notch, important molecules in embryonic development, TGF-β participates, too. This last factor is the main member of a family of 40 pleiotropic cytokines, involved in some processes such as proliferation, apoptosis, differentiation, migration, stem-like phenotype, regulation of immune responses. Three isoforms are, by now, better characterized (TGF-β1, 2, 3) because ubiquitous. The pathways activated by the interaction of TGF-β with the receptor are mediated from the SMAD, a family composed by 8 proteins classified as R-SMAD (*Receptor-activated SMADs*), as SMAD 1, 2,

3, 5, 8; coSMAD (*common mediator SMADs*) as SMAD4 and I-SMAD (*Inhibitory SMADs*), SMAD 6, 7. Without TGF-β the SMAD are not active, instead, answering to its effect, R-SMAD form heterotrimeric complexes with SMAD4 which organize with other factors in the nucleus to regulate gene expression. Another kind of pathway down line of TGF-β is defined not canonical and utilizes other regulatory proteins like MEK/ERK, GTPasi Rho-like, p38/MAPK and PI3K/Akt, as it is outlined in figure 14 [183; 184; 185].
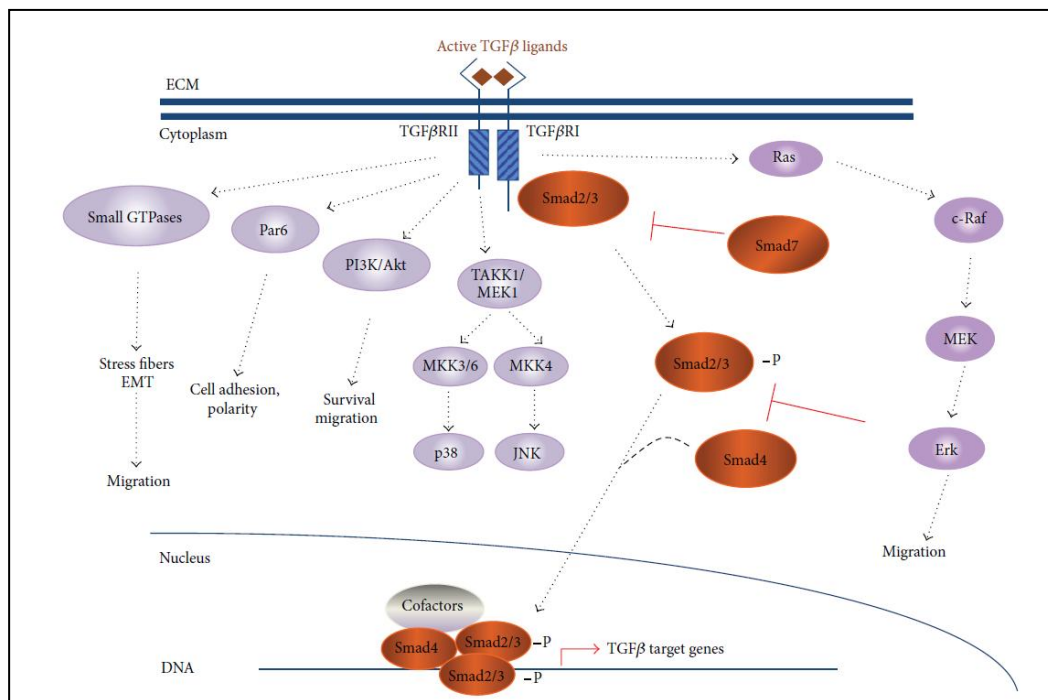
Figura 3.3: Pathways of TGF-β dependent or not from SMADs [186].

TGF-β shows antiproliferative effects on normal epithelial, endothelial, neural cells such as on the immune system, particularly the T linfocyte, in which it regulates the expression of genes that are involved in cell cycle phases G1/S. For example, TGF-β induces the expression of inhibiting molecules of the Cdk (*Cicline-dependent kinases*) as CDKN2B or CDKN1A, on the contrary, it inhibits the oncogene expression like c-Myc and ID 1, 2 and 3 (*Inhibitor of DNA binding protein*) [186]. An experimental example can be in KO (*Knock Out*) mice for Smad3 in which the rate of growth of keratinocytes is enhanced and also wound healing can repare more rapidly [187]. Furthermore, in hepatoma cells, is has been shown that TGF-β induces

apoptosis through the proteins SMAD and the DAPK (*Death Associated Protein Kinase*) [188]. Therefore, during tumor development, the pathway of TGF-β loses its function following some mutations of TGF-βR1, TGF-βR2, SMAD 2, 3 and 4, particularly in gastric, colonrectal, prostate and pancreatic cancers [189]. But when neoplatisc cells cross the check mechanisms and begin the dissemination, starting from the primary tissue, TGF-β participates as promoter of the invasion and of metastatisation. In fact, the effect of TGF-β is upstream of yet cited transcriptional factors such as Snail, Slug, Zeb1 and 2, Twist. For example, the signal of SMAD2 keeps repressed the E-cadherin, cingulin, claudin-4 and calicrein-1 expression [190; 191]. Numerous experiments allowed to create a sort of parallelism between TGF-β and hypoxic condition, which constitutes an important part of tumorigenesis and ends with the activation of HIF1α (*Hypoxia Induced Factor 1 α*) and of uPAR receptors (*uroknase Plasminogen Activator receptors*), considerable conditions in the acquisition of a mesenchymal phenotype, in fact some possible reoxygenation can conduct to MET [192]. Other important factors in EMT (and in its reversion), both inducers like intracellular signal trasnductors, chromatin regulation molecules, transcriptional factors, splicing regulators and miRNA and mediators as cell-cell or cell-ECM adhesion molecules, organizers of cytoskeleton remodeling, chemokines and cytokines and stem-like phenotype markers are classified in figure 3.4 [193].
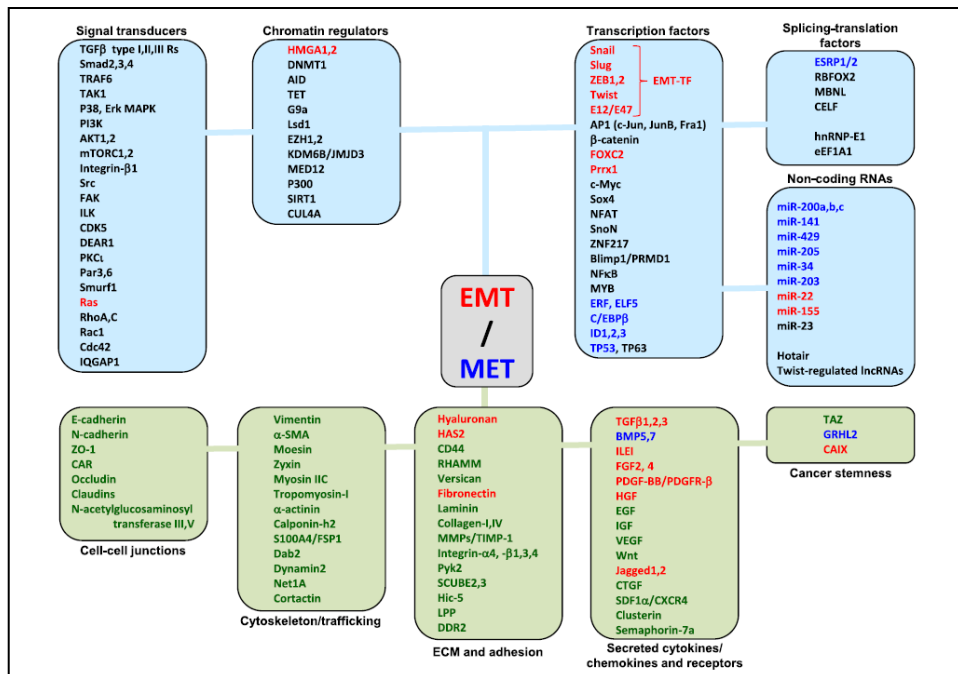
Figure 3.4: Summary representation of EMT/MET program [193].

3.5 EMT in pancreatic cancer progression

Both chronic pancreatitis and pancreatic cancer tissues demonstrate active EMT profile [194]. The EMT phenomenon in PC cell lines and surgically resected tissues has been documented, for example it was found, *in vitro*, that L3.6pl, Colo357, BxPC3, HPAC, CFPAC-1 and SU86.86 cells expressed high levels of epithelial marker E-cadherin; however, MIA PaCa-2, PANC-1, AsPC-1, Hs766T and MPanc96 cells had high level of expression of mesenchymal markers like vimentin and ZEB1. Among those cell lines, gemcitabine-resistant PC cells such MIA PaCa-2, PANC-1 and AsPC-1 showed strong expression of vimentin, and ZEB-1 suggesting that the gemcitabine-resistant cells elicits EMT phenotype which could be in part responsible for drug resistance [195; 196]. Importantly, increased expression of fibronectin, vimentin, N-cadherin and decreased expression of E-cadherin were correlated with invasion, metastasis and poor survival. These results suggest that a population of distinct PC cells, which show EMT phenotypes, exists in PC and could promote the progression and aggressiveness of PC [197; 198]. The expression of N-cadherin is another critical event in EMT; a clear mechanism linking the effect of TGFβ with the N-cadherin expression explains that, when the TGF-β pathway is activated, SMAD proteins, mainly SMAD4, subsequently translocate into nucleus, where they influence, trough the SBEs (*SMAD binding elements*), the expression of several genes, including CDH2, encoding for N-cadherin. In fact, the knockdown of SMAD4 causes a decrease N-cadherin expression with a resulting decrease of migration and invasion of human pancreatic ductal epithelial cells and a similar result is obtained after CDH2 knockdown [199]. Furthermore, in gemcitabine-resistant cells it was found a high expression of HIF1α and, more importantly, the inhibition of this factor caused partial reversal of EMT phenotype, suggesting that HIF1α was critically involved in gemcitabine-resistant-mediated EMT [200]. The analysis of EMT statuses, clinicopathologic factors and prognoses report a significant correlation between EMT status and CA19-9 levels, peritoneal washing cytology, portal vein invasion and lymph node metastasis. Multivariate analysis demonstrated that perineural invasion, lymph node metastasis and EMT status were significant prognostic factors [201].

CHAPTER 4

ANNEXIN A1

4.1 Introduction

The Annexins belong to a family of soluble and hydrophilic proteins correlated by their structure, that interact with the plasma membrane, through the anionic phospholipids, in a calcium-mediated fashion [202]. They have been discovered at the end of 70's and have been identified both in mammalian organisms and in mildews or plants. The name Annexin derives from the Latin "adnexio", meaning their main properties to bind and to keep themselves joined to plasma membranes. So two principal parameters are important to identify an annexin protein: the capability to interact with the negative membrane phospholipids though the Calcium (Ca^{2+}) and the presence of a repeated segment of 70 amino acids defined as "annexin repetition". This repetition is particularly preserved in about all annexins, instead the NH_2-terminal part is more variable. The role of these proteins appears quite important, both in cytosol and at the plasma membranes, as confirmed by their presence in 65 animal species. Annexins represents by now about 2% of all cell proteins [203; 204].

4.2 Annexin A1 structure

Annexin A1 (ANXA1) is the first characterized member of the yet described annexin family, comprising 12 other members. Its structural nucleus is constituted by four homologous segments and is surrounded by a C-term, which accommodates the sites binding Ca^{2+} cations, and an N-term. As shown in figure 4.1, the convex side is situated in front of plasma membrane, on the other hand, the concave one is accessible for the interactions with the N-term of the same protein or with other molecular partners [205].
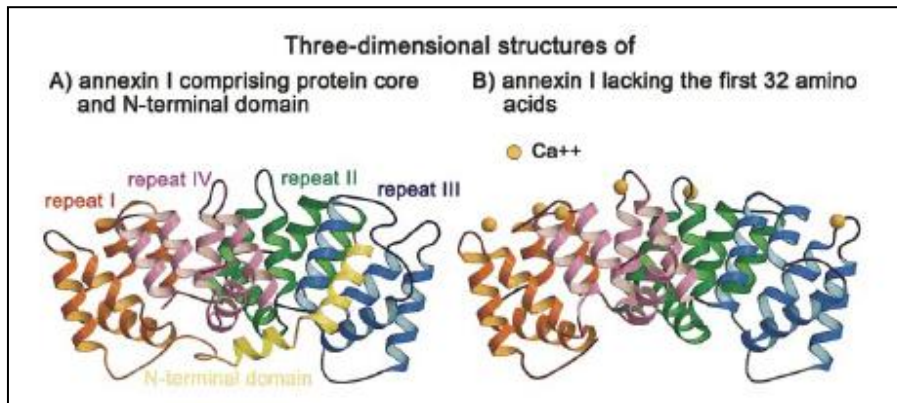
Figure 4.1: Ribbon diagrams of (a) one monomer of recombinant porcine annexin 1 comprising protein core and the N-terminal domain and (b) human annexin 1 lacking the first 32 amino acid residues. The yellow N-terminal helix in (a) is replacing the two-turn blue helix in (b). Bound calcium ions are illustrated as yellow spheres [206].

The first annexin described with its crystal structure was the Annexin A5, but the first longer annexin studied by high resolution crystallography has been just the ANXA1. This one has a N-terminal domain of 44 amino acids, of which the first 10-14 represent a site binding S100A11 (Fig. 4.2); particularly, this portion comprises phosphorylation sites for Protein Kinase C (PKC) and tyrosine-kinases, and other ones for glycosylation, acetylation and proteolysis reaction. The C-terminal domain or *core* presents, between each of its four repetitions, segments of 17 amino acids that are specific for the bind to the Ca^{2+} [207; 208; 209].
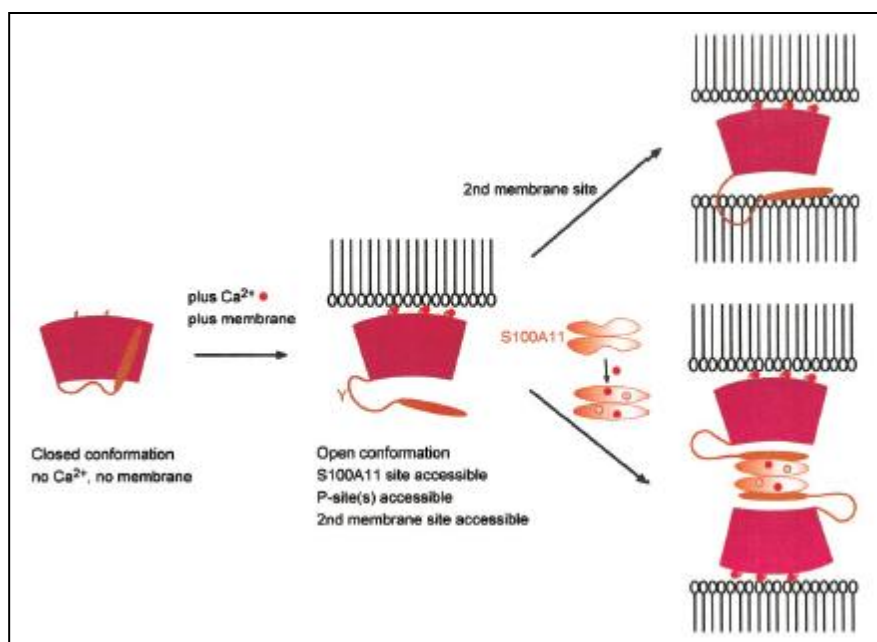
Figure 4.2: In the crystal structure of Ca^2-free ANXA1 (red), the NH_2-terminal-helix, which contains the S100A11 binding site (brown), is replacing helix D of the third repeat. Ca^2-dependent membrane binding could be accompanied by a conformational change establishing the Ca^2-bound crystal structure of the ANXA1 core and, most likely, a more accessible NH_2-terminal domain. As a result, the NH_2-terminal domain can interact with a second membrane surface or the S100A11 dimer, which itself requires Ca^2 binding to establish an interaction-competent conformation. An hypothetical ANXA1/S100A11 heterotetramer would represent an entity capable of linking membrane surfaces [210]

The gene of ANXA1 has been the first one to be cloned, it is localized on the human chromosome 9, particularly at 9q12-21.2 and codes for a protein of 38,71 kDa. The promoter is particularly preserved and presents consensus sequences for some molecules [211].

About its subcellular localization, studies using cell fractionation and immunogold labelling indicate that, ANXA1 exists in three distinct pools: (i) in the cytoplasm, (ii) embedded in membrane structures, and (iii) attached to the outer surface of the plasma membrane [212; 213].

4.3 ANXA1: an anti-inflammatory protein

Originally named as lipocortin 1, ANXA1 has been first identified as protein with anti-inflammatory functions, in fact its promoter is strongly

regulated by glucocorticoids, and in several *in vitro* and *in vivo* models mediates their effects [214; 215; 202]. It is now evident that the association between glucocorticoids and ANXA1 is more complex than initially observed. Dexamethasone and other steroids regulate the expression of ANXA1 since its promoter has a canonical Glucocorticoid Response Element (GRE). More delayed augmentation of cell surface expression of ANXA1 is consequent to gene activation. [215; 216; 202; 217]. ANXA1 was initially characterized for its ability to inhibit prostanoid release, an effect that underlined its efficacy in the rat paw oedema model [218; 219]. ANXA1 was also able to elicit an anti-pyretic response that was clearly associated with an inhibition of prostaglandin E2 production in the third ventricle [220]. ANXA1 acts on specific enzymes as phospholipase A2 (PLA_2), both through direct and indirect inhibition [221; 222]. Other inhibited enzymes are the macrophage iNOS (inducible Nitric Oxide Synthase) through the induction of Interleukin-(IL)10 expression, and COX2 [223; 224; 225]. Even if the ANXA1 gene deletion does not represent a lethal event, as confirmed in the papers of Hannon *et al* and Yang *et al*, in null mice for ANXA1 there is an over-expression of some pro-inflammatory enzymes as iNOS, COX-2 and $cPLA_2$ above all in thyme and lungs, suggesting that this inducible enzyme could be indirectly influenced by this protein [226; 227; 228; 229; 230]. ANXA1 is not so abundant within neutrophils, comprising ∼2–4% of total cellular protein, but it is the major proresolving agent, inducing both neutrophil apoptosis and their phagocytic clearance by macrophages [231; 232; 233]. Furthermore, migrated neutrophils upregulate ANXA1 gene activity, contributing to the abundant presence of this protein in exudates, as shown in rodent and human settings [234; 235]. Again mimicking the action of glucocorticoids, ANXA1 promotes inflammatory cell apoptosis associated with transient rise in intracellular calcium and caspase-3 activation [236].

Also in rats, ANXA1 can modulate lipopolysaccharide (LPS)-induced neutrophil accumulation [237]. ANXA1 induces anti-inflammatory/proresolution effects in these cells, including suppression of IL-6, IL-1β and TNF-α, production of IL-10, negatively regulating phosphorylation of p38 [238; 239; 240].

In the years, lots of studies created a substantial body of evidence that suggests that many effects of ANXA1 are exerted through a cell surface receptor mediated mechanism. A key paper by Walther *et al.* [241] implicated the formylated peptide (fMLP) receptor subtype FPR in the transduction of the ANXA1 signal in leukocytes. FPR1 is a member of a family of G-protein coupled receptors expressed in migratory cells and many other tissues, FPR2 is important in human polymorphonuclear leucocytes (PMN) and ANXA1

compete with other receptor known ligands. Endogenous ANXA1 and FPR2 co-immunoprecipitate is found in murine extravasated PMN *in vivo*. Acetyl 2–26, the N-terminal ANXA1 mimetic peptide, retains the ability to promote the detachment of adherent leucocytes in FPR1 null mice suggesting that FPR2 is a candidate receptor for this peptide [241; 242; 243]. The ANXA1/FPR2 pathway has a central role in the resolution process and in the modulation of monocyte recruitment, neutrophil extravasation and apoptosis [244; 245].

In conclusion, in cell types including peripheral blood leucocytes (PBMC), it has been shown that ANXA1-derived peptides Ac2-26 can inhibit antigen-driven cellular proliferation and cytokine production and also other effects like classified in table 4.2 [246].

Peptide Ac2-26		
	IL-1β inflamed air-pouch (mouse)	↓ Leukocyte migration
	IL-8 inflamed air-pouch (mouse)	↓ Leukocyte migration
	FMLP-induced neutropenia (mouse)	↓ Neutropenia
	Albumin extravasation in the skin (mouse)	↓ Skin oedema
	Heart ischaemia–reperfusion (rat)	↓ Infarct size by up to 50%
		↓ IL-1β and MPO levels in infarcted hearts
	Mesenteric microcirculation activated by ischaemia–reperfusion (mouse)	↓ Leukocyte adhesion and emigration but not rolling
		↓ Plasma protein extravasation
	Carrageenan paw oedema (rat)	↓ Oedema
	Carrageenan-induced arthritis (rat)	↓ The disease severity (intra-articular injection)
	Glacial acetic acid-induced gastric ulcers (mouse)	↑ Ulcer healing upon a 4 day treatment
	Contusive spinal cord injury (rat)	↓ PLA₂ and MPO activities
		↓ Glial fibrillary acidic protein (4 weeks post injury)
		↑ White matter sparing *in vivo*
	Metabolic inhibition of cardiac myocytes (rat cells)	↓ Cellular injury
	Ovalbumin-induced pleurisy (rat)	↓ Mast cell degranulation and plasma protein leakage
		↓ PMN and eosinophil accumulation
		↓ Eotaxin release in exudates
	Splanchnic artery ischaemia–reperfusion (rat)	↓ The progressive fall in blood pressure
		↓ PMN accumulation
		↓ Bowel injury
	Glycogen-induced peritonitis (mouse)	↓ PMN accumulation
	Ovalbumin-induced sensitization (mouse)	No effect on skin eosinophil recruitment
	Zymosan-induced peritonitis (mouse)	↓ PMN migration (4 h)
		↓ Monocyte migration (24 h)
	In vitro model of septic shock (rat heart)	Abrogation of the fall in the inotropic response to isoprenaline
		↓ COX-2 mRNA
		No effect NOS-2 mRNA
	Mesenteric microcirculation activated by zymosan (mouse)	↓ Leukocyte adhesion and emigration (s.c.)
		↑ Detachment of adherent leukocytes (i.v.)
	Intestinal ischaemia–reperfusion (mouse)	↓ Tissue injury
		↓ TNF-α levels
		↓ Lethality
	Neutrophil/endothelial interaction under flow (human cells)	↓ PMN adhesion
	Phagocytosis of apoptotic neutrophils (human cells)	↑ Clearing by macrophages

Table 4.1: List of experimental systems where the anti-inflammatory actions of ANXA1 fragments have been analyzed [245].

4.4 ANXA1 post-translational modifications

Lots of ANXA1 functions depends on its post-translational modifications, its activity is regulated by many chemical modifications including covalent ones. Summarizing the results and recent literature, it can be concluded that ANXA1 is phosphorylated by several kinases. This phosphorylation is not Ca^{2+}-dependent but the phosphorylated ANXA1 binds the phospholipids in a Ca^{2+}-dependent manner: the conformation of ANXA1 changes by Ca^{2+} binding followed by the release of the N-terminal domain [247]. It was shown by Futter *et al.* that ANXA1 is a substrate of EGF-R kinase in multivesicular bodies (MVBs), important for stimulated EGF-R internalization. The ANXA1 phosphorylation has been suggested being responsible for the MVBs inward vesiculation induced by EGF-R activation, furthermore, ANXA1 phosphorylation is linked with EGF-R internalization suggesting that the endosomal EGF-R kinase may be involved in the protein phosphorylation [248; 249]. Even if the phosphorylated ANXA1 residue in this study is not shown, EGF-R has as the main target the residue Tyr21. Then, Varticovski *et al.* showed that Tyr21 and Ser27 of ANXA1 are phosphorylated by protein tyrosine kinases and protein kinases A/C (PKA/C), respectively [250]. It was also reported that phosphorylation of Tyr21 in ANXA1 inhibits its ability to aggregate chromaffin granules [251; 252]. As shown in figure 4.3, Schlaepfer and Haigler have reported that from the Tyr24 to Ser45, these residues are phosphorylated by PKC [253].
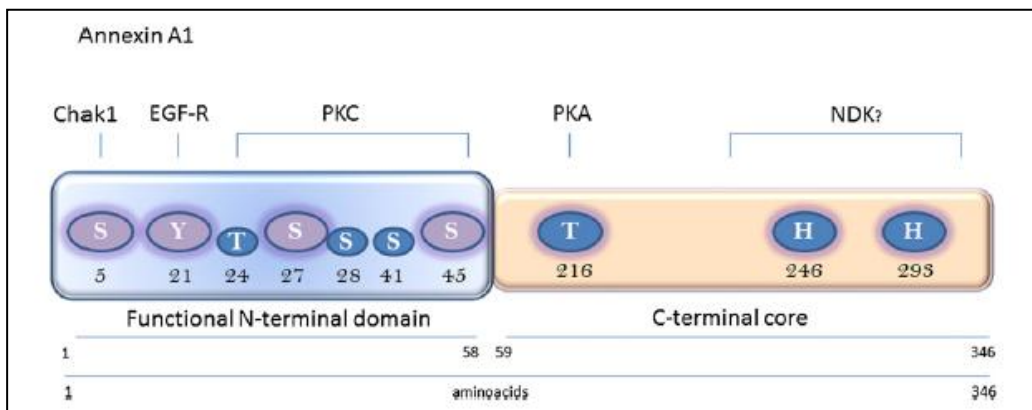
Figure 4.3: Schematic representation of the target residues and principal kinases involved in ANXA1 phosphorylation. S, T, H and Y are respectively Serine, Threonine, Histidine and Tyrosine [247].

Although PKC and annexins have some features in common, such as binding of calcium and phospholipids and association with cytoskeletal elements, there are no structural similarities between them. The PKC-dependent sites are located in a consensus sequence motif (Ser/Thr-Val-Arg/Lys), interestingly, other annexins, such as ANXAIII, VII, VIII and X, which possess the putative PKC substrate motif are also potential substrates for PKC [254]. Supporting this aspect, it has been constructed a plasmid with mutations on three single nucleotides like $A^{11}R$, $V^{22}K$ and $V^{36}K$ that cannot undergo to phosphorylation and then proteolitic cleavage probably by the serin-proteases, proteinases 3, like shown in PMN [255].

Following the analysis of the most important ANXA1 points of modification, is has been shown that Ser27 phosphorylation induces a conformational change, which is probably related to the described membrane aggregation property [256]. The phosphorylation of ANXA1 on Ser27 is crucial for migration to cell surface and maybe to protein externalization; glucocorticoids induce rapid serine phosphorylation and membrane translocation of ANXA1 via a novel glucocorticoid receptor (GR)-dependent mechanism, which requires MAPK, PI3K and Ca^{2+}-dependent PKC pathway and it is now clear that the phosphorylation of Ser27 residue and protein migration to the cell membrane are implicated in hormones release. Finally, the serine phosphorylation is essential not only for the protein migration but also for the involvement of isoprenyl lipids [257; 258; 259; 260].

Not only phosphorylations appear important for ANXA1 functions; SUMOylation may interfere with the inward vesiculation process of MVBs and thus late events in EGFR trafficking [261]. A structural analysis of ANXA1 revealed that Lys257 is located in a hot spot where Ca^{2+} and Small Ubiquitin-related MOdifier-1 (SUMO-1) bind and where a nuclear export signal and a polyubiquitination site are also present. Also, Tyr21 is buried inside an α-helix structure in the Ca^{2+}-free conformation implying that Ca^{2+} binding and the subsequent expelling of the N-terminal α-helix in a disordered conformation, is permissive for its phosphorylation. So SUMOylation can be regulated by an external signal (EGF) and can indicate the presence of a cross-talk between the N-terminal and C-terminal domains of ANXA1 through post-translational modifications [262].

Generally, phosphorylation, much more than other kinds of modifications, induced the N-terminal peptide cleavage by a number of proteases, including elastase, calpain, plasmin, cathepsin D and proteinase 3 [264; 265; 266; 267]. The N-terminal truncated ANXA1 is known to be capable to mediate lots of protein functions such as proinflammatory effects and promotion of neutrophil transendothelial migration [268]. In their work,

Rescher *et al*, hypothesize that the neutrophils produce elastase to create a compensatory mechanism between the inflammatory reaction and the anti-inflammatory effects of ANXA1 [265].

4.5 ANXA1 in cancer

ANXA1 performs multiple functions in tumors. Lots of experimental data about characterization of ANXA1 expression and localization show that the role of this protein can change according to the different cancer models [269].

4.5.1 ANXA1 in prostate cancer

In human prostate adenocarcinoma, particularly in androgen-stimulated prostate cancer, ANXA1 is decreased if compared to benign prostate epithelium; the loss of protein expression is an useful indicator for cancer proliferation and progression and a potential parameter to evaluate the anticancer drug resistance. ANXA1 negatively mediates IL-6 expression and play a proapoptotic role by mediating p38 and JNK [270; 271; 272; 273; 274; 275]. *In vitro*, ANXA1 expression reduced tumourigenicity and cell viability in prostate cancer cell lines by enhancing activation of pro-apoptotic signaling pathways [276]. The inverse expression of CK18 and ANXA1 has been well characterized also in prostate cancer cells: luminal cells, with epithelial phenotype present poor level of ANXA1, instead the basal cells (expressing CK5) has high level of this protein. Furthermore it has been reported that ANXA1 from prostate-derived cancer-associated fibroblasts (CAF) is capable of inducing EMT, promoting *de novo* generation of cancer stem cells (CSCs) and stimulating the CSC population from prostate cancer cells [277]. Another important event during the EMT and prostate tumor progression is the break in the dynamic dialog between ANXA1 and cytokeratin 18 (CK18), a cytoskeleton protein, considered as one the most important epithelial markers. In normal breast tissue but also in benign lesion or breast carcinoma, the difference in the expression between ANXA1 and CK18 is not significant. During the EMT, in luminal cells becoming mesenchymal ones, CK18 is lost, on the other hand, ANXA1 expression increases, in this way, ANXA1 cannot co-localize with CK18/CK8, a protein complex involved in the cytoskeleton organization. A very similar situation appears in the prostate cancer where the ANXA1 has been studied in the acquisition of a more aggressive phenotype: the more invasive prostate cancer cells show not only

EMT but also CSCs markers and express an increased level of ANXA1. When the ANXA1 expression decreases, the invasive and migratory capability of these cells falls down together with all the detected markers for EMT and CSCs (like NANOG, Oct-4, ALDH7A1, CD44 and CD133 as well as Snail and Sox2), beyond to other genes involved in the acquisition of chemoresistance as ABCG2 [278].

4.5.2 ANXA1 in colon rectal cancer

In colon rectal cancer (CRC) ANXA1 promotes progression, invasion and metastasis, as demonstrated by *in vitro* and *in vivo* systems and positively correlates with *K-ras* gene mutations in tumorigenesis. The protein stimulates CRC cell migration through activating the FPR [279; 280; 281; 282; 283].

4.5.3 ANXA1 in lung cancer

ANXA1 is up-regulated in A549-LAC and H446-SCLC lung cancer cells and patients' tissues; ANXA1 is associated with progression, metastasis, drug resistance and differentiation of this cancer [284; 285; 286]. In a study about lung cancer, the authors reported that the expression of ANXA1, A2 and A3 closely related to cisplatin resistance and an up-regulation in cisplatin resistant patients' tissues appears both in mRNA and protein levels [287].

4.5.4 ANXA1 in melanoma

A very well characterized model in which ANXA1 has been studied is melanoma. The protein is up-regulated in metastatic B16 mouse cells and subsequent syngeneic primary tumors when compared with non-metastatic B16F10 cells. ANXA1 promotes the invasion and metastasis of melanoma through its interaction with the FPRs [288; 289; 290].

4.5.5 ANXA1 in breast cancer

In breast cancer (BC), ANXA1 can play a paradoxical role. The protein is down-modulated in estrogen-resistant cells, compared with the non-malignant ones. ANXA1 might act as a stress protein protecting cells from heat- and estrogen-induced growth arrest, DNA damage and proliferation in MCF-7 cells, possibly through enhanced ERK activation and inhibited JNK activation [291; 292]. ANXA1 knockdown by siRNA attenuates proliferations of MCF-7 and MDA-MB-231, suggesting a mitogen function through FPR

activation [293; 294]. It is reported that ANXA1 may act as an EMT/metastasis suppressor for BC: RNAi-mediated ANXA1 knockdown induced EMT and metastasis in nonmetastatic cells. Strikingly, restored Anxa1 expression reversed EMT and abolished the metastasis of BC [295]. Therefore, ANXA1 negatively regulates the proliferation of breast epithelial cells and contributes to maintaining normal breast biology. Furthermore, ANXA1 expression is associated with a highly invasive basal-like BC subtype. Its knockdown in invasive basal-like BC cells reduces the number of spontaneous lung metastasis, whereas its re-expression enhanced the cell's metastatic capacity. ANXA1 promotes the metastasis by enhancing TGF-β/Smad signaling and actin reorganization, which facilitates an EMT-like switch, thereby allowing efficient cell migration and invasion of metastatic BC cells [296]. ANXA1 could be utilized as an additional marker to better discriminate basal-like BC from other subtypes, with an inverse correlation with cytocheratin 18, marker of luminal cell, in fact ANXA1 appears much more in mioepithelial cells compared with epithelial ones [297; 298]. ANXA1 knockdown inhibits the migration and invasion of MDA-MB-231. Consequently, ANXA1 down-regulation decreases MMP-9 mRNA and protein levels, as well as its activity, which further suppresses the activity of NF-kB [299]. All these information suggest that ANXA1 can perform a double role in BC development, functioning as oncogene and oncosuppressor. In addition, ANXA1 -/- mice showed a particular reduction of the known EMT markers like vimentin, as well as myosin light-chain kinase which has been reported to induce Rho-kinase mediated assembly to stress fibers known to be implicated in the EMT [300].

4.5.6 ANXA1 in pancreatic cancer

ANXA1 is over-expressed in PDAC tissues and up-regulated 1.7-fold in TS-1-resistant cells; ANXA1 correlates with poor differentiation, prognosis and drug resistance of PC [301; 302; 303].

4.6 ANXA1 externalization

Secreted eukaryotic proteins use an N-terminal signal peptide to direct their co-translation on Endoplasmic Reticulum (ER)-bound ribosomes into the ER lumen, after which they progress to the Golgi apparatus and are ultimately exported through secretory vesicles to the cell surface or to the extracellular environment [304]. ANXA1 sequence analysis revealed the lack of an N-terminal signal peptide, required for classical externalization of the protein,

suggesting that ANXA1 could be externalized through non-classical secretory pathways [305]. Furthermore, it has been often observed that following its externalization, ANXA1 undergoes a proteolytic cleavage on its N-terminal end [306; 265; 292]. Different studies aimed to characterize ANXA1 externalization process and it appears that the protein could be externalized through five mechanisms.

- ANXA1 externalization depends on a myristoylation process, since sequence of ANXA1 includes potential sites for this modification and the PKC targets its myristoylated substrate to the plasma membrane. ANXA1 lipidation could be a prerequisite step for membrane targeting and a process facilitatin the protein passage across the plasma membrane [307].
- The ATP-Binding Cassette (ABC)-A1 is a transporter involved in ANXA1 secretion even if the authors found that its inhibition does not completely abrogate ANXA1 externalization, suggesting that other non-classical mechanisms might contribute to protein release [308].
- In PMNs, upon adhesion to endothelial cells, granules translocate and fuse with the plasma membrane, during a process called degranulation, leading to release of ANXA1 in the extracellular compartment [309].
- Following the activation of flippases and scramblases, the bud-lipid bilayer becomes inside-out orientated with phosphatidylserine being exposed to the outside. Since ANXA1 has a great affinity for acidic phospholipids, the hypothesis of microparticles surface associated ANXA1 is addressed [310].
- After the fusion process of exosomes, small endosome-derived vesicles, ranging in size from 40 to 100 nm in diameter, with the bilayer membrane, all the proteins associated with them could be externalized; among them it has been recognized ANXA1 [311].

CHAPTER 5

Formyl Peptide Receptors

5.1 Introduction

Studies conducted throughout the 1980s led to the identification of the Formyl Peptide Receptors (FPR) as a little class of trans-membrane seven domains receptors, coupled to G protein (GPCR) (Fig. 5.1); they are known to be important in several mechanisms for immune defense and discovered for the first time in mammalian leucocytes [312].

The FPR gene family has a complex evolutionary history. The principal ligands for FPRs are bacterial and mitochondrial formylated peptides, actively secreted by invading pathogens or passively released from dead and dying host cells after tissue injury. The binding of the N-formyl methionine motifs of bacterial and mitochondrial-derived peptides to FPRs was initially described over 3 decades ago and was the starting point for the subsequent dissection of the many G-protein signaling within neutrophils. All major neutrophil functions stimulated by fMLP (fMet-Leu-Phe) can be inhibited by treatment of the cells with pertussis toxin [313].

Using low-stringency hybridization with FPR cDNA as the probe, two separate but relatively conserved low-affinity receptors, initially termed FPR-like 1 (FPRL1) and FPR-like 2 (FPRL2), were cloned from an mRNA of neutrophil-like promyelocytic HL-60 cells. These receptors have been renamed FPR2/ALX and FPR3, respectively, as more has become known about their distinct biochemical and physiological roles. All three receptors are clustered together on chromosome 19q13.3 and share significant sequence homology. FPR1 has 69% amino acid identity with FPR2 and 56% with FPR3, whereas FPR2 and FPR3 share 83% identity. Despite the relatively high level of sequence homology, FPR2/ALX is a low-affinity receptor for fMLF, with a Kd of 430 nM [314; 315]. Subsequent studies demonstrated that the recombinant FPR1 is able to mediate fMLF-induced actin polymerization and chemotaxis in transfected HL-60 cells [316].
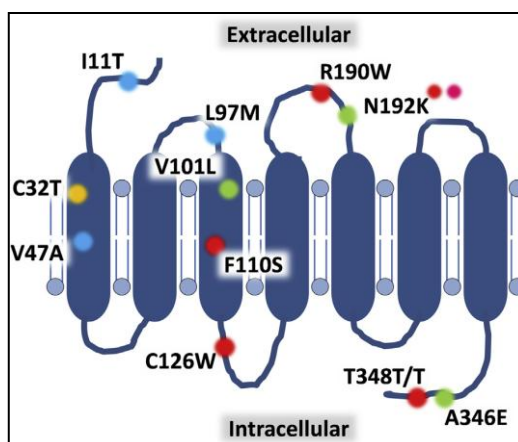
Figure 5.1: Structure of the FPR1 receptor and key polymorphisms within the protein. (green), polymorphisms associated with disease states including juvenile and aggressive periodontitis (red), hypertension in young adults (orange), gastric cancer (pink; denotes D192K) and those that have been observed but whose functional significance remains uncertain (blue) [317].

Unlike FPR1 and FPR2/ALX, FPR3 transcripts are not found in neutrophils. Instead, it can be detected together with transcripts for FPR1 and FPR2/ALX in monocytes, although the expression pattern changes with monocyte differentiation. In particular, in the process of monocyte differentiation into immature dendritic cells (DC), the cellular expression of FPR2/ALX progressively declines, whereas FPR2/ALX expression remains unchanged during monocyte differentiation into macrophages. There is a progressive loss of FPR1 during differentiation of immature DC to mature DC, such that FPR3 becomes the predominant human FPR in mature DC. The biological significance of differential expression of FPRs in monocytes, macrophages, and DCs has not yet been clearly delineated [318; 319].

5.2 FPR mechanism of action

5.2.1 FPR1

As shown in figure 5.2, after binding of ligand to FPR1, conversion of guanosine diphosphate (GDP) to guanosine triphosphate (GTP) induces dissociation of the α from the βγ subunits, activating phospholipase C β (PLCβ). Hydrolysis of phosphatidylinositol 4,5-bisphosphate (PIP2) by PLCβ generates inositol 1,4,5-trisphosphate (IP3), which releases calcium from

endoplasmic reticulum stores activating calmodulin (CaM)/calcineurin pathway, and DAG, which activates PKC isoforms. PKC is also able to induce NF-kB translocation to the nucleus. The G protein βγ subunit recruits phosphoinositide-3 kinase (PI3K) to the plasma membrane, thereby enhancing the activity of Src-like tyrosine kinases, which phosphorylate docking proteins such as the Shc adaptor proteins. A functional association between Shc, Grb2 and Sos follows, leading to the activation of the Ras-Raf-MEK-ERK pathway and therefore transcriptional regulation. ERK1/2 play also a role in FPR-mediated oxidant production: these kinases are known to catalyze the phosphorylation of p47phox prompting membrane translocation of cytosolic factors. Assembly of a membrane complex of NADPH oxidase is key to its conversion of molecular oxygen to superoxide. The stimulation of FPR receptors leads also to the activation of low molecular weight G proteins of the Rho family (Rho, Rac and Cdc42 -Cell division control protein 42-), via the activation of guanine-nucleotide exchange factors (GEFs) such as Vav1 or pRex1. The Rho GTPases are key regulators of many functions, including cell adhesion, chemotaxis and superoxide generation. Rac and Cdc42 are involved in the remodeling of the actin cytoskeleton at the leading edge of migrating cells. The activation of Cdc42 is thought to release the auto-inhibited conformation of the Wiskott–Aldrich syndrome protein (WASP), a multi-domain protein that is an activator of the nucleating Arp2/3 complex. Concluding, the activation of FPR triggers a range of intracellular kinase pathways, resulting in the induction of a variety of cell functions, including neutrophil chemotaxis, degranulation, superoxide anion production and activity; the predominant signaling pathways are those of PI3K, mitogen-activated protein kinase (MAPK) and PLC [320; 321].
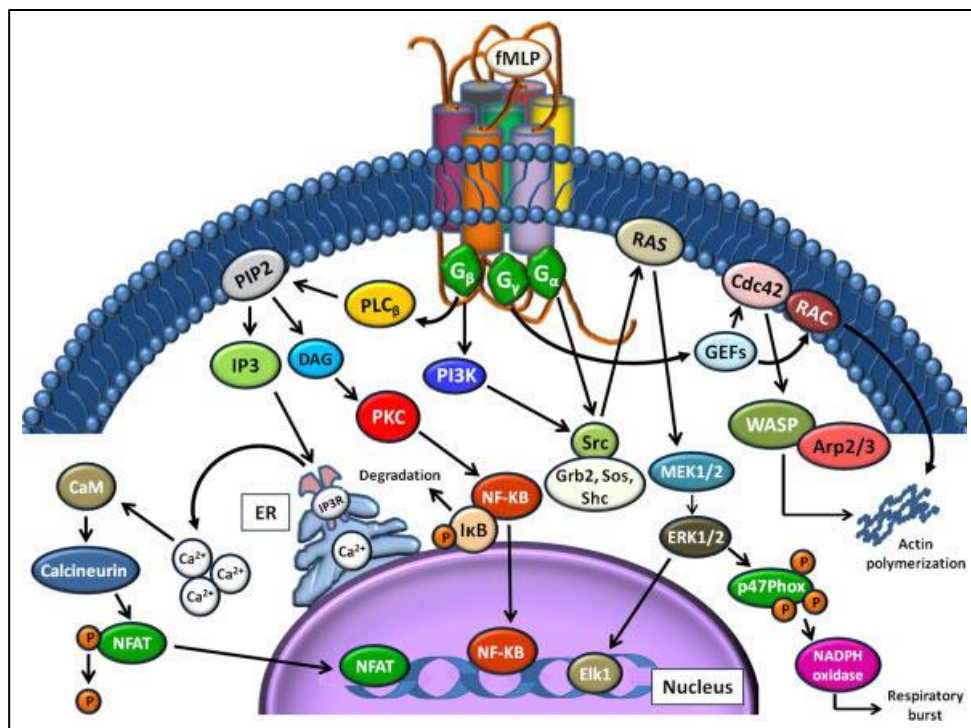
Figure 5.2: Schematic signalling pathways of an activated FPR [320].

5.2.2 FPR2

Binding of serum amyloid A or the cathelicidin-associated antimicrobial peptide leucine-leucine-37 (LL37) to FPR2/ALX results in proinflammatory responses with neutrophil NF-kB activation and cytokine release, increased neutrophil recruitment to sites of inflammation and increased neutrophil lifespan. In contrast, binding of ANXA1 inhibits neutrophil migration, promotes neutrophil apoptosis, increases the rate of macrophage phagocytosis of apoptotic cells and skews the macrophages toward a less proinflammatory phenotype. These effects elicited from ligand binding to the same receptor have recently been attributed to different dimerization states after agonist binding that alter receptor conformation and subsequent intracellular signaling [322; 323; 324].

5.2.3 FPR3

Distinct from the other members of the FPR family, the function of FPR3 remains relatively poorly understood. While not expressed on human

neutrophils, it is found in eosinophils, monocytes, macrophages, and DCs, leading to speculation that it may play a role in the pathogenesis of allergic disease. FPR3 is relatively insensitive to formylated peptides and few specific endogenous ligands have been identified. F2L, an endogenous 21 amino acid acetylated amino-terminal peptide, is the most specific ligand described to date [325; 326]. Derived from cleavage of heme binding protein 1 by cathepsin D, F2L activates FPR3 in low nanomolar concentrations. In doing so, it induces monocyte intracellular calcium flux, ERK1/2 phosphorylation and chemotaxis while also augmenting LPS-mediated IL-12 production in DCs, thereby inhibiting their maturation. Humanin, a neuroprotective peptide, also binds with high affinity to both FPR2 and FPR3 [327; 321]. Despite the high sequence homology with FPR2/ALX, the behavior of FPR3 is surprising, with significantly higher basal levels of receptor phosphorylation and internalization and relative insensitivity to common FPR2/ALX ligands. This observation has led to the hypothesis that it may also act as a decoy receptor to bind extracellular ligands, thereby regulating the function of other formylated peptide receptors. Although there is likely to be some functional overlap with FPR2/ALX, the true functional role of FPR3 and its relevance *in vivo* remain to be determined [328].

5.3 Ligands of FPR family

5.3.1 Agonists

With the exception of the eicosanoid LXA4, all the ligands of FPRs are peptides and, recently, it has been possible to add to the list of formyl peptides, also the low molecular weight synthetic compounds which derive from proteins libraries. The yet cited fMLP acts with its own amino acidic residues in different three receptor tasks, the formyl group and the carbonyl one of the phenylalanine are important for the bind between two molecules [313].

Beyond the N-formylpeptides, a large number of endogen peptides, also not formylated ones, has been identified as agonists, above all for the FPR2/ALX. Serum amyloid A (SAA) protein is an acute-phase protein the serum concentration of which is increased in response to trauma, acute infection and other environmental stress causing acute-phase responses; it has been the first endogen agonist identified in the mammalian organisms. Interacting with FPR2/ALX, it functions as chemotactic factor for monocytes, neutrophils, mast cells and T lymphocytes; stimulates production of

metalloproteases and cytokines and increases expression of cytokine receptors [329; 330].

The 42-amino acid form of β amyloid peptide which is a cleavage product of the amyloid precursor protein in the brain and a pathologic protein in Alzheimer's disease ($A\beta_{42}$), was also found to activate FPR2/ALX. It provokes migration and activation of monocytes and microglia, as shown by the increased flux of Ca^{2+} which enhances its own endocytosis [331; 332].

A cecropin-like peptide from *Helicobacter pylori*, Hp(2–20), was found to attract monocytes and basophils to the gastric mucosa in response to bacterial infection. Hp(2–20) was identified as an agonist at FPR2/ALX and FPR3. Despite the absence of an *N*-formyl group in this case, Hp(2–20) is a full agonist capable of stimulating superoxide production [333; 334].

In addition to HIV-1 proteins, other viral proteins contain sequences that can serve as ligands for FPRs when tested in the form of synthetic peptides. In Herpes simplex virus type 2, a gG-2p20 peptide corresponding to amino acids 190 to 205 of the secreted glycoprotein sgG-2 activates neutrophils and monocytes via FPR1. The gG-2p20–induced activation of phagocytes releases ROS that inhibits NK cell cytotoxicity and accelerates apoptotic cell death [335; 336].

LL-37, an enzymatic cleavage fragment of the neutrophil granule protein cathelicidin and its mouse homolog CRAMP are agonists for FPR2/ALX. LL-37 is expressed by leukocytes and epithelial cells and secreted into wounds and onto the airway surface. In addition to its microbicidal activity, LL-37 induces directional migration of human monocytes, neutrophils and T lymphocytes, a function mediated by FPR2/ALX. Other studies showed that LL-37-induced angiogenesis is mediated by FPR2/ALX in vascular endothelial cells. Decreased vascularization during wound repair observed in mice deficient for CRAMP indicates that cathelicidin-mediated angiogenesis is important for cutaneous wound neovascularization *in vivo*. LL-37 seems to be a multifunctional peptide with a central role in innate immunity against bacterial infection and in the induction of arteriogenesis important for angiogenesis [337; 338].

In 2005, it has been identified F2L as agonist of FPR3. It is a peptide with the acetylated N-terminal portion, deriving from a natural protein cleavage capable to bind the eme group. This molecule enhances the migration of immature DCs and monocytes also at low concentrations [339].

LXA4 (5*S*,6*R*,15*S*-trihydroxy-7,9,13-*trans*-11-eicosatetraenoic acid) is a potent mediator biosynthesized from arachidonic acid. It is a small molecule with physical chemical properties that displays multilevel control of processes relevant in acute inflammation via specific and selective actions on multiple

cell types via specific receptors. In particular, LXA4 has been reported to interact directly with both human FPR2/ALX and CysLT1 (Cysteinyl leukotriene receptor 1). It also induces signals that regulate production of chemokines, cytokines (for example TNF) and growth factor receptors (as VEGFR) in human leukocytes, vascular cell types and mucosal epithelial cells, each contributing to regulate the resolution of inflammation [340; 341].

As previously described, ANXA1 is an important agonist of FPRs, particularly it has been a major affinity of the ANXA1 full length on FPR1 and of its N-terminal peptide Ac2-26 on FPR2. Besides all the reported information about the anti-inflammatory effects of ANXA1 on FPRs, focusing for example on the capability of ANXA1 to promote intestinal epithelial migration through activation of FPR1-, Rac1- and NOX1-dependent redox signaling, it has been investigated also the importance of Ac2-26 and FPR2 in atherogenesis and identified a prominent protective effect [342; 343; 344]. Furthermore ANXA1 can promote skeletal muscle cell and skin fibroblasts migration by acting through FPRs [345; 346]. Recently, several studies have been published about the role of the interaction of ANXA1 and FPRs in cancer [347; 294; 283]
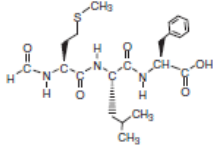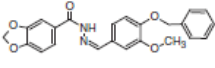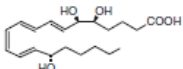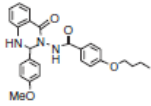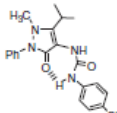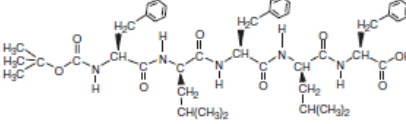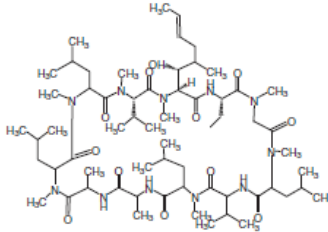
5.3.2 Antagonists

Biochemical studies reported that replacing the formyl group of fMLP with tertiary butyloxycarbonyl group (*t*-Boc) it is possible to obtain an antagonist effect; the most used compounds are Boc1 (*t*-Boc-Met-Leu-Phe) and Boc2 (*t*-Boc-Met-D-Leu-D-Phe). If it is utilized at high concentration (100μM), Boc2 inhibits FPR2/ALX, instead at lower concentration (nM), both Boc1 and Boc2 act as antagonists of FPR1, finally, at a quantity that is higher than micromolar Boc2 blocks both FPR2/ALX and FPR1. Moreover, Boc2 is less selective at elevated quantity, differently from WRW-WWW (Trp-Arg-Trp-Trp-Trp-Trp-CONH$_2$) which inhibits selectively FPR2/ALX also at high doses. This peptide inhibits the augmentation of intracellular Ca^{2+} and the consecutive neutrophil migration and ROS formation induced by Aβ$_{42}$ [348; 349].

Cyclosporin H (CsH) is a cyclic undecapeptide produced by fungi with an effect of selective inverse agonist on FPR1, with a greater power than Boc1 and Boc2. It has not immunogenic activities, in fact, its capability to inhibit the neutrophil activation and the O_2^- formation, induced by fMLP, and the chemotactic effect on leucocytes is due exclusively to its interaction with FPR1 [350].

Some agonist and antagonist compounds and their structure are summarized in table 5.1.

FPR1-selective agonists	fMLF (M.W. 437.55)	AG-14 (M.W. 404.42)	
FPR2/ALX-selective agonists	Lipoxin A4 (M.W. 352.47)	Quin-C1 (M.W. 445.51)	Compound 43 (M.W. 384.86)
Antagonists	t-Boc –FLFLF (M.W. 785.51)	Cyclosporin H (M.W. 1202.61)	

Table 5.1: Chemical structure of selected ligands for the FPRs [313].

5.4 Regulation of FPRs

After a prolonged stimulation by fMLP, the cell response is reduced and cells begin to appear resistant to administration of other agonists. This phenomenon could be explicated through the homologous or heterologous desensitization. In the first case, the GPCR FPR is phosphorylated in its Ser and/or Thr residues by a G protein coupled kinase (GRK); the phosphorylation sites become as recognition and binding ones for the β-arrestin with which the receptor, probably, is internalized. In the second case, instead, it is hypothesized that the interaction with the ligand triggers some pathways which request the intervention of kinases as PKC or PKA [351; 313].

5.5 FPRs in cancer

Besides their involvement in inflammatory disorders, FPRs have been implicated in the regulation of tissue repair and angiogenesis; the evidence for their central role at the intersection between inflammation, physiologic angiogenesis and pathologic neovascularisation links the receptors to cancer [352]. On one hand FPRs participate in intestinal, lung and retinal pigment epithelial cell restitution but, on the other hand, the role in cancer seems to be context-specific [353; 354; 355]. Recently, FPR1 has been shown to be expressed by highly malignant glioblastoma cells. Upon activation by ANXA1, released by necrotic glioma cells, FPR1 transactivates EGFR and consequently promotes glioma cell chemotaxis, invasion, growth and production of angiogenic factors. Depletion of FPR1 markedly reduced the malignancy of glioma cells both *in vitro* and *in vivo* [356; 357; 358]. By contrast, in a mouse colon carcinogenesis model, FPR2 knockout in epithelial, but not in immune cells, markedly increased tumor formation and a positive association between a specific FPR1 polymorphism and gastric cancer has recently been described, particularly the stimulation of FPR1, FPR2 and FPR3 induces the EMT, cell proliferation, survival and invasiveness of gastric cancer cells [359; 360; 361; 362].

PC has a poor prognosis, even if diagnosed early. It typically spreads rapidly and its detection appears very difficult in early stages; signs and symptoms may not appear until PC is quite advanced and complete surgical removal is not sufficient. These reasons are the major ones why PC is a leading cause of cancer death.

Beyond the anti-inflammatory function, ANXA1 may also play a tumor suppressor or enhancer role depending on the type of tissue and organ. During PC progression, ANXA1 is found over-expressed as shown by immunohistochemical analysis or multi tissue array studies, both of them carried out on patients' biopsies. The increase of its expression correlates with the most advanced stages of tumor, nevertheless a specific role for ANXA1 in this cancer has not been yet defined. Therefore, this work presents as principal aim the investigation of the role of ANXA1 in human PC. The *in vitro* initial approach, based on the use of immortalized cell lines, allowed to focus the attention on several aspects of tumor development, such as migration and invasion.

CHAPTER 6

MATERIAL AND METHODS

6.1 Cell Cultures

MIA PaCa-2, human PC cells, were cultured in DMEM (Lonza) containing L-Glutamine 2 mM, 10% heat-inactivated fetal bovine serum (FBS; Lonza) and 2,5% heat inactivated horse serum (HS; Lonza). PANC-1, human pancreatic epithelioid carcinoma cells, were kept in DMEM containing L-Glutamine 2 mM and 10% heat-inactivated fetal bovine serum (FBS; Lonza). BxPC-3, human pancreatic adenocarcinoma cells, were cultured in RPMI 1640 (Lonza) containing 10% heat-inactivated fetal bovine serum (FBS; Lonza). CAPAN-2, human PDAC cells, were kept in McCoy's 5a Medium Modified (Lonza) with 10% heat-inactivated fetal bovine serum (FBS; Lonza). All the media were supplemented with antibiotics (10000 U/ml penicillin and 10 mg/ml streptomycin; Lonza). Cell lines were purchased from ATCC (Rockville, USA) and were stained at 37°C in 5% CO_2 -95% air humidified atmosphere.

6.2 Cytosol and membrane extracts

MIA PaCa-2 and PANC-1 cells were washed twice with PBS, detached with trypsin-EDTA 1x in PBS (Euroclone), harvested in PBS and centrifuged for 5 minutes at 600 x g at 4°C. After that, the pellets were resuspended in 4 ml of lysis buffer (Tris HCl 20 mM, pH 7,4; sucrose 250 mM; DTT 1 mM; protease inhibitors, EDTA 1 mM in water), sonicated (5 seconds pulse - 9 seconds pause for 2 minutes, amplitude 42%) and then centrifuged at 4°C for 10 minutes, at 5000 x g. The obtained supernatants were ultra-centrifuged for 1 hour at 100000 x g at 4°C, until to get new supernatants that represent cytosol extracts. Each resulting pellet was resuspended in 4 ml of lysis buffer and ultra-centrifuged for 1 hour at 100000 x g at 4°C. The pellets were then resuspended in 250 µl of solubilization buffer (Tris HCl 20 mM, pH 7,4; DTT 1 mM; EDTA 1 mM; Triton X-100 1%, in water) and left overnight on orbital shaker at 4°C. After that, the solution was centrifuged for 30 minutes at 50000 x g at 4°C: the supernatants represent membrane extracts. To detect membrane expression of ANXA1 we also use an EDTA Wash method: cells, kept on ice, were washed twice with PBS and then with a buffer 5 mM EDTA and protease inhibitors for 10 minutes.

6.3 Nuclear extracts

MIA PaCa-2 and PANC-1 cells were washed twice with PBS, detached with trypsin-EDTA 1x in PBS (Euroclone), harvested in PBS and centrifuged for 5 minutes at 600 x g at 4°C. The pellets were resuspended in 500 µl of buffer A (Hepes pH 7.9 10 mM, EDTA pH 8.0 1 mM, KCl 60 mM, N-P40 0.2%, DTT 1 mM, PMSF 1 mM, protease inhibitors) and then left on ice for 10 minutes. After that, the samples were centrifuged at 660 x g for 5 minutes at 4°C, resuspended in 50 µl of buffer B (Tris HCl pH 7.8 250 mM, KCl 60 mM, DTT 1 mM, PMSF 2 mM, glycerol 20% v/v in PBS) and centrifuged again at 9500 x g for 15 minutes at 4°C. The obtained pellets were resuspended in 100 µl of buffer C (Hepes pH 7.9 10 mM, EDTA pH 8.0 1 mM, KCl 60 mM, DTT 1 mM, PMSF 1 mM, protease inhibitors) and centrifuged at 660 x g for 5 minutes at 4°C. The samples were then washed twice with 1 ml of buffer C, resuspended in 50 µl of buffer B and exposed to 3 cycles of freeze/thawing. Finally, the samples were centrifuged at 9500 x g for 15 minutes at 4°C: the pellets represent the nuclear extracts.

6.4 Supernatant analysis

Cell growth media were harvested, frozen at -80°C and lyophilized. Dried samples were suspended in lysis buffer containing protease inhibitors and left at 4°C for 30 minutes. After centrifugation, the supernatants were filtered through Amicon Ultra-15, PLTK Ultracel-PL Membrane, 10 kDa (Millipore). The filtrates were loaded on a Chromabond HR-X micro-column (Macherey-Nagel) and eluted with 70% ACN and 95 % ACN. Eluted samples were analyzed by LC/MS/MS using an Orbitrap XL instrument (Thermo Scientific) as reported elsewhere [363].

6.5 Western blotting analysis

Expression of ANXA1 was examined by SDS-PAGE. Total intracellular proteins were extracted from the cells by freeze/thawing in lysis buffer containing protease inhibitors. Protein content was estimated according to Biorad protein assay (BIO-RAD). Samples (20 µg protein) were loaded onto 10% denaturing-polyacrylamide gel and separated by SDS-PAGE. The separated proteins were then transferred electrophoretically to nitrocellulose membranes (Immobilon-NC, Millipore). Membranes were blocked with 5% non-fat dry milk in TBS-Tween 20 (0.1% v/v) and then incubated overnight at 4°C with the primary antibodies. Proteins were visualized using the enhanced chemioluminescence detection system (Amersham Pharmacia Biotech) after

incubation overnight at 4 °C with primary polyclonal antibodies against ANXA1 (1:10000; Invitrogen), ERK and p-ERK (1:1000; Cells Signaling), CK 8 (1:1000; Abcam) monoclonal ones against vimentin (1:1000; Santa Cruz Biotechnologies), cyclin A (1:1000; Santa Cruz Biotechnologies), ALDH7A1 (1:1000; Abcam), α-tubulin (1:1000; Sigma-Aldrich) and GAPDH (1:1000 Santa Cruz Biotechnologies) and then at room temperature with an appropriate secondary rabbit or mouse antibody (1:5000; Sigma-Aldrich). Immunoreactive protein bands were detected by chemioluminescence using enhanced chemioluminescence reagents (ECL; Amersham), the blots were exposed and analyzed to Las4000 (GE Healthcare Life Sciences).

6.6 siRNA transfection

The 4, 6, 7 and 8 siRNA sequences against ANXA1 were purchased from Qiagen and used at a final concentration of 5 nM. siRNA Oligo-Scrambled (Santa Cruz Biotechnology) was used as control at the same concentration. siRNAs were transfected using Lipofectamine 2000 Reagent (Life technologies Corporation), according to the manufacturer's instructions. Cells were harvested after 72 hours from transfection.

6.7 Confocal Microscopy

After the specific time of incubation, MIA PaCa-2, PANC-1, BxPC-3 and CAPAN-2 cells were fixed in p-formaldehyde (4% v/v in PBS) for 5 minutes. The cells were permeabilized in Triton X-100 (0.5% v/v in PBS) for 5 minutes, and then incubated in goat serum (20% v/v PBS) for 30 minutes, and with rabbit anti-ANXA1 antibody (1:100; Invitrogen), mouse anti-FAK (1:100; BD Transduction Laboratories), mouse anti-E-cadherin (1:250; Abcam), mouse anti-vimentin (1:500; Abcam), mouse anti-lamin A/C (1:450; Novocastra) overnight at 4°C. After two washing steps with PBS, cells were incubated with anti-rabbit and / or anti-mouse AlexaFluor (488 and/or 555; 1:1000; Molecular Probes) for 2 hours at RT and then with FITC-conjugated anti-F-actin (5µg / ml; Phalloidin-FITC, Sigma) for 30 minutes at RT in the dark. The coverslips were mounted in glycerol (40% v/v PBS). A Zeiss LSM 710 Laser Scanning Microscope (Carl Zeiss MicroImaging GmbH) was used for data acquisition. To detect nucleus, samples were excited with a 458 nm Ar laser. A 555 nm He-Ne laser was used to detect emission signals from ANXA1 stain. Samples were vertically scanned from the bottom of the coverslip with a total depth of 5 mm and a 63X (1.40 NA) Plan-Apochromat

oil-immersion objective. Images were generated with Zeiss ZEN Confocal Software (Carl Zeiss MicroImaging GmbH).

6.8 Flow cytometry

MIA PaCa-2 and PANC-1 cells were harvested at a number of 1×10^6 and centrifuged at 30000 x g for 5 minutes. The pellets were then incubated on ice for 1 hour in 100 µl of PBS containing a primary polyclonal antibody against FPR-1 (1:500, Santa Cruz Biotechnology) or a primary monoclonal antibody against FPR-2 (1:100, Genovac). After that, MIA PaCa-2 and PANC-1 cells were washed twice and incubated on ice for 1 hour in 100 µl of PBS containing AlexaFluor 488 anti-rabbit (1:1000; Molecular Probes) or Alexa-Fluor 488 anti-mouse (1:1000; Molecular Probes). About the expression of CD44, cells were incubated on ice for 30 min in 100 µl of PBS containing APC-conjugated CD44 anti-human antibody, APC-conjugated human IgG1 was used as scrambled. The cells were analyzed with Becton Dickinson FACScan flow cytometer using the Cells Quest program.

6.9 PCR

MIA PaCa-2 and PANC-1 cells were seeded at an initial density of 1×10^6 in a 100 mm Petri dish and incubated for 48 hours in growth medium allowing cells to reach 90% confluency. Total RNA was extracted from cells using Trizol (Invitrogen) [24]. Total RNA (5 µg) was used to synthesize cDNA using a reverse transcription kit (Roche). PCR was conducted by using the following primers:

FPR-1 primer pair: (fwd 5'-CAA GAT GGA GAC AAA TTC CTC TC-3') and (rev 3'-GAG CAG AGC CAT CAC CCA GGG CCC AA-5');

FPR-2 primer pair: (fwd 5'-CTG TAC TTT CAA CTT TGC ATC C-3') and (rev 3'-ATT TCC CAA CTC CAC TTA CC-5');

The predicted FPR-1 and FPR-2 products are 469 bp and 773 bp respectively. The FPR-1 and FPR-2 genes were amplified using PCR under the following conditions: pre-denaturation at 94°C for 2 minutes, 35 cycles of denaturation at 94°C for 30 seconds, annealing at 60°C for 30 seconds, extension at 72°C for 30 seconds and a final extension at 72°C for 10 minutes. The products were stored at 4°C. A portion (5 µl) of the PCR product was electrophoresed on a 1% agarose gel in a Tris-acetate-EDTA buffer. The gel was stained with ethidium bromide and was scanned and analysed to Las4000 (GE Healthcare Life Sciences).

6.10 RNA isolation and quantitative RT-PCR assay

mRNA levels of MIA PaCa-2 WT, PGS and ANXA1 KO were analysed by Real- time PCR using the Light Cycler 480 II instrument (Roche). Total RNA was extracted from cultured cells using TriPure Isolation Reagent (Roche), 1μg of total RNA was reverse transcribed into cDNA with Transcriptor First Strand cDNA Synthesis Kit (Roche). 5μl of 1:10 diluted cDNA were used in a 20μl reaction using Light Cycler 480 Probes Master and Real Time Ready Catalog Assay primers (Roche) for CK18 (Forward AATGGGAGGCATCCAGAACGAGAA, Reverse TTCTTCTCCAAGTGCTCCCGGATT) and HPRT1 (Forward GACCAGTCAACAGGGGACAT, Reverse CCTGACCAAGGAAAGCAAAG) following the manufacturer instruction protocol. Results were analysedusing the Delta–Delta CT method.

6.11 Measurement of intracellular Ca^{2+} signalling

Intracellular Ca^{2+} concentrations [Ca^{2+}] were measured using the fluorescent indicator dye Fura 2-AM, the membrane-permeant acetoxymethyl ester form of Fura 2, as previously described [364]. Briefly, MIA PaCa-2 and PANC-1 cells (5 × 10^3/multiwell 24 culture dishes) were washed in PBS and re-suspended in 1 ml of Hank's balanced salt solution (HBSS) containing 5 μM Fura 2-AM for 45 minutes. Thereafter, cells were washed with the same buffer to remove excess of Fura 2-AM and incubated in Ca^{2+}-free HBSS/0.5 mM EGTA buffer for 15 minutes to allow hydrolysis of Fura 2-AM into its active-dye form, Fura 2. MIA PaCa-2 and PANC-1 cells then were transferred to the spectrofluorimeter (Perkin-Elmer LS-55). Treatment with ionomycin (1 μM), fMLP (50 nM, Sigma Aldrich), with Ac 2-26 (1 μM, Tocris Bioscience) or Boc-1 (10 μM, Bachem AG) was carried out by adding the appropriate concentrations of each substance into the cuvette in Ca^{2+}-free HBSS/0.5 mM EGTA buffer. The excitation wavelength was alternated between 340 and 380 nm, and emission fluorescence was recorded at 515 nm. The ratio of fluorescence intensity of 340/380 nm (F340/F380) was used to estimate intracellular free calcium. Results are indicated as delta increase of fluorescence ratio (F340/F380 nm) induced by ionomycin - basal fluorescence ratio (F340/F380 nm).

6.12 *In vitro* wound-healing assay

MIA PaCa-2 and PANC-1 cells were seeded in a 12-well plastic plate at 5×10^5 cells per well. After 24 hours incubation, cells reached 100% confluency and a wound was produced at the centre of the monolayer by gently scraping the cells with a sterile plastic p10 pipette tip. After removing incubation medium and washing with PBS, cell cultures were incubated in the presence of fMLP (50 nM), Ac2-26 (1 μM), Boc-1 (10 μM) or in growth medium as control. In case of transfection with siANXA1s, cells were plated at a number of 2×10^5, after 24 hours were transfected with siANXA1s and with scrambled siRNAs and, 72 hours after transfection, wound was produced. The wounded cell cultures were then incubated at 37°C in a humidified and equilibrated (5% v/v CO_2) incubation chamber of an Integrated Live Cell Workstation Leica AF-6000 LX. A 10x phase contrast objective was used to record cell movements with a frequency of acquisition of 10 minutes. The migration rate of individual cells was determined by measuring the distances covered from the initial time to the selected time-points (bar of distance tool, Leica ASF software). For each condition five independent experiments were performed. For each wound five different positions were registered, and for each position ten different cells were randomly selected to measure the migration distances. Statistical analysis were performed by using GraphPad Prism software (GraphPad Software Inc., version 5.0). Data are presented as means ± SEM. Values $p < 0.05$ were considered as significant.

6.13 Matrigel Invasion Assay

MIA PaCa-2 and PANC-1 invasiveness was studied using the Trans-well Cell Culture (12 mm diameter, 8.0-fim pore size) purchased form Corning Incorporated (USA). The chambers were coated with Matrigel (Becton Dickinson Labware) that was diluted with 3 volumes of DMEM serum-free and stored at 37°C until its gelation. Cells were plated in 350 μl of DMEM serum-free at a number of 9×10^4/insert in the upper chamber of the trans-well. 1,4 ml of DMEM with or without FBS were put in the lower chamber and the trans-well was left for 24 hours at 37°C in 5% CO_2 -95% air humidified atmosphere. After that, the medium was aspirated, the filters were washed twice with PBS 1x and fixed with 4% p-formaldehyde for 10 minutes, then with 100% methanol for 20 minutes. The filters so fixed, were stained with 0,5% crystal violet prepared from stock crystal violet (powder, Merck Chemicals) by distilled water and 20% methanol for 15 minutes. After that, the filters were washed again in PBS 1x and cleaned with a cotton bud. The number of cells that had migrated to the lower surface was counted in twelve random fields using EVOS light microscope (10X) (Life technologies Corporation).

6.14 MTT assay

MIA PaCa-2 WT, PGS and ANXA1 KO cells were seeded at $1,5 \times 10^4$ cells/well in a 96-well plate and incubated for the indicated times (24, 48 and 72 hours) at 37°C. At the ends of the selected experimental times, MTT stock solution (5 mg/ml) was added to all wells of an assay (25 µl per 100 µl medium), and plates were incubated at 37°C for 4 hours. At the end of each experimental point, cells were lysed and the dark blue crystals dissolved with 100 µl of a solution containing 50% (v/v) N, N-dimethylformamide, 20% (w/v) SDS with an adjusted pH of 4.5. The optical density (OD) of each well was measured with a microplate spectrophotometer (Titertek Multiskan MCC/340) equipped with a 620 nm filter. The viability of cells was calculated as: % viable cells = [OD (550 nm-690 nm) ZA/OD (550 nm-690 nm) negative control] × 100.

6.15 Analysis of apoptosis

The effect of gemcitabine 10µM (Sigma Aldrich) on the cell death was checked by propidium iodide (PI) staining and flow cytometry. Briefly, cells supernatant were harvested at 24, 48 or 72h from te administration of gemcitabine, centrifuged at 200 x g for 10 min at room temperature. The seeded cells were washed in PBS and resuspended in 500 µl of a solution containing 0.1% sodium citrate, 0.1% Triton X-100 and 50 µg/ml PI (Sigma Aldrich). These cells were added to the supernatant pellets and incubated at 4°C for 30 min in the dark. Cell nuclei were analyzed with FACScan cytometer (Becton Dickinson) using the Cell Quest evaluation program. Cellular debris were excluded from the analysis by raising the forward scatter threshold and the DNA content of the nuclei was registered on logarithmic scale. The percentage of the cells in the hypodiploid region was calculated.

6.16 Cell cycle analysis

1×10^6 cells were seeded in a 6-well plate, after 24h the growth medium was replaced by a medium without serum to induce a chronicity about cell cycle. After 24h of starvation cells complemented medium was added again for 24, 48 and 72h. Cells were harvested and fixed in cold 70% ethanol at -20°C. Cell cycle profiles were evaluated by DNA staining with 2,5 mg/ml PI in PBS supplemented with 100 U/ml ribonuclease A for 30 min at room temperature in the dark. Samples were analyzed with a FACScan cytometer (Becton Dickinson) using Cell Quest evaluation program. The

distribution of cells in distinct cell cycle phases was determinate using ModFit LT cell cycle analysis software.

6.17 Molecular cloning by Gene/CRISPR *(clustered, regularly interspaced, short palindromic repeat)* -Cas9 *(CRISPR associated protein 9)* technique

The CRISPR/Cas system is a powerful tool for functional screens *in vitro* and *in vivo*, it has been seized upon with a fervor enjoyed previously by small interfering RNA (siRNA) and short hairpin RNA (shRNA) technologies and has enormous potential for high-throughput functional genomics studies [365; 366]. The functions of CRISPR and CRISPR-associated (Cas) genes are essential in adaptive immunity in select bacteria and archaea, enabling the organisms to respond to and/or eliminate invading genetic material. These repeats were initially discovered in the 1980s in *E. coli*, but their function wasn't confirmed until 2007 by Barrangou and colleagues, who demonstrated that *S. thermophilus* can acquire resistance against a bacteriophage by integrating a genome fragment of an infectious virus into its CRISPR locus [367; 368]. Three types of CRISPR mechanisms have been identified, of which type II is the most studied, in fact the simplicity of the type II CRISPR nuclease, with only three required components (Cas9 along with the crRNA – CRISPR RNA- and trRNA –transactivating crRNA-) makes this system amenable to adaptation for genome editing. This potential was realized in 2012 by the Doudna and Charpentier labs [369]. By now, RNA–directed Cas9 endonuclease became a versatile tool for site-specific genome modification in eukaryotes; particularly, this nickase can be used to efficiently mutate genes without detectable damage at known off-target sites and, due to its high ease in building constructs, it has been widely used in humans, mice, rabbits, monkeys and several other species [370]. The plasmid structure is based on the presence of a four genes: cas9 but also cas1, cas2 and csn2, upstream there is the sequence for the tracrRNA as shown in figure 6.1 [371].
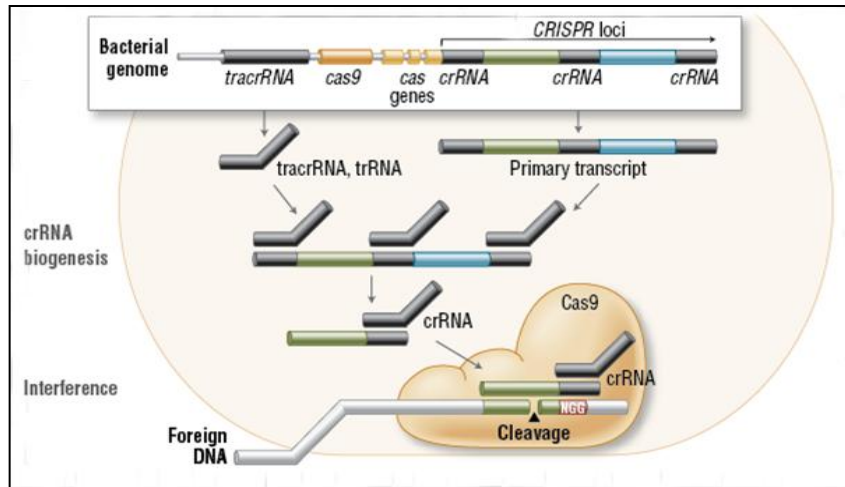
Figure 6.1: CRISPR loci is then transcribed and processed into crRNA during crRNA biogenesis. During interference, Cas9 endonuclease complexed with a crRNA and separate tracrRNA cleaves foreign DNA containing a 20-nucleotide crRNA complementary sequence adjacent to the PAM sequence.

The mechanism is based on the action of CRISPR/Cas9 which generates site-specific DNA double-strand breaks (DSBs) that can be repaired by Non-Homologous End Joining (NHEJ) pathway, resulting in insertions and/or deletions (indels) which disrupt the targeted locus. Alternatively, if a donor template with homology to the targeted locus is supplied, the DSB may be repaired by the homology-directed repair (HDR) pathway allowing for precise replacement mutations to be made [372; 373]. In particular, in this system, single-guide RNAs (sgRNAs) direct Cas9 nucleases to induce DSBs at targeted genomic regions. The 5′ end of sgRNAs includes a nucleotide (Fig. 6.2) sequence of around 20 nucleotides that is complementary to the targeted region defined as a PAM (Protospacer-Adjacent Motif) sequence consisting of either an NGG or NAG trinucleotide [374; 375].
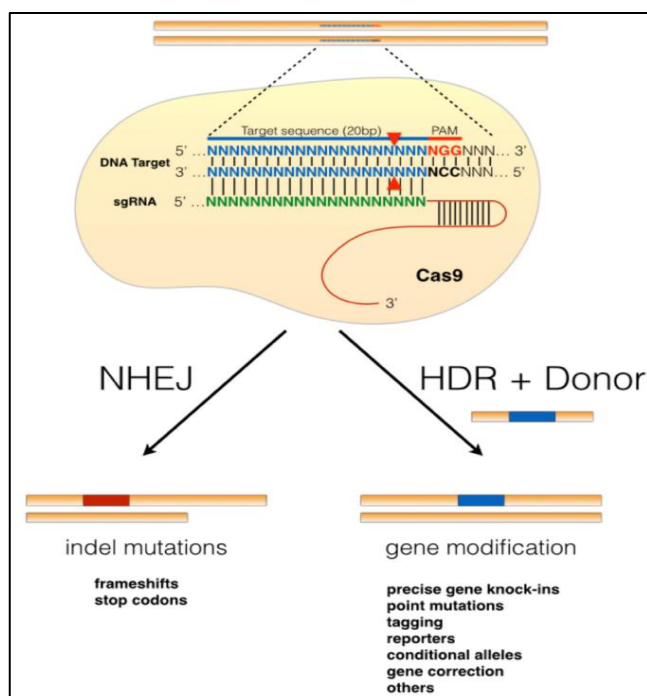
Figure 6.2: Genome engineering utilizing the CRISPR-Cas9 system [376].

The genome-wide CRISPR/Cas9 knockout technology shows greater promise compared with other loss-of-function screen techniques such as RNA interference (RNAi), because it is able to knockout genes at the DNA level and it can be considered also more efficient than more established methods, such as TALENs (transcription activator-like effector nucleases) or ZFNs (zinc-finger nucleases) [377]. However, the data generated by these screens pose several challenges to computational analysis. First, studies are often carried out with no or few replicates, which necessitates a proper statistical model to estimate the variance of the read counts and to evaluate the statistical significance of comparisons between treatment and control samples. Second, as different sgRNAs targeting the same gene might have different specificities and knockout efficiencies, a robust method is needed to take these factors into account in the aggregation of information from multiple sgRNAs. Third, depending on different screen libraries and study designs, the read count distributions of the CRISPR/Cas9 knockout screening experiments are different, as positive selection often results in a few sgRNAs dominating the total sequenced reads [378; 379; 380; 381].

6.17.1 Transfection of plasmid DNA and clones selection.

AS1 ANXA1 KO plasmid and PGS scrambled plasmid were purchased from TwinHelix srl (Milan, srl). MIA PaCa-2 cells were transfected AS1 ANXA1KO plasmid and with PGS scrambled vector using Lipofectamine 2000 Reagent (Life technologies Corporation), according to the manufacturer's instructions. After 48 hours from transfection, cells were replaced with fresh medium, and re-seeded when the cells became confluent. One week later, the transfected cells were subject to neomycin (G418, Euroclone spa) selection at concentrations of 700 μg/ml (the antibiotic dose was established by a previous dose-response curve starting from 200 μg/ml until to 1 mg/ml); the purpose was to maximize recombination and minimize the random insertion. When all control cells (no transfected cells) died because of the antibiotic, cells with plasmids, which formed several clusters in the plate, were harvested and replaced in 96 well plate following the method of the limit dilution. The wells with a single cell were selected. When it expanded, cells were harvested and replaced in a 12 well plate, then in larger plates. We performed Western blotting to test the obtained clones and only those ones which did not show ANXA1 were later analyzed.

6.18 Mass spectrometry of protein extracts

6.18.1 LC-MS/MS analysis

Total intracellular proteins were extracted from the cells by freeze/thawing in lysis buffer containing protease inhibitors. Protein content was estimated according to Biorad protein assay (BIO-RAD). Samples (150 μg protein) analysis was performed using a classical proteomic approach. Specifically, 30 μg of protein extract from each sample were resolved on a 1D SDS-PAGE. Resulting gel lines were cut in 10 bands, and subjected to in-gel digestion procedure. The gel pieces were washed with water and dehydrated in acetonitrile. The bands were then reduced with 25 μM DTT and alkylated with 50 μM iodoacetamide prior to be hydrolysed. All bands were digested using trypsin, by adding 30 μl of a 13 ng/μl trypsin 25 mM ammonium bicarbonate solution. Reaction was performed incubating the mixture overnight at room temperature to achieve complete digestion. The resulting peptide mixtures were extracted from the polyacrylamide with 50 % acetonitrile - 5 % formic acid, and then analysed by high resolution LC/MS/MS. The LC–MS system was a LTQ-Orbitrap mass spectrometer (Thermo Fisher Scientific Inc.) hybrid mass spectrometer system. The HPLC column was a Dionex 15 cm × 75 μm internal diameter Acclaim Pepmap C18,

2 µm, 100 Å reverse phase capillary chromatography column. The extracts (5 µl) were injected into the column and the peptides eluted by an acetonitrile/0.1 % formic acid gradient at a flow rate of 0.25 µl/min were introduced into the source of the mass spectrometer on-line. The microelectrospray ion source is operated at 2.5 kV. The digest was analyzed using the data dependent multitask capability of the instrument, acquiring full scan mass spectra to determine peptide molecular weights and product ion spectra to determine amino acid sequence in successive instrument scans.

6.18.2 Data analysis

All MS/MS samples were analyzed using MaxQant software. MS/MS peak lists generated by the mass spectrometer were searched against the Human UniProtKB/SwissProt protein sequence complete proteome database. Searches were performed selecting alkylation of cysteine by carbamidomethylation as fixed modification, and oxidation of methionine and N-terminal acetylation as variable modifications. Mass tolerance was set to 5 ppm and 0.6 Da for parent and fragment ions, respectively. The false discovery rate for both peptides and proteins were set at 0.01. "High-scoring" corresponded to proteins that were above the significant threshold in MaxQuant searches (5 % probability of false match for each proteins above this score).

6.18.3 Statistical analysis

The statistical analysis of the MaxQuant results was done in Perseus (Version1.5.0.31). At first, proteins only identified by one peptide were removed. Relative protein quantification was done based on LFQ intensities of at least two unique and razor peptides per protein. Significant protein expression differences between the two groups were identified using a T-test analysis with a P value < 0.05.

6.18.4 GO analysis

The two lists of the differentially expressed proteins were subjected to PANTHER classification system, version 9.0 (http://www.pantherdb.org/), for molecular function-based gene ontology analysis. Genes were categorized into multiple different functional groups, including binding, catalytic activity, enzyme regulator, nucleic acid binding transcription factor activity, protein binding transcription factor activity, receptor activity, structure molecule activity, transporter activity, and others.

6.19 Orthotopic pancreatic cancer xenografts in immunodeficient mice

The orthotopic implantation was performed as reported in [382]. Briefly, female, 5 weeks old Severe Combined Immunodeficiency (SCID) mice were anesthetized by inhalation of isoflurane (4% for the induction and "% for the maintenance). The abdomens were shaved and prepped with a betadine solution. The entire operation was done in a sterile hood, with sterile technique maintained throughout. A 1-cm incision was made in the left upper quadrant of the abdomen, and the pancreas was exposed by retraction of the spleen. 1×10^6 MIA PaCa-2 wild type, MIA PaCa-2 PGS and MIA PaCa-2 ANXA1 KO were resuspended in a mixture of 20 µl of sterile PBS and 20 µl of matrigel (BD Transduction Laboratories) (1:1) and injected directly into the pancreas of, using a 29 gauge needle of a Hamilton syringe. The peritoneum was then closed with 5.0 dissolvable suture (AgnTho´s AB) and the skin incision closed with wound clips (Azlet). After 5 weeks from the implantation, mice were sacrificed and organs like pancreas with tumor mass and liver were collected and analyzed.

6.20 H&E tissue staining

The livers were harvested, whashed in PBS 1x and fixed in a solution of p-formaldehyde and TritonX-100 (0.5% and 0.1% v/v in PBS, respectively) O/N at 4°C. Then they were incubated in a sucrose solution (15% p/v in deionized water) O/N at 4°C to guarantee the cryoprotection. The organs were cut into two parts, mounted in OCT and immediately frozen in isobutyl alcohol mixed with dry ice. The obtained blocks were stored at -80°C. Frozen liver sections were cut on a Leica CM 1950 cryostat at 10–12 µm, mounted directly on super frost slides (Thermo Scientific), and air dried for 10–30 min before processing for hematoxylin and eosin (H&E) staining. Slides mounted cryostat sections were dehydrated for 5 min with acetone previously refreshed at -20°C for 15 min and rehydrated to water. Slides were placed in hematoxylin stain for 9 min, rinsed in alcoholic acid, differentiated in 80% alcohol and stained in 0.01% eosin for 2.5 min, rinsed in 95% ethanol, dehydrated with absolute ethanol and cleared in xylenes for 4 min before coverslipping with a mix of xylenes:mounting 1:1. The images were taken through the Axio Observer microscope (4, 10 and 40X) (Carl Zeiss MicroImaging GmbH).

6.21 Statistical analysis

All results are the mean ± SEM of at least 3 experiments performed in triplicate. The optical density of the protein bands detected by Western blotting was normalized against tubulin levels. Statistical comparisons between groups were made using two-way ANOVA or unpaired, two-tailed t-test comparing two variables. Differences were considered significant if $p < 0.05$ and $p < 0.01$.

CHAPTER 7

RESULTS

7.1 Expression of ANXA1 in PC cell lines

ANXA1 role in PC progression is poorly described. Therefore, we initially focused to define how ANXA1 is expressed and localized in several human primary PC cell lines like MIA PaCa-2, PANC-1, BxPC-3 and Capan-2. These cells show many differences about their origin, genotype and phenotype, as adhesion, migration, invasion and angiogenesis capacities [383]. Particularly:

- BxPC-3 was cultured from a 61-year-old woman's adenocarcinoma of the body of the pancreas [384].
- Capan-2 originated from a 56-year-old male with pancreatic adenocarcinoma. The primary tumor involved the head of the pancreas and infiltrated the duodenal wall distal to the ampulla [385].
- MIA PaCa-2 was derived from the pancreas adenocarcinoma of a 65-year-old man, the tumor involved the body and tail of the pancreas and had infiltrated the periaortic area [386].
- PANC-1 was cultured from a 56-year-old male with an adenocarcinoma in the head of the pancreas which invaded the duodenal wall. Metastases in one peripancreatic lymph node were discovered during a pancreaticoduodenectomy [387].

The main differences about gene mutation are summarized in table 7.1:

Cell Line	KRAS	TP53	CDKN2A/p16	SMAD4/DPC4
BxPC-3	WT	220 Cys	WT	HD
Capan-2	12 Val	WT Intron 4 Δ200 bp splice site	WT	WT
MIA PaCa-2	12 Cys	248 Trp	HD	WT
PANC-1	12 Asp	273 His; 273 Cys	HD	WT

Table 7.1: The four most common mutations in pancreas cancer (WT—wild type, Δ—deletion, bp—base pair, HD—homozygous deletion) [383].

Western blotting analysis in figure 7.1 showed that all cell lines expressed ANXA1. Only MIA PaCa-2 cells revealed two bends for ANXA1 (37 and 33kDa) at variance with the other cell lines (see the paragraph 7.4).
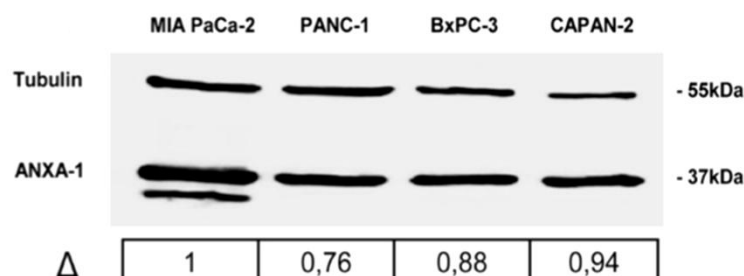
Figure 7.1: Total ANXA1 expression in MIA PaCa-2, PANC-1, BxPC-3 and CAPAN-2 cells was analyzed by Western blot with anti-ANXA1 antibody. Protein normalization was performed on tubulin level.

Next, we characterized MIA PaCa-2, PANC-1, BxPC3 and CAPAN-2 cells on the basis of their phenotype since the more aggressive and invasive cancer cells had a higher basal EMT signature [388]. Confocal microscopy analyses confirmed more aggressive features for MIA PaCa-2 and PANC-1 as, differently from BxPC-3 and CAPAN-2, these cancer cells possess a marked mesenchymal phenotype characterized by up-regulation of the mesenchymal marker vimentin and down-regulation of the epithelial marker E-cadherin (Figure 7.2 A, B, C) [168].
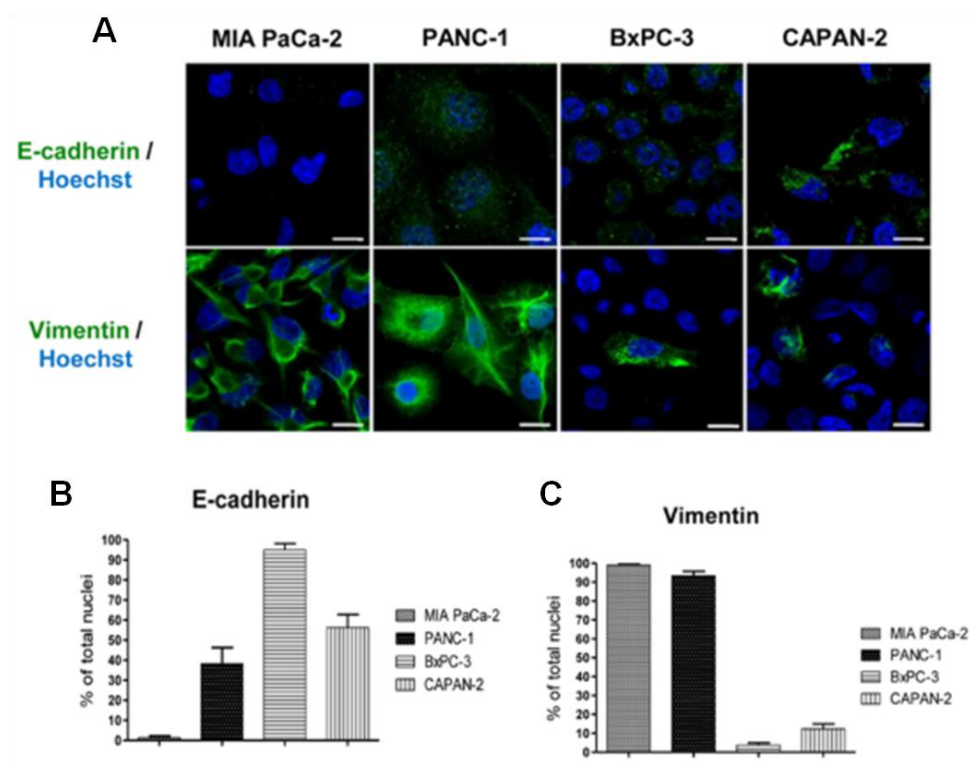
Figure 7.2: A, Cultured human MIA PaCa-2, PANC-1, BxPC-3 and CAPAN-2 cells fixed and labeled with fluorescent antibody against E-cadherin and Vimentin (green). **C,** Quantitative analysis of E-cadherin expression in MIA PaCa-2, PANC-1, BxPC-3 and CAPAN-2 cells. **D,** Quantitative analysis of vimentin expression in MIA PaCa-2, PANC-1, BxPC-3 and CAPAN-2 cells

7.2 Localization of ANXA1 in PC cell lines

Tumor cell invasion and metastasis processes involve many proteins that are required for normal cell motility. As it is known that ANXA1 plays a role in normal cell migration [345; 346] and in cancer cell invasion and metastasis [296; 289], we also analyzed by confocal microscopy ANXA1 localization in the cellular motility structures identified by using focal adhesion kinase (FAK) or F-actin staining. In the figure 7.3 (panels c, f) we show that ANXA1 co-localized in both MIA PaCa-2 and PANC-1 cells with FAK, a protein commonly expressed in adhesion hot spots of migrating/invasive cells. Moreover, we show an actin-like filamentous ANXA1 organization and an enrichment of the protein at burble ends and extrusions in MIA PaCa-2 cells (Fig. 7.3, panel i). Also in PANC-1 cells ANXA1 co-localized with F-actin protein although this cell line is characterized by a less mesenchymal-like phenotype (Fig. 7.3, panel n).
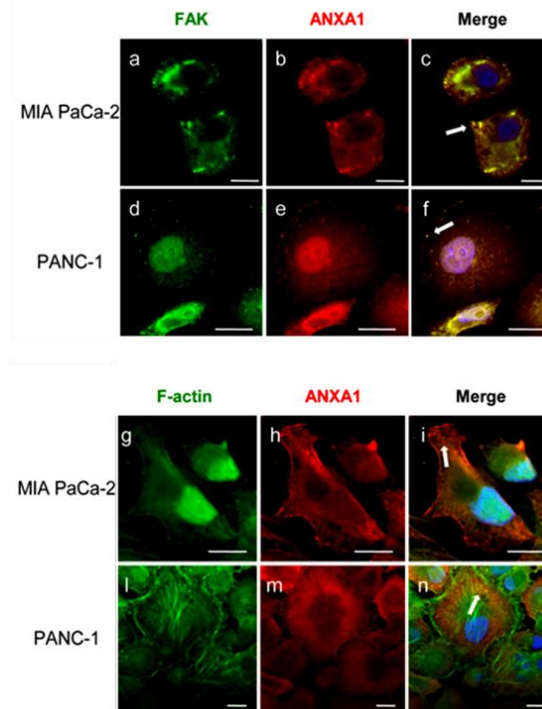
Figure 7.3: Immunofluorescence analysis to detect FAK (panels a, d), ANXA1 (panels b, e, h, m), and F-actin (panels g, l) in MIA PaCa-2 and PANC-1. Nuclei were stained with DAPI. The merged image shows overlapping localization of the proteins

(panels c, f, I, n). Magnification 63x.The data are representative of 5 experiments with similar results. Bar=10μm.

7.3 Effects of ANXA1 knockdown on MIA PaCa-2 and PANC-1 cell migration and invasiveness

As it is known from previous reports and confirmed by our data using confocal microscopy, PANC-1 and MIA PaCa-2, at variance with CAPAN-2 and BxPC-3, show a more aggressive phenotype, particularly MIA PaCa-2 that have an higher tumorigenic potential [383; 389].

We observed that in MIA PaCa-2 and PANC-1 cell lines, ANXA1 localized in the regions that are involved in the cell movement. As the migration and invasion processes start once cells form actin- and FAK-rich protrusions that adhere to the matrix and create the tension forces necessary for cell motility [390], we hypothesised a role for the protein in these processes. The expression of ANXA1 was greatly reduced in MIA PaCa-2 (Fig. 7.4A) and PANC-1 (Fig. 7.4D) cells by specific siRNA transfection. Thus a Wound healing migration assay was performed on cellular monolayer of ANXA1 knockdown cells. The confluent cultures were scraped at the middle of well to create a wound and cell migration was monitored by time-lapse video-microscopy at the site of the described wound. We measured the migration distances of selected cells at different time points as described in Material and methods section. In ANXA1 knockdown MIA PaCa-2 (Fig. 7.4B) and PANC-1 (Fig. 7.4E) cells the rate of migration decreased in a significant manner, if compared with the wild type control and with scrambled RNA transfected cells.

The matrigel invasion assay was also performed in ANXA1 knockdown MIA PaCa-2 and PANC-1 cells to investigate the role of ANXA1 on their invasion ability. As shown in figure 7.4C and 7.4F, siRNAs against ANXA1 markedly suppressed the invasiveness of both PC cell lines. To confirm the technical efficiency of our experiment, we used a serum free control to eliminate any chemoattractant condition: in this way we found significantly less invading cells on the lower surface of matrigel.
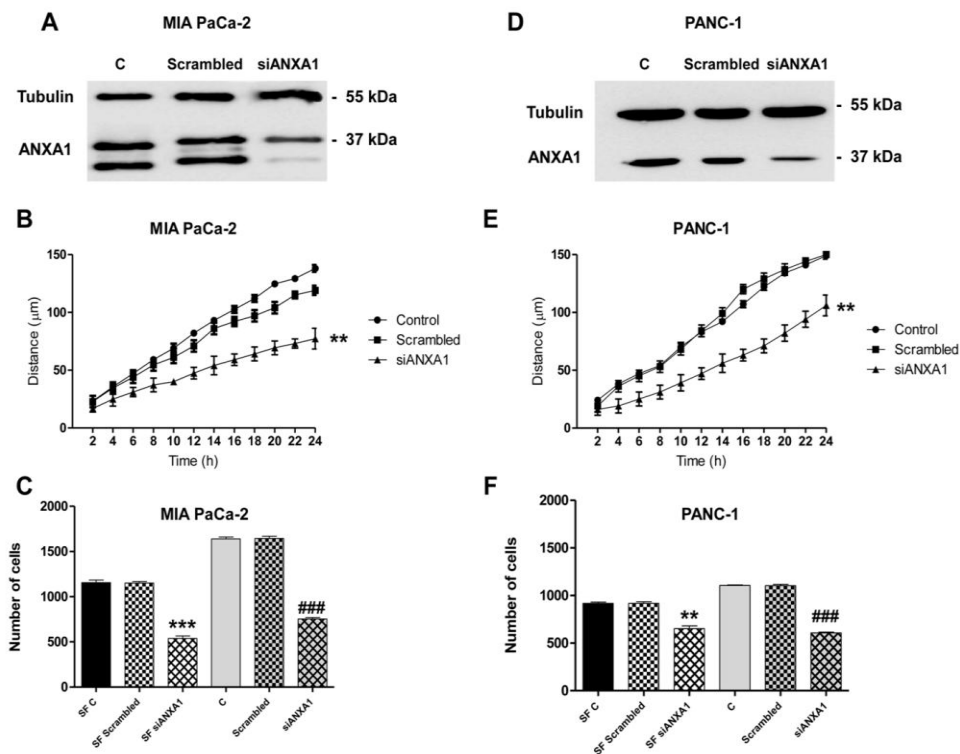
Figure 7.4: A, Western blot using an anti-ANXA1 antibody on protein extracts from MIA PaCa-2 or PANC-1 cells (**D**) treated or not with siRNAs direct against ANXA1 (siANXA1). Protein normalization was performed on tubulin levels. **B,** Results of Wound healing assay on MIA PaCa-2 (**B**) or PANC-1 cells (**E**) transfected with siANXA1s or scrambled siRNAs; ** $p<0.01$ vs untreated control. The data are representative of 5 independent experiments ± SEM.
Invasiveness rate of MIA PaCa-2 (**C**) or PANC-1 cells **F,** In invasion assays a total of 90,000 cells were transfected or not with siANXA1s (5nM) or scrambled siRNAs (5nM) for 72h and plated as described in Material and methods section. Invasiveness rate was founded out by counting stained cells on the lower surface of the filters. Data represent mean cell counts of 12 separate fields per well ± SEM of 5 experiments. ** $p<0.01$ vs serum free (SF) control; *** $p<0.001$ vs SF control; ### $p<0.001$ vs control.

7.4 Localization and cleavage of endogenous ANXA1 in MIA PaCa-2 and PANC-1 cells

Cellular migration and invasion events can be triggered by a number of molecular signals, such as chemoattractants and mechanical forces, that are sensed by receptors on the cell surface or within cells to lead to a migratory response [391].

The extracellular form of ANXA1 has been described to play a role in cancer cell invasion and metastasis. Although the protein does not possess classical signal sequences to target the protein for export, both the full-length and truncated forms are often observed in extracellular environments. Moreover, it appears that proteolytic cleavage of ANXA1 is required for protein secretion, because the majority of ANXA1 released from neutrophils is N-terminally cleaved [257; 391; 392; 393; 394; 395; 396]. Based on these information, our characterization experiments continued with the analysis by Western blot of ANXA1 expression in sub-cellular compartments of MIA PaCa-2 cells. In particular, we obtained membrane, cytosol and nuclear protein extracts as described in Material and methods section. The ANXA1 membrane expression was detected by both fractioned protein extracts and EDTA wash, with which we obtained the proteins that bind plasma membrane through calcium. In MIA PaCa-2 extracts, we found both, full length (37kDa) and cleaved (33kDa) forms of ANXA1 protein at plasma membrane and in the cytosol but not in the nucleus where only the 37kDa ANXA1 form was expressed. Conversely, PANC-1 did not show the ANXA1 cleaved form and the protein expression in sub-cellular compartments was characterized by a small amount onto membrane and in the nucleus, if compared with MIA PaCa-2 cells.

Both full length (37kDa) and cleaved (33kDa) forms of ANXA1 were also observed in MIA PaCa-2 supernatants, whereas no protein secretion was observed in the PANC-1 supernatants (Fig. 7.5).
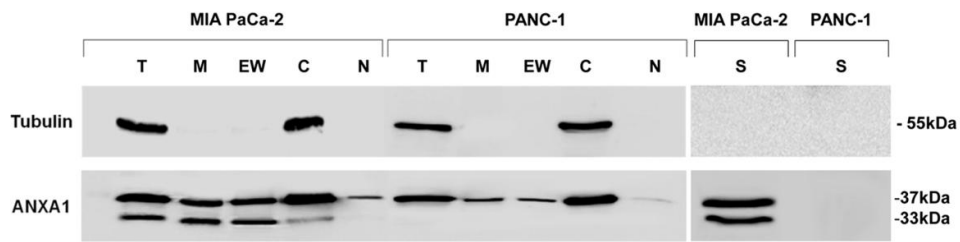
Figure 7.5: Cellular compartments were obtained as described in Methods section. Total (T), membrane (M), EDTA Wash (EW), cytosolic (C), nuclear (N) and supernatants (S) ANXA1 expression in protein extracts from MIA PaCa-2 and PANC-1 was examined by Western blot with anti-ANXA1 antibody. The protein bands were normalized on tubulin levels. The data are representative of 5 experiments with similar results.

7.5 Analysis of the secreted forms of ANXA1

Based on the previous findings, we focused on the appearance of a 33kDa form only in MIA PaCa-2 cells, both in total (Fig. 7.1) and supernatant extracts (Fig. 7.5). Therefore, in order to detect possible ANXA1 fragments released from the cells a multi-step fractionation of MIA PaCa-2 supernatants was performed. Obtained samples were analyzed by LC-HRMS/MS as described in Material and methods section. A peptide showing a molecular weight of 2744.324 was detected; on the basis of its molecular weight and of the CID induced fragmentation spectrum (Fig. 7.6), this peptide was identified as the fragment 4-26 of ANXA1.
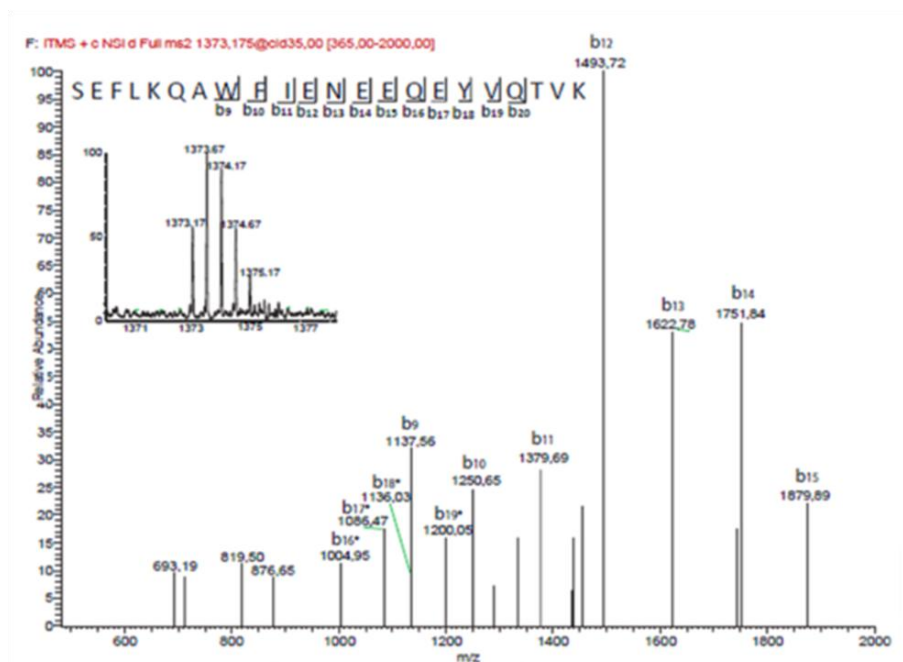
Figure 7.6: LC-HRMS/MS spectrum, peaks refer to all the discovered peptide fragments. The data are representative of 5 experiments with similar results.

7.6 Expression of FPRs in MIA PaCa-2 and PANC-1 cells

Cancerous cell capability to migrate and invade tissues is a decisive aspect of cancer development and metastasis and entails the coordination of several cellular events, such as cytoskeletal reorganization, dynamic cell-matrix adhesion and remodeling [390].

Regulatory action on cell surface by extracellular ANXA1 is reported to be mediated by signaling through FPRs [345; 346; 397; 283] that are reported to regulate cell migration by actin polymerization.

In order to verify the role of ANXA1-FPR interaction in MIA PaCa-2 and PANC-1 cell migration and invasiveness, we first assessed FPR expression in these cell lines by cytofluorimetric analysis (Fig. 7.7A): we found that FPR-1 and FPR-2 were expressed in both cell lines. These findings were confirmed by qualitative PCR (Fig. 7.7B).
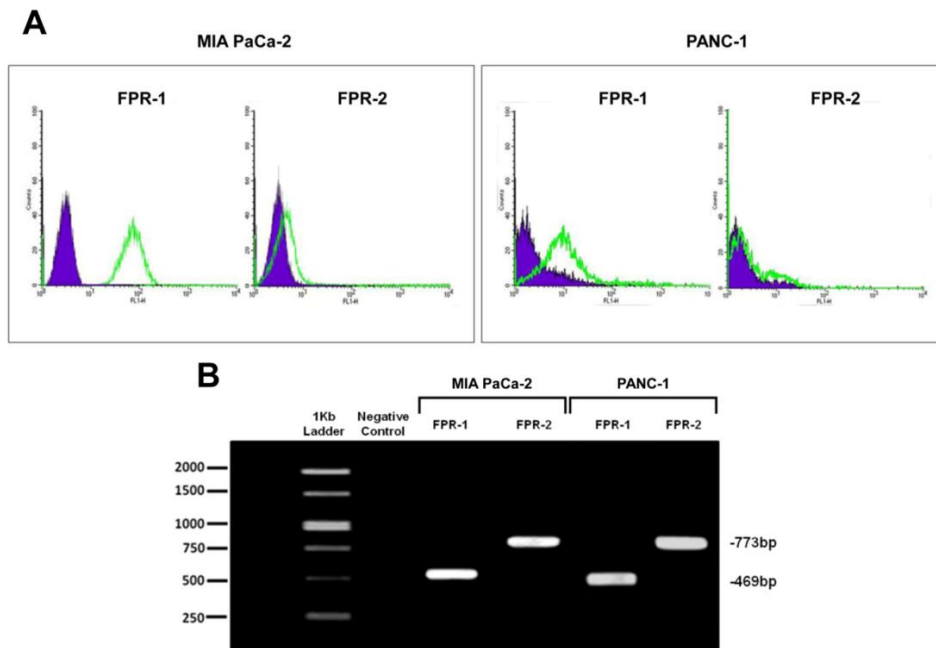
Figure 7.7: A, Cell surface expression of FPR-1 and FPR-2 in MIA PaCa-2 and PANC-1 cells was analyzed by flow cytometry. The violet areas in the plots are relative to secondary antibody alone. FPR-1 and FPR-2 signals are showed with green bends. **B,** Expression of FPR-1 and FPR-2 in MIA PaCa-2 and PANC-1 cells analyzed by PCR.

7.7 Activation of FPRs in MIA PaCa-2 and PANC-1 cells

It is known that the interaction between ANXA1 and FPRs causes a series of cellular responses, such as the ERK phosphorylation and the increase of intracellular [Ca^{2+}] concentration. The N-terminal mimetic peptide of ANXA1, Ac2-26, can activate all three human FPRs, promoting calcium fluxes and cell locomotion. To determine whether ligand binding to FPRs induces similar signal transduction in MIA PaCa-2 and PANC-1, we examined the stimulated release of calcium from intracellular stores. Cells were incubated in Ca^{2+} free medium and loaded with the fluorescent calcium indicator Fluo-2AM before stimulation with Ac2-26 (1 µM) or the natural FPR agonist fMLP (50 nM) together or not with the FPR pharmacological antagonist Boc-1 (10 µM) that is able to antagonize, at this concentration, all three human FPR isoforms. The spectrofluorimetric assay (Fig. 7.8) shows that fMLP and peptide Ac2-26 were able to increase the mobilization of intracellular Ca^{2+} in both MIA PaCa-2 and PANC-1 cells. In fact, no significant differences between ionomycin (used as reference compound) and fMLP or Ac2-26 were observed. The effects of fMLP and Ac2-26 peptides were inhibited by the pharmacological pan-antagonist Boc-1 in both cell lines.
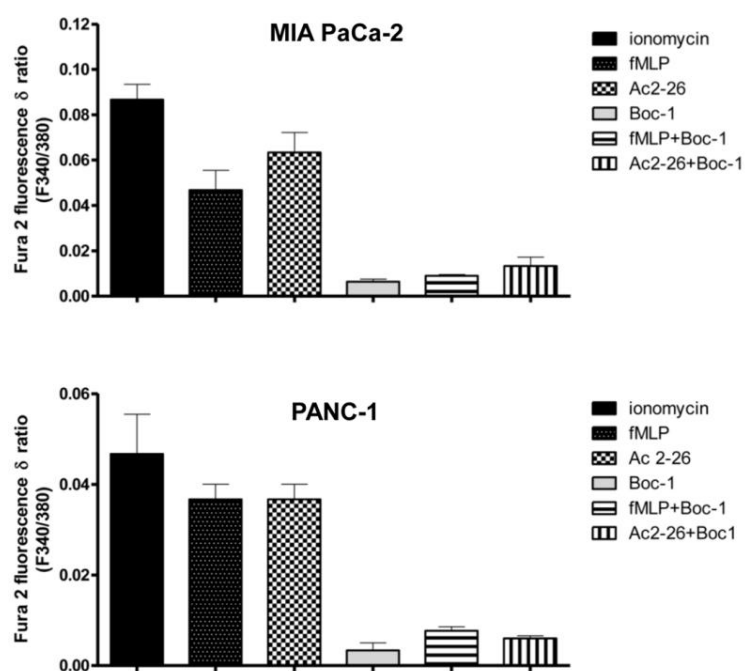
Figure 7.8: Effects of fMLP (50 nM), Ac-2-26 (1 µM) and FPR pan-antagonist Boc-1 (10 µM) on the FPR-induced rise in intracellular Ca^{2+} in MIA PaCa-2 or PANC-1 cells. The histograms show the fluorescence ratio calculated as F340/F380 nm in absence of extracellular Ca^{2+}. Control represents ionomycin-stimulated cells. Data are means ± SEM (n=5).

7.8 Effects of activation of FPRs on MIA PaCa-2 and PANC-1 cells in migration and invasion assays

The role of ANXA1 in cancer progression is still discussed; this protein may have specific functions in different tumoral models. For example, in gastric and colon carcinomas ANXA1 has a pro-invasive role through its interaction with FPRs [347; 283].To determine if ANXA1 influences cell migration acting through FPRs, we performed a Wound healing migration assay on cellular monolayer in both the analyzed cell lines.

For MIA PaCa-2, results in figure 7.9A show an increase in migration speed of cells treated with Ac2-26 (1 µM) or fMLP (50 nM) compared to control cells. The FPR pan-antagonist Boc-1 (10 µM) significantly inhibited basal and stimulated migration. When treated with Ac2-26 and fMLP, MIA PaCa-2 cells showed an increased invasion speed through coating of matrigel. Again, Boc-1 antagonist (10 µM, Fig. 7.9C) reduced in a significant manner MIA PaCa-2 stimulated cell invasion.

At the same time, we used PANC-1 cell line as basis for comparison, as these cells did not show either the ANXA1 cleaved form or the externalized one. Similarly for MIA PaCa-2, results of the Wound healing migration assay on cellular monolayer showed an increase in migration speed of the cells treated with Ac2-26 or fMLP when compared to control cells and a reverted effect in cells treated with the pan-antagonist Boc-1 (Fig. 7.9B and D).
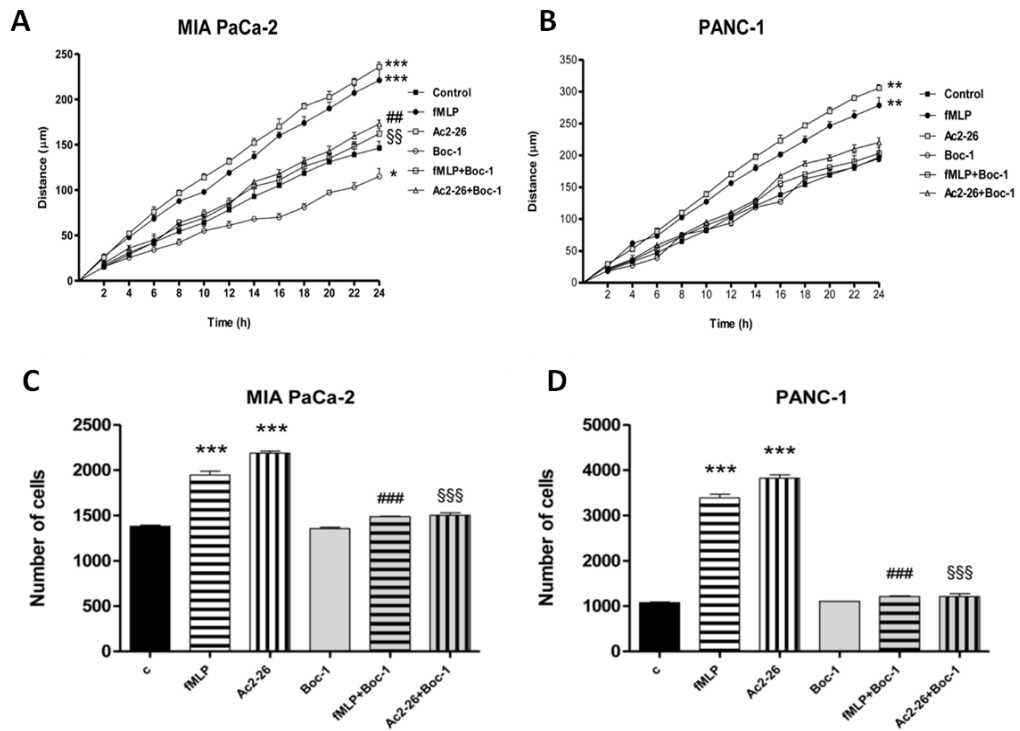
Figure 7.9: Wound healing assay on MIA PaCa-2 (**A**) or PANC-1 cells (**B**) treated or not with fMLP (50nM), Ac2-26 (1µM), Boc-1 (10 µM), fMLP + Boc-1 or Ac2-26 + Boc-1; * $p<0.05$, ** $p<0.01$, *** $p<0.001$ vs untreated control; ## $p<0.01$ and §§ $p<0.01$ vs respective controls. Invasiveness rates were measured as described in Material and methods section and are represented in **C** for MIA PaCa-2 and **D** for PANC.1. Data represent mean cell counts of 12 separate fields per well ± SEM of 5 independent experiments.

7.9 Effects of extracellular ANXA1 on MIA PaCa-2 and PANC-1 cells in migration and invasion assays

To confirm the direct effect of extracellular ANXA1 on MIA PaCa-2 and PANC-1 cells, we used an ANXA1 blocking antibody showing its ability to reduce in a significant manner MIA PaCa-2 basal cell migration (Fig. 7.10A) and invasion (Fig. 7.10C). Interestingly, ANXA1 blocking antibody had no effects on PANC-1 cell motility, both about migration ability (Fig. 7.10B) and invasiveness (Fig. 7.10D), confirming the absence of its targeted protein in the extracellular environment for this cell line.
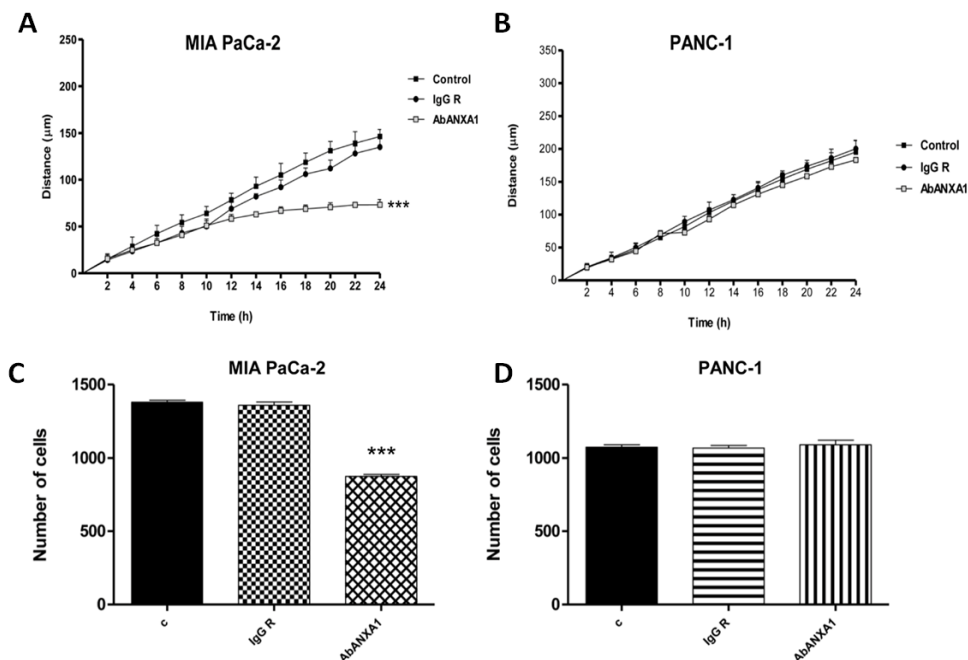
Figure 7.10: Wound-healing assay on MIA PaCa-2 (**A**) or PANC-1 cells (**B**) treated or not with ANXA1 blocking antibody (AbANXA1) or scrambled rabbit IgG (IgG R); *** p<0.001 vs untreated control. All wound-healing data are representative of 5 experiments ± SEM. Invasiveness rate of MIA PaCa-2 (**C**) or PANC-1 cells (**D**) treated or not with AbANXA1 or IgG R; *** p<0.001 vs untreated control. Invasiveness rates were measured as described in Methods section. Data represent mean cell counts of 12 separate fields per well ± SEM of 5 independent experiments.

7.10 Effects of MIA PaCa-2 supernatants on PANC-1 cell migration

Our data suggest a double role of ANXA1 in PC cell motility. In one way the protein acts in the intracellular environment thanks to its involvement in cytoskeleton reorganization, as confirmed by immunofluorescence assay showed in figure 7.3. In another one, ANXA1 externalized form appears to bind FPRs and trigger some molecular pathways that lead to cell migration and invasion. Substantial evidences support that ANXA1 membrane translocation and its consequent externalization are modulated by some post-transductional modifications. In particular, Ser27 phosphorylation triggers a proteolytic cleavage by which protein loses its N-terminal fragment [257]. As previously described, the greater part of biological ANXA1 activity is due to this peptide which is especially important in several extracellular functions of the protein [398].

Furthermore, we considered the higher migratory and invasive rate of MIA PaCa-2 compared with PANC-1 cells [383]. In order to confirm that the secreted forms of ANXA1 protein were able to induce PC cell migration and invasion in autocrine and paracrine manner, we performed further experiments adding MIA PaCa-2 supernatants to PANC-1 cells and *viceversa*. As shown in figures 7.5 and 7.6, MIA PaCa-2 supernatants containing all the secreted forms of ANXA1 protein (37kDa, 33kDa and 3kDa) significantly increased PANC-1 cell migration rate. Conversely, the administration of PANC-1 supernatants on MIA PaCa-2 cells had no effects on migration speed of the latter ones. Moreover, the administration of MIA PaCa-2 conditioned supernatant containing ANXA1 blocking antibody on PANC-1 cells did not increase the migration rate of these cells.
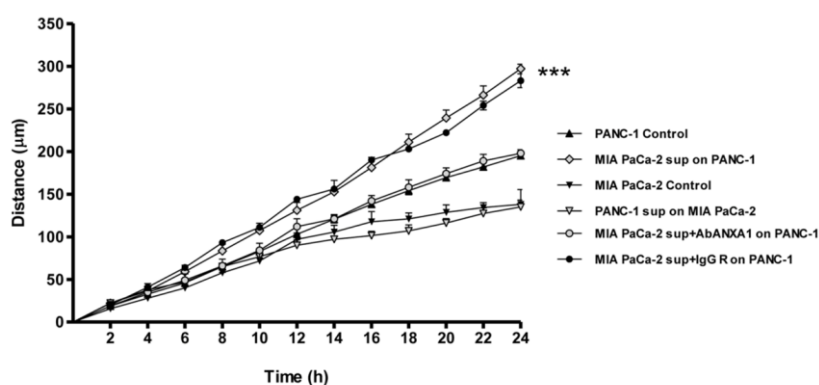
Figure 7.11: Effects of MIA PaCa-2 supernatants on PANC-1 cells and *viceversa* in a Wound healing assay. *** $p<0.001$. Data are means ± SEM (n=5).

7.11 Creation of genomic ANXA1 deletion in MIA PaCa-2 cell line using CRISPR/Cas9 technique

Working with cellular model systems, RNAi (as in case of siRNA) has represented a powerful tool for functional genomics. However, limitations of this approach have included incomplete reduction in target mRNA transcript levels, heterogeneity of effect of independent reagents targeting the same gene and known off-target effects including seed-based and non-seed effects. Genome editing strategies promise to address many of these concerns and represent an exciting, complementary approach for prospective genetic perturbation [399]. Therefore, we opted for the use of CRISPR/Cas9 technique, as reported in Material and Methods section, to obtain the genomic deletion of ANXA1 gene.

Plasmid map and specific sequence targeting a small portion (from nucleotide 274 to 292) of ANXA1 coding sequence are represented in figure 7.12A and B, respectively. We obtained 12 ANXA1 knockout (KO) clones of MIA PaCa-2 cell line which has been chosen because of its aggressive phenotype and the marked *in vivo* tumorigenity. ANXA1-KO clones were all analyzed by Western blotting. In figure 7.12C only 3 of them are reported and compared with MIA PaCa-2 wild type (WT) and the scrambled vector (PGS), used as technical and biological controls. The expression of ANXA1 has been normalized considering tubulin levels.

Figure 7.12: A, Commercial plasmid map; **B,** Targeting sequence of plasmid, the sequence of alignment are signed by green arrows; **C,** B11, D6, G2 and G5 are 4 of 12 clones KO for ANXA1, the absence of ANXA1 has been compared with MIA PaCa-2 WT and PGS and normalized basing on tubulin level.

7.12 Comparative proteomic analysis of MIA PaCa-2 PGS and ANXA1 KO derived sub-line MIA PaCa-2

Once we obtained ANXA1 KO-MIA PaCa-2 from MIA PaCa-2 WT cells as previously described, we examined the total protein extract by LC-MS/MS together with MIA PaCa-2 PGS to characterize proteins putatively affected by the absence of ANXA1. Also MIA PaCa-2 WT cells were analyzed but no significant differences were found when compared to PGS protein extract The adopted procedure has been described in detail in Material and Methods section. The total protein extract was performed in biological triplicate and three ANXA1-KO clones have been taken. According to the statistic tests, in ANXA1 KO MIA PaCa-2 26 proteins appear down-modulated, on the other hand, 36 were over-expressed. These proteins belong to pathways involving several processes which are represented in the pie chart in figure 7.13A. They are metabolism, cell proliferation, cell trafficking, cytoskeleton organization and other processes. We paid particular attention about this cytoskeleton organization signaling because the importance that ANXA1 has in remodeling of F-actin and other correlated proteins. The proteins are reported in table 7.13B and they are specified by fold change, relative p value (for all < 0,05) and the gene name.

PROTEIN ID	GENE NAME	PROTEIN NAME	FOLD CHANGE	BIOLOGICAL FUNCTION	p VALUE
P05787	KRT8	Keratin, type II cytoskeletal 8	0	Structural molecule activity	1,41E-06
F8VZY9	KRT18	Keratin, type I cytoskeletal 18	0	Structural molecule activity	0,042453
P53621	COPA	Coatomer subunit alpha;Xenin;Proxenin	7,740548847	Structural molecule activity	0,013284
P48643-2	CCT5	T-complex protein 1 subunit epsilon	3,47838083	Microtubule organization	0,035743
H0YD13	CD44	CD44 antigen	2,789712509	Cell adhesion	0,024194
O75369-2	FLNB	Filamin-B	1,579505107	Connection of cell membrane constituents to the actin cytoskeleton	0,000111
P43243	MATR3	Matrin-3	0,303521	Structural molecule activity	0,017219
P14625	HSP90B1	Endoplasmin	0,390034	Actin rod assembly	0,000784
P12814-2	ACTN1	Alpha-actinin-1	0,390837	Actin filament organization	0,002918
Q13813-3	SPTAN1	Spectrin alpha chain, non-erythrocytic 1	0,415984	Structural molecule activity	0,04326
P02545	LMNA	Prelamin-A/C;Lamin-A/C	0,532087	Nuclear assembly, chromatin organization, nuclear membrane and telomere dynamics	0,000837
Q13263	TRIM28	Transcription intermediary factor 1-beta	0,561538	Nucleosome remodeling	0,044216
P08670	VIM	Vimentin	0,671009	Structural molecule activity	0,009402

Figure 7.13: A, Pie chart of the different cell pathways affected by the absence of ANXA1; **B,** Differentially expressed proteins identified by mass spectrometry involved in the process of cytoskeleton organization.

7.13 Validation of protein identified as differentially expressed in the LC-MS/MS analysis

To validate the LC-MS/MS-obtained results, as well as to further evaluate the nature and importance of some of the identified proteins that changed expression between ANXA1 KO MIA PaCa-2 and MIA PaCa-2 PGS cells lines, other kinds of experiments have been performed.

Of particular note, ANXA1 KO MIA PaCa-2 showed reduced expression of of vimentin, a protein of the intermediate cytoskeletal filaments and a known EMT marker. We confirmed the down-modulation of this protein by Western blot analysis, as shown in figure 7.14A, and by immunofluorescence assay (Fig.7.14D, panel g, h, i). Moreover we established also the down-modulation of Lamin A/C (Fig. 7.14D, panel l, m, n), another protein belonging to the cytoskeletal intermediate filaments, which apperas misregulated in some cancers. The lamins are components of the nuclear lamina, a fibrous layer on the nucleoplasmic side of the inner nuclear membrane which is suggested to provide a framework for the nuclear envelope and may interact with chromatin. Nuclei are mechanically linked to the cytoskeleton through lamin-interacting proteins that span the nuclear envelope. Nuclear lamina also mediates structural linkages between the nucleus and cytoskeleton, through the linker of nucleoskeleton and cytoskeleton (LINC) complex just consisting of lamins and an interacting outer nuclear membrane protein, which in turn binds cytoskeletal elements [400].

Furthermore, we demonstrated the increase of CD44 level by FACS technique, using APC-conjugated antibody. CD44 has a particular importance in cell adhesion on hyaluronic acid of ECM, in fact only when it undergoes a proteolytic cleavage, it becomes not more capable to guarantee the adhesion and cell begin to migrate [401; 402; 403]. In figure 7.14B, the purple line is overlapped on the green one and they respectively refer to the CD44 expression in MIA PaCa-2 PGS and in MIA PaCa-2 WT; the black line is relative to the protein expression in ANXA1 KO MIA PaCa-2 and, finally, the blue line refers to the APC-conjugated human IgG1 using as technical control.

Cytokeratin 8 (CK8) and 18 (CK18) have a structural role in simple epithelia. Additionally, they play a role in a signaling that modulates cell attachment, protein synthesis, G1/S phase transition, and in stress adaptation. Furthermore, CK18 can be applied to detect therapy-induced tumor apoptosis and necrosis [404; 405; 406]. Several reports showed that there is an inversely correlation between CK18 and ANXA1 expression, such as in our case [298]. By RT-PCR in figure 7.14C, executed as reported in Material and method section, we showed the increase of cytokeratin (CK) 18,

using the levels of the protein hypoxanthine phosphoribosyltransferase 1 (HPRT) as house-keeping gene. Additionally, the Western blot in figure 7.14A proved the increase of CK8.

Cell migration requires precise control, which is altered or lost when tumor cells become invasive and metastatic. The first protein we analyzed was F-actin because of its important role in cell migration. In fact, its polymerization mediates the mechanical energy to induce the formation of lamellopodia. These ones are characterized by a network of actin and myosin; particularly actin spreads out in parallel bundles to mediate the interaction with integrins and other focal adhesion molecules. In this way the cell directional advancing is guaranteed [407]. ANXA1 co-localizes with F-actin in the basal conditions, that is in cells in which the cytoskeleton protein is well spread in filamentous and organized in bundles protruding towards the plasma membrane. On the contrary, in ANXA1 KO MIA PaCa-2 cells we found a disorganized cytoskeleton and F-actin appeared concentrated all around plasma membrane and depolymerized in the cytosol. This is known as cortical F-actin and is not capable to induce cell migration as previously described (Fig.7.14D, panel d, e, f).
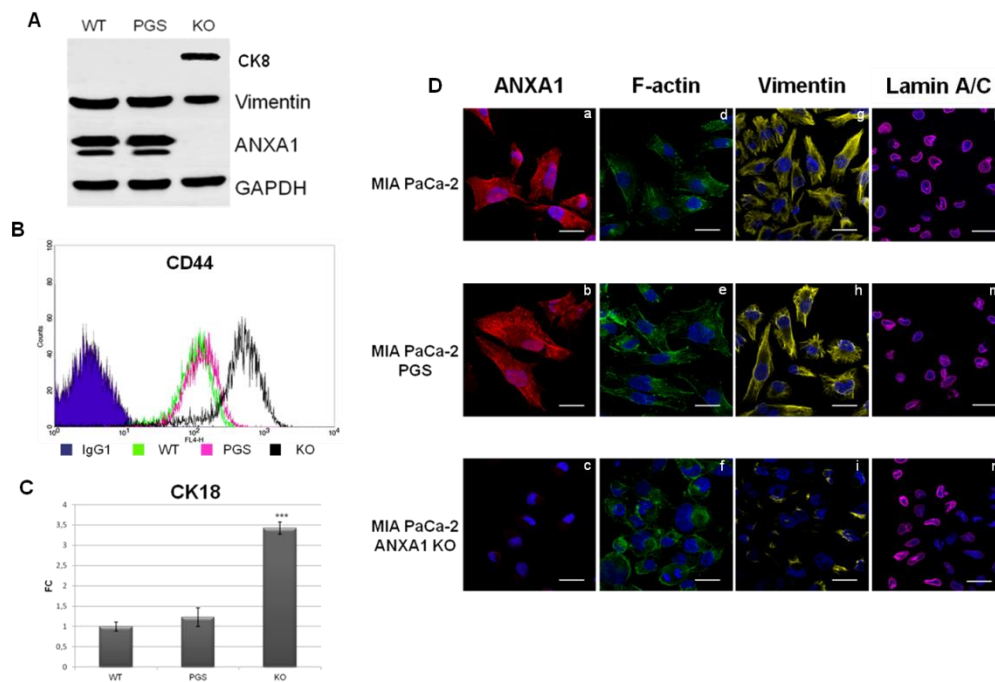
Figure 7.14: A, Western blot showing CK8, vimentin, ANXA1 and GAPDH expression on MIA PaCa-2 WT, PGS and ANXA1 KO. **B,** Cell surface expression of CD44 was analyzed by flow cytometry. The violet areas in the plots are relative to human IgG1; CD44 signals are showed with green bends for MIA PaCa-2 WT, in pink bends for MIA PaCa-2 PGS and in black ones for MIA PaCa-2 ANXA1 KO. **C,** RT-PCR for CK18 mRNA expression measured on levels of HPRT in the same experimental models. **D,** Immunofluorescence analysis to detect ANXA1 (panels a, b, c), F-actin (panels d, e, f) vimentin (panels g, h, i) and Lamin A/C (panel I, m, n) in MIA PaCa-2 WT, PGS and ANXA1 KO. Nuclei were stained with DAPI. The merged image shows overlapping localization of the proteins (panels c, f, I, n). Magnification 63x. Bar=10μm.
The results relative to ANXA1 KO MIA PaCa-2 are representative to almost three analyzed clones with a similar behavior.

7.14 Effects of ANXA1 knockout on MIA PaCa-2 migration and invasion

Based on the information by immunoflurescence assay particularly about the F-actin distribution and in order to confirm the previous data with ANXA1 siRNA, we performed the same functional assays to analyze the migration and invasion ability of ANXA1 KO MIA PaCa-2 cells. Both Wound healing assay and invasion through coating of matrigel were executed on three KO clones compared with WT and PGS cells. In figure 7.15 it is possible to observe a significant reduction of migration rate (about the 40%) (Fig. 7.15A and B) and a stronger loss of invasion capability (about the 80%) (Fig.7.15C and D). Also in this case, the invasion experiment was performed with and without (data not shown) FBS on the lower chamber of transwells.
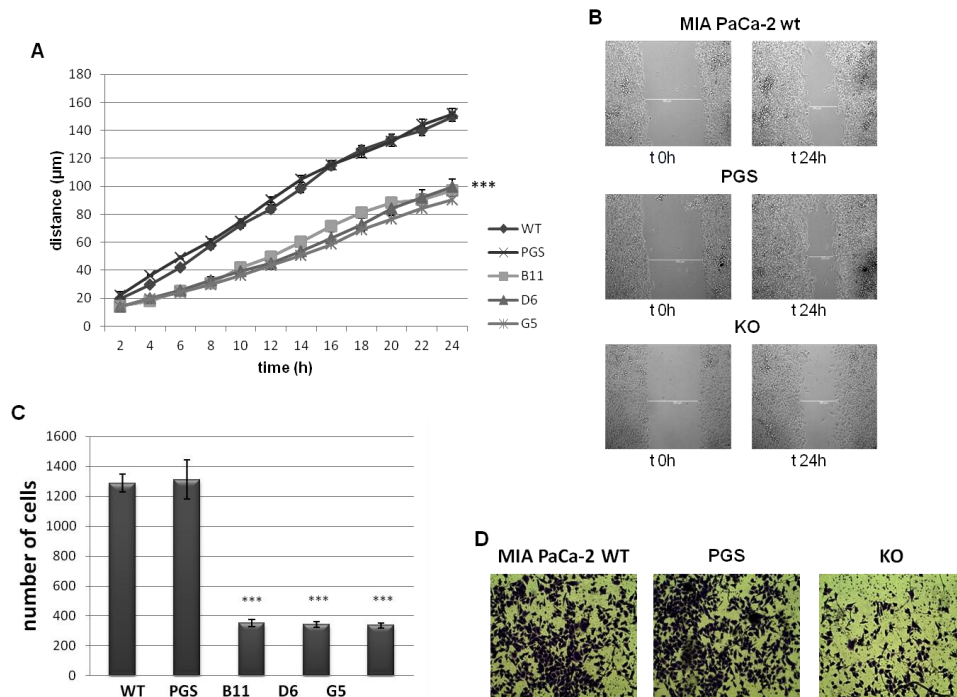
Figure 7.15: A, Results of Wound healing assay on ANXA1 KO MIA PaCa-2; ** p<0.01 vs untreated control. The data are representative of 5 independent experiments ± SEM. **B,** Representative images captured by TIME LAPSE microscope of the migration process of MIA PaCa-2 WT, PGS and ANXA1 KO. **C,** Invasiveness rate of ANXA1 KO MIA PaCa-2. Data represent mean cell counts of 12 separate fields per well ± SEM of 5 experiments. **D,** Representative imagines of analyzed fields of invasion assay. ** p<0.01 vs serum free (SF) control; *** p<0.001 vs SF control; ### p<0.001 vs control.

7.15 ANXA1 KO MIA PaCa-2 cells respond to the pro-migratory and pro-invasive effects of Ac2-26

The proteomic study has not identified any modification in the expression of the main proteins which are involved in the intracellular signaling triggered by FPRs. Furthermore, both FPR-1 and FPR-2 expressions are retained in MIA PaCa-2 ANXA1 KO compared with MIA PaCa-2 WT and PGS, as shown by cytofluorimetric assay in figure 7.16A. In order to confirm the activation of FPRs pathways in MIA PaCa-2 ANXA1 KO clones, receptor agonist (Ac2-26) and antagonist (Boc-1) have been used in migration and invasion assays. Both Wound healing assay and cell invasion through the coating of matrigel confirmed that Ac-2-26, the ANXA1 mimetic peptide, induced a significant increase of migration and invasion rate if compared with the controls. Interestingly, when treated with Ac2-26, MIA PaCa-2 KO clones migrate and invade in a very similar way of control MIA PaCa-2 WT and PGS, as evident in figure 7.16B and 7.16C, reporting the invasion assay. In the same manner of MIA PaCa-2 WT and PGS, Boc-1 reverted the Ac2-26 effects.
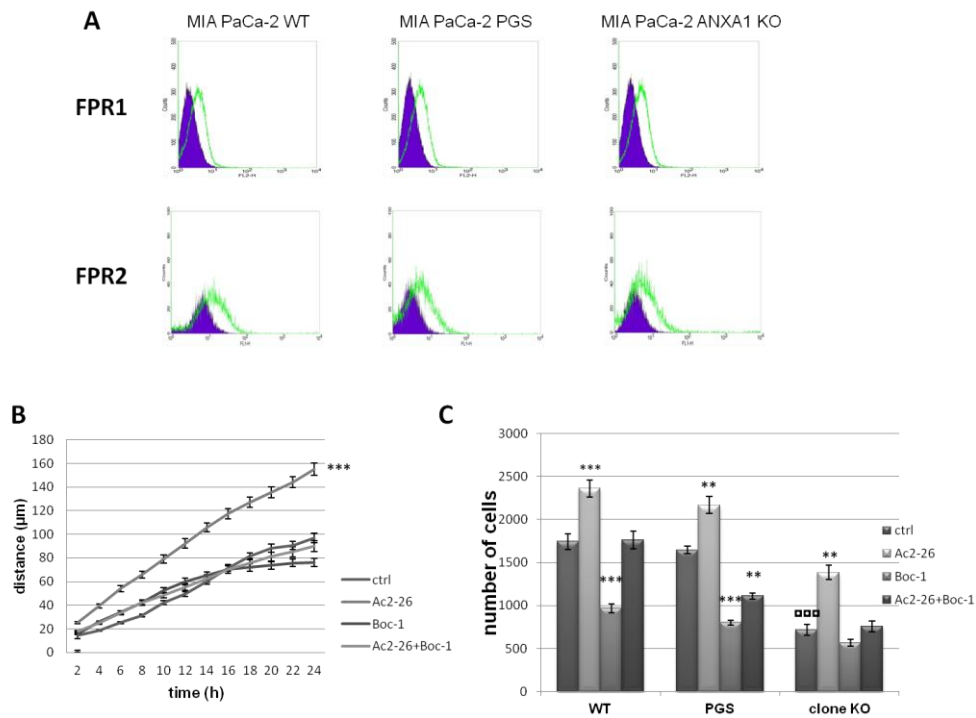
Figure 7.16: A, Cell surface expression of FPR-1 and FPR-2 in MIA PaCa-2 WT, PGS and ANXA1 KO cells was analyzed by flow cytometry. The violet areas in the plots are relative to secondary antibody alone. FPR-1 and FPR-2 signals are showed with green bends. **B,** Wound Healing assay on MIA PaCa-2 ANXA1 KO treated or not with Ac2-26 (1µM), Boc-1 (10 µM) and Ac2-26 + Boc-1. The migration rate has been calculated as reported in Material and methods section, ** $p < 0.01$ vs all the other experimental points. Invasiveness rates were measured in **C** ** $p < 0.01$ and *** $p < 0.001$ vs untreated control and ▫▫▫ $p < 0.001$ vs MIA PaCa-2 WT and PGS not treated controls. Data represent mean cell counts of 12 separate fields per well ± SEM of 5 independent experiments. The data relative to clone ANXA1 KO are representative of three analyzed clones.

7.16 Effects of ANXA1 knockout on MIA PaCa-2 proliferation

Based on the information obtained thanks to proteomic analysis, to complete the investigation of the functional role of ANXA1 in our experimental models, we analyzed also cell growth and proliferation rate. Therefore, ANXA1 KO MIA PaCa-2 show a faster propagation rate with respect to MIA PaCa-2 WT and PGS technical control. So, through an MTT assay, the result was confirmed as shown in the graph in figure 7.17A. The major proliferative capacity of these cells is represented also by a more prompted cell cycle in the direction of S/G2 phases (Fig. 7.17B). For this reason we analyzed by Western blot the expression of other proteins that could play a critical role, using antibody against the Cyclin A (Fig. 7.17C). Cyclin A is particularly interesting among the cyclin family because it can activate two different cyclin-dependent kinases (CDKs), CDC2 and CDK2, and functions in both S phase and mitosis, it starts to accumulate during S phase and is abruptly destroyed before metaphase implicating the control of DNA replication; ectopic expression of cyclin A in mammalian cells accelerates the entry of G1 cells into S phase [408]. Furthermore, confirming the data obtained by the proteomic analysis, we showed also the increase of Aldehyde dehydrogenase7A1 (ALDH7A1), by Western blot shown in figure 7.17D. This is a protein mainly involved in the process of cell detoxification, as it is a member of the alcohol metabolism, but there are several experimental data which correlated ALDH7A1 cytosol localization with the regulation of cell cycle. Particularly, in some tumor models, the effects of tumorigenic signals induce the increase of protein expression. In addition, it has been reported that using shALDH7A1, the levels of cyclin A significantly decrease [409; 410]

On the other hand, the classical ERK family (p42/44 MAPK) is known to be an intracellular checkpoint for cellular mitogenesis: in cultured cell lines, mitogenic stimulation by growth factors correlated with stimulation of p42/44 MAP kinase [411]. After the activation of receptor tyrosine kinases (RTKs) or GPCRs by growth factors or mitogens several signals are triggered until the phosphorylation of ERK1/2 by MEK1/2, on both threonine and tyrosine. The phosphorylated ERK1/2 translocate to the nucleus where they activates multiple transcription factors ultimately resulting in effector protein synthesis and causing changes in cell proliferation and survival [412]. The increase of the phosphorylated isoform of ERK is represented in Western blot in figure 7.17E.
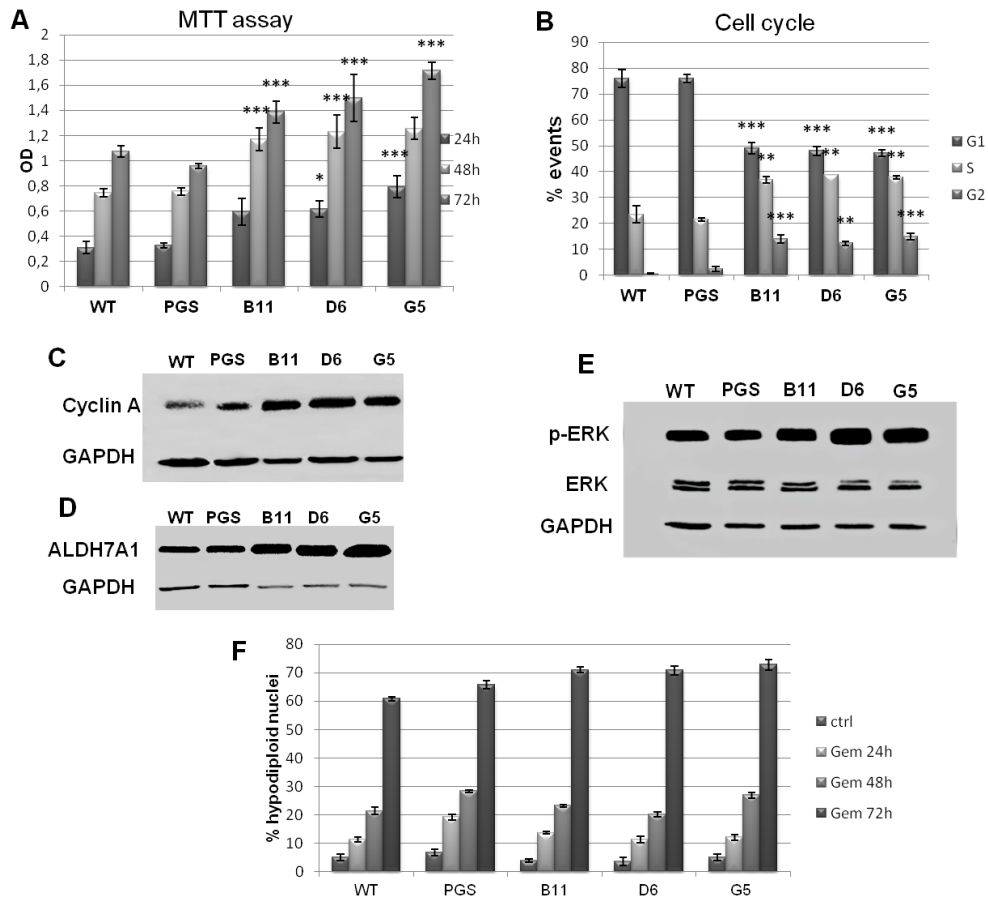
Figure 7.17: A, MTT assay at 24, 28 and 72h on MIA PaCa-2 WT, PGS and ANXA1 KO (clones B11, D6, G2, G4 and G5). **B,** Cell cycle analysis thorough PI staining, the graph is representative of 72h of culture, after 24h of serum starvation.
C, Western blot of Cyclin A expression on the same experimental points. **D,** Western blot showing ALDH7A1 expression. **E,** ERK and phospho-ERK on MIA PaCa-2 WT, PGS and ANXA1 KO clones as B11, D6 and G5. All protein levels are normalized on GAPDH ones. All the shown data are representative of 5 experiments with similar results.

7.17 ANXA1 is not involved in apoptosis induced by gemcitabine

In several system, such as tumoral or inflammatory ones, ANXA1 has been described as a protein involved in apoptosis mechanisms. In PC system there is no evidences about this aspect. However we investigated the apoptosis induced by gemcitabine, the false nucleotide still used in PC chemotherapy, to test the sensitivity of MIA PaCa-2 ANXA1 KO compared to MIA PaCa-2 WT and PGS. Generally, MIA PaCa-2 cell line does not answer significantly to gemcitabine and cells appear quite resistant to lots of chemotherapic molecules, probably due to the membrane expression of high levels of MUC1 and MUC4 that increase the phosphorylation of pro-apoptotic protein Bad in association with the increased phosphorylation of HER2 and ERK [131; 134]. As reported in figure 7.18, MIA PaCa-2 cells show a worthy sensitivity to gemcitabine 10 μM only at 72h and there are no significant changes in response to the molecule among WT, PGS and ANXA1 KO cells. This data confirms that ANXA1 in PC is not involved in apoptotic process.
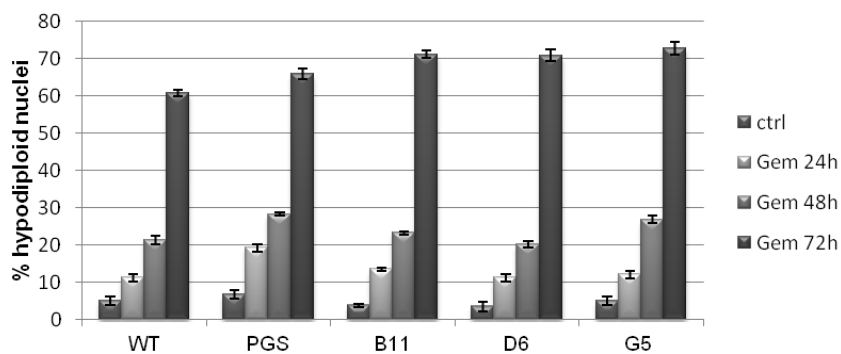
Figure 7.18: Analysis of hypodiploid (apoptotic) nuclei by cytofluorimetric assay of the effect of gemcitabine 10 μM at 24, 4 and 72h on MIA PaCa-2 WT, PGS and three clones ANXA1 KO. Tha data are representative of 5 experiments with similar results.

7.18 KO of ANXA1 decreases the metastatic potential of highly aggressive MIA PaCa-2 cells *in vivo*

Since the initial phases of the study about cancer of the digestive apparatus, MIA PaCa-2 cells were chosen to establish human pancreatic tumor xenografts both for subcutaneous and orthotopic models [413]. In order to validate *in vivo* the data collected *in vitro* about the effect of ANXA1 in PC progression, the generated cell lines were implanted directly into the pancreas of SCID female mice as reported in Material and methods section. The animal wellness has been checked during all the experimental period evaluating their motility and measuring once a week the weight: no significant weight loss has been found, (Fig.7.19A). After 5 weeks from the implantation, mice were sacrificed and the tumors generated in the pancreas were evaluated. KO of ANXA1 had no effect on primary cancer growth. As shown in figure 7.19B, the tumor mass in mice implanted with MIA PaCa-2 ANXA1 KO did not appear smaller in a significant manner if compared with those extracted from mice implanted with MIA PaCa-2 WT and PGS. This aspect is confirmed also through the evaluation of tumor weight displayed in the graph in figure 7.19C. But we also determined whether ANXA1 depletion from highly invasive MIA PaCa-2 cells can reduce metastasis formation. For this purpose, we analyzed the livers of the animals since they represent the first affected organ form PC metastatic process. The livers harvested from mice injected with MIA PaCa-2 WT and PGS presented numerous metastasis which were particularly notable since they emerged as white spots on the surface of a brick-red organ. Additionally, the interested livers lost their own physiological integrity with indented profiles and reduced compactness. On the other hand, the livers extracted from the animals implanted with MIA PaCa-2 ANXA1 KO retained their characteristic colour and tissue density and showed reduced metastatic lesions (Fig. 17.9D). Furthermore, the tissues processed with H&E (Fig. 17.9E) revealed distinctly stained areas in a well defined larger zone. It is possible to highlight smaller cells with a different morphology and staining in the upper areas of the H&E images of the relavite MIA PaCa-2 WT and PGS mice livers. The image of the liver of mice implanted with ANXA1 KO MIA PaCa-2 cells revealed a more regular tissue. These findings on the liver sections confirm the infiltration of tumor metastasis.
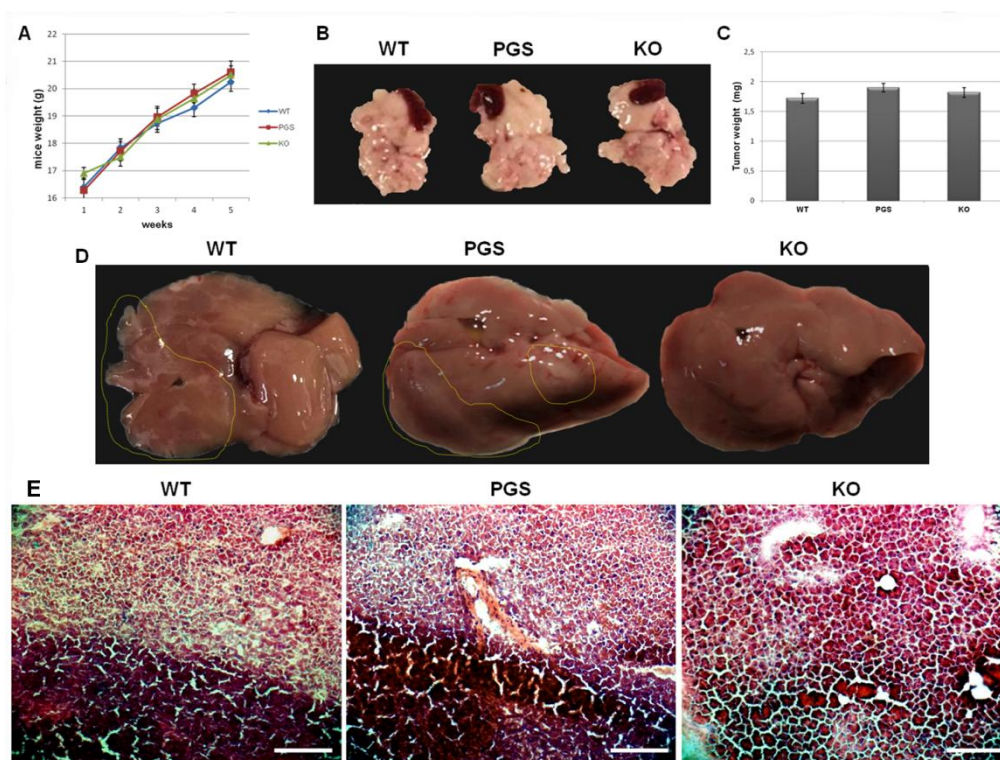
Figure 7.19: A, Average body weight of mice measured weekly from the implantation until the sacrifice. **B,** An exemplar image, including also the spleens, of the tumor volumes generated in pancreas by MIA PaCa-2 WT, PGS and MIA PaCa-2 ANXA1 KO. **C,** Histogram of tumor weights. **D,** Photos of mice livers, the selected areas represented the parts affected by metastatic lesions. **E,** The relative liver sections have been stained through H&E. Bar=100μm.
The results relative to ANXA1 KO MIA PaCa-2 are representative to almost three analyzed clones with a similar behavior.

ANXA1 is the first characterized member of annexin superfamily, it was discovered as an antinflammatory protein but, in the last 20 years, ANXA1 has been involved in a broad range of molecular and cellular processes, including inhibition of cell proliferation, the regulation of cell migration, differentiation and death both in physiological and pathological models [414]. In tumors ANXA1 performs multiple functions and it appears to behave either as a tumour suppressor or an oncogenic gene. More studies are required to investigate in detail the role of ANXA1 in cancer progression since its mechanism of action has not been yet completely clarified.

About its involvement as oncogenic factor, ANXA1 participates in the maintenance of a stem-like/aggressive phenotype in prostatic carcinoma, where the protein seems overall down-modulated [287]. On the other hand ANXA1 contributes to tumor progression inducing cell migration and invasion, leading to metastatization, drug-resistance and poor prognosis, as shown in breast cancer, colon and gastric carcinoma and melanoma, all tumors where the protein is up-regulated [287; 289; 290; 282; 283; 296; 299; 415].

It has been shown that ANXA1 over-expression in the tissues from patients with PC is correlated with poor differentiation and prognosis and seems to be associated with malignant transformation and cancer development [302; 303].

Furthermore, in PC there is an abnormally high expression of a number of important tyrosine kinase growth factors and receptors, like the EGF family, which may contribute to the neoplasia growth by autocrine and paracrine effects. Immunohistochemistry studies showed that EGFR over-expression positively correlates with advanced tumor staging and lymph node metastasis [303; 416]. For example, activating mutations of the K-*ras* oncogene have also been shown to promote a remarkable array of cellular effects such as proliferation, survival and invasion with poor prognosis and poor response to many existing therapies [17; 70]. ANXA1 is commonly reported as a substrate of EGFR, which is involved in the post-transductional modifications (phosphorylations) that the protein undergoes to be, later, cleaved and/or translocated to other sub-cellular compartments, above all to plasma membrane. In PC the constantly activated EGFR pathway could promote ANXA1 up-regulation and modifications which might be associated with PC acquired aggressive behavior.

In this PhD project, we report that ANXA1 might have a role in PC cell migration and invasiveness and consequently to be involved in the metastatic capability *in vivo*.

First of all, we started analyzing ANXA1 expression and localization in MIA PaCa-2, PANC-1, BxPC-3 and CAPAN-2 PC cell lines and we found that

all of them expressed high and similar levels of ANXA1. Many recent experimental evidences report that *in vitro* tumor models could present at least two phenotypes that frequently overlap. The better characterized phenotypes can be classified in a less aggressive epithelial-like and a more aggressive mesenchymal-like ones [163; 389; 383]. In the latter, ANXA1 is mainly localized in the regions involved in cellular motility, suggesting an intracellular role for the protein in the processes of cell migration/invasion. Since CAPAN-2 and BxPC-3 cells show a less aggressive phenotype, we chose to use only MIA PaCa-2 and PANC-1 cells that present more marked mesenchymal features.

In particular, concerning cellular motility, ANXA1 actions are exerted in the intracellular environment where it contributes to the dynamic reorganization of the actin cytoskeleton, but also extracellularly *via* FPRs in autocrine/paracrine manner [417]. For this reason, we first investigated the placement of ANXA1 in the sub-cellular compartments involved in motility, where the protein co-localizes with FAK and F-actin, two proteins particularly known to mediate the migration process [418]. Then, about the second aspect, we investigated the expression and activation of FPRs, as ANXA1 receptor partners. FPRs are expressed in several cellular populations and bind a variety of exogenous and endogenous ligands that elicit differential biological responses. ANXA1 and its N-terminal mimetic peptide, Ac2-26, are endogenous FPR ligands. Flow cytometry and PCR analyses showed that MIA PaCa-2 and PANC-1 cells express FPR-1 and FPR-2. Moreover, experiments on the mobilization of intracellular calcium have confirmed the activity of the FPRs in these cell lines, following stimulation with the Ac2-26 peptide. We found no receptor activation in presence of Boc-1, a molecule that at a dose of 10 μM can be considered as able to block all the three receptor isoforms [313].

To find a functional role of ANXA1, we used specific siRNAs to down-regulate its expression in both MIA PaCa-2 and PANC-1 cells and we found a significant decrease of the migration rate and a marked suppression of the invasiveness of these cells, confirming that intracellular ANXA1 is involved in PC cell migration/invasion. Exogenous administration of Ac2-26 was also able to increase migration speed and invasiveness of cells through coating of matrigel, compared to relative controls. The specificity of Ac2-26-induced effects on wound closure and invasiveness through the FPRs was confirmed by administration of the FPR pan-antagonist Boc-1. These data confirm the involvement of the main pathway which follows the activation of FPRs since the triggered Rho GTPases pathway is a key regulator of many functions, including cell adhesion, chemotaxis and superoxide generation. Particularly,

Rac and Cdc42 are involved in the remodeling of the actin cytoskeleton at the leading edge of migrating cells. The activation of Cdc42 is thought to release the auto-inhibited conformation of the Wiskott–Aldrich syndrome protein (WASP), a multi-domain protein that is an activator of the nucleating Arp2/3 complex [320].

ANXA1 has been shown to localize to the cell surface of various cell types including leukocytes, endothelial cells, lung epithelial cells and synoviocytes where it is thought to be important in biological functions [247; 419; 258; 420]. As previously reported, the ANXA1 translocation to plasma membrane and its secretion, through a not yet known mechanism, are outcomes of post-transductional modifications and/or proteolytic cleavages. These modifications concern Tyr21 which is the target of EGFR kinase and Ser27 phosphorylation by PKC that induces a conformational change, including proteolytic cleavages, probably related to the described membrane aggregation properties [257; 421]. As shown through compartmentalized protein extractions, we also report the presence of the full-length form (37kDa) accompanied by the appearance of the 33kDa cleavage product of ANXA1 only in MIA PaCa-2 cells. Furthermore, these two forms are secreted outside the cells, since they appeared in cellular supernatants. LC-HRMS/MS, used to characterize secreted forms of ANXA1, showed a peptide with molecular weight of 2744.324 demonstrating, for the first time, the presence of the fragment 4-26 of ANXA1 in the extracellular environments. Since we found that MIA PaCa-2 cells exhibit a strong level of extracellular ANXA1 in all the isoforms (37, 33 and 3kDa), we have hypothesized an important role for the secreted protein in regulating PC cell migration/invasion. To demonstrate this hypothesis, we tested the effect of a blocking antibody which, binding the protein, inhibits its binding to FPRs. The effect is the reduction of motility of MIA PaCa-2 cells. Our results are consistent with the observed role of ANXA1 in head neck squamous cancers where the protein over-expression was associated with increased tumour invasiveness and metastasis and in SK-CO15 intestinal epithelial cells where ANXA1 regulated cellular invasive behaviour acting through FPRs [422; 283]. Moreover, we showed that ANXA1 blocking antibody had no effects on PANC-1 cell motility, confirming that, differently from MIA PaCa-2, no secreted forms of ANXA1 protein were observed in protein supernatant extracts from PANC-1 cells. However, it is evident an increase in migration and invasiveness rate of cells treated with Ac2-26: these findings are consistent with the expression of FPR-1 and FPR-2 that we found on the surface of these cells. Consequently, we reasoned on the role of the extracellular protein in PC cell line migration and invasiveness and we supposed that the more invasive behavior of MIA PaCa-2 than PANC-

1 cells could be due to the presence of secreted forms of ANXA1 [423; 424]. To further confirm this aspect, we found that the addition of MIA PaCa-2 supernatant to PANC-1 cells significantly stimulated PANC-1 migration rate. Conversely, PANC-1 supernatant administration on MIA PaCa-2 cells had no effects on cell motility, confirming that the secreted forms of ANXA1 protein may be able to induce PC cell migration and invasion [425].

Among the other PC cell lines, MIA PaCa-2 cells are commonly used to induce tumor xenografts in nude mice because of their strong capability to develop not only the largest tumoral mass but also metastasis [383]. So we chose this cell line to create KO ANXA1 clone in order to further investigate the role of this protein *in vitro* but above all *in vivo*. The technology used to induce the KO has been the Gene CRISPR/Cas9; this latter makes use of the endonuclease activity of the enzyme Cas9, directed to the gene target by a gRNA transcripted just by the plasmid. The generated effect consists of a DSB on a portion of the targeted coding sequence which will be repaired by the NHEJ pathway [365; 366]. Finally we obtained, through the limit dilutions approach, the ANXA1 KO clones together with the MIA PaCa-2- PGS, a scrambled DNA plasmid we have used as technical control, and the MIA PaCa-2 WT. This technology has been devised to prevent off target effects that are very common in these experimental setups [370]. To characterize in detail the MIA PaCa-2 ANXA1 KO with respect to MIA PaCa-2 PGS and WT, a proteomic analysis was performed to evaluate the expression of which proteins could be directly or not affected by the absence of ANXA1. Among the detected proteins, of particular interest were the proteins of the cytoskeleton that are involved in the maintenance of its stability and plasticity. In addition, changes in expression of other components of the ANXA family were not observed confirming the absence of important off target effects. Among the cytoskeleton proteins, the expression of F-actin was not modified whilst the phalloidin staining proved a confused distribution in the cytosol and the lack of lamellopodia and stress fibers, the well documented sub-cellular structures which are known to be assigned to cell motility. It is widely accepted that actin stress fibers promote cell migration, forming an assembly mechanism which exhibited an uniform polarity, that is pointing towards the leading edge, with their constituent filament barbed ends [426]. Since cell motility is driven by the assembly of both protrusive and contractile actin filaments, the disruption of this organization led us to investigate again the migration and invasion processes, confirming their strong reduction in MIA PaCa-2 ANXA1 KO. These results, taken together, show that ANXA1, in the intracellular environment, directly mediates the cytoskeleton integrity and distribution, controlling the rate of the actin filament assembly and

disassembly. However, the potential role of extracellular ANXA1 is likely retained because the expression and activation of FPRs is not affected by the absence of the protein. In fact, in presence of agonist, the Ac2-26 peptide, and antagonist, Boc-1, the MIA PaCa-2 ANXA1 KO cells migrate and invade following the same trend of the parental control MIA PaCa-2 WT and MIA PaCa-2 PGS. Thus, the capability of ANXA1 to act in the extracellular environment, binding FPRs and triggering the increase of migration and invasion rate, has been further confirmed.

Based on our findings, it is possible to assert that ANXA1 overall contributes to the maintenance of a more aggressive phenotype of PC cells. Its KO induces not only a strong decrease of migration and invasion speed, but also a greater proliferation rate, a typical aspect of more differentiated tumors, which could be, in this way, more easily attacked by the chemotherapic agents. Nevertheless, ANXA1 is not involved in the apoptosis process mediated by gemcitabine, the main anti-tumoral agent still used in the clinical practice.

With the purpose to investigate the role of ANXA1 *in vivo*, orthotopic xenotrapiants with MIA PaCa-2 WT, PGS and ANXA1 KO have been created in SCID mice. ANXA1 KO did not affect primary tumor growth, but significantly reduced the number of metastases, above all the liver ones.

Taken together these results indicate that ANXA1 is important in migration and invasiveness of PC cells. Furthermore, it has been shown that the EMT process may not be necessary to metastatization: two studies in *Nature* report that EMT is not required for metastasis in mouse tumor models. Both in a lung and pancreatic carcinoma models, the EMT suppression did not affect the number of circulating tumor cells, the ability of tumor cells to form tumor spheres *in vitro* or the overall frequency of metastasis [427; 428]. Moreover, carcinogenesis is a multistep process: to reach the malignant phenotype, multiple alterations affecting several levels of growth control are required. It is important to consider the origin tissue of tumor; in the case of PC, the pancreatic ductal basal cells are an important regulator of the differentiation of the pancreatic epithelium. The pancreas is composed of simple epithelia with a keratin (CK) profile very similar to liver: the pancreatic duct cells exhibit, as the bile duct cells (CKs 7, 19, 20) and the hepatocytes have the same CKs as pancreatic acinar cells (CKs 8 and 18), also present in the luminal side of ducts (Fig. D.1) [429]. In addition in the pancreas, the ductal keratin profile (CKs 7, 19) is associated with poor differentiation and/or potential stem cells or progenitors. In epithelia where the location of the progenitor cells is known, like for instance the epidermis, this location (basal layer) coincides with the distribution of CK 19, whereas the differentiated cells

lack CK 19 expression. The CK profile can be actually used to distinguish the several phases of physiological morphogenesis, both in the embryonic development and in case of damage, and pathological tumor development [430]. Particularly, "basalness" has now acquired a dual meaning and could be related with an epithelial or progenitor/stem cell origin [431]. The possible association between EMT and the existence of a basal-like phenotype has been also demonstrated in a study of human breast cancer, suggesting that EMT may not be a sign of overall tumor dedifferentiation but, rather, the manifestation of a specific phenotype of stem cell origin showing more aggressive behavior [180]. In fact, cells with a basal phenotype probably have a higher proclivity to develop EMT changes and subsequently undergo invasion [432]. Several analysis reported a negative correlation between the high expression of the luminal CK 8/18 and the existence of metastasis [296; 432]. In our ANXA1 KO MIA PaCa-2 cells, we found a significant up regulation of the CK couple 8/18, a data that can be considered particularly consistent with the acquired ANXA1 KO cells behavior both *in vitro* and *in vivo*. Our analyses demonstrate an inverse relationship between the presence ANXA1 expression and the degree of tumor differentiation, an important histopathological criteria in tumor characterization and the definition of prognosis for patients.
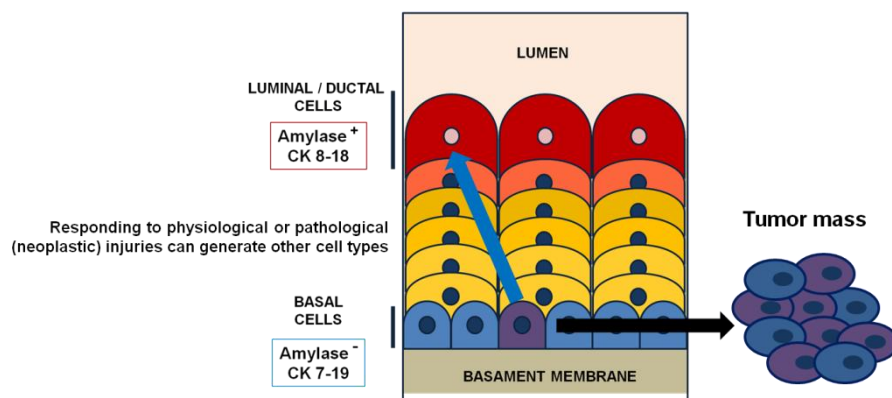
Figure D.1: the normal pancreatic ducts epithelium is composed of a bilayer of basal and luminal cells, these latter are discernible by amylase, among the other possible markers, and the CK couple 8/18. It is also synthesized the expansion of tumor mass from a single progenitor described as a basal phenotype (amylase$^-$; CK7/19$^+$) in response to oncogenic stimulation. In parallel, the same undifferentiated cell has the potentiality to became a luminal one to recover the eventually damaged epithelial layer

These findings raise the possibility that ANXA1 could regulate metastasis *in vivo* and may represent a novel approach to cancer treatment. However, further studies are needed to address this point. It could be interesting to make additional functional studies to determine the role of ANXA1 in generating stem-like, so less differentiated, tumor phenotypes and to correlate it to PC patients' prognosis, rate of tumor metastatization, response to chemotherapy, and, generally, time survival.

APPENDIX

COMPUTATIONAL DESIGN OF PROTEIC INHIBITORS OF ANXA1

A.1 Background

Annexins participate in membrane-related events such as the mediation of membrane-membrane contacts, the regulation of membrane-cytoskeleton linkages and ion transport across membranes. In this section it is described the structural aspect of ANXA1. Generally, it is reported that each annexin is composed of two parts, a major C-terminal core domain and a minor N-terminal tail domain. The similar properties of all annexins regarding Ca^{2+} and phospholipids seem to be due to the C-terminal core domains that show highly conserved sequences and structures. Since the N-terminal tail domains of annexins differ widely in length and sequence, it has been proposed that these portions can preserve the functional protein specificity. Although the 3D structures of more than 10 annexins [433], are presently available, the knowledge of the N-terminal domain structure is very scant because these domains are either naturally short or truncated [434, 435; 436; 437]. In this last case, for example, ANXA1 lacks the residues 1-26 since the residue Lys-26 is prone to tryptic digestion [437].

Annexins are excellent models for studying the folding mechanisms of multidomain proteins. All of them have a core domain that contains four (in the case of ANXA6 eight) homologous repeats (numbered I to IV) of five α-helices each. These repeats are arranged into a slightly curved disc with the Ca^{2+}-binding sites on the convex side. These N-terminal domains are different in sequence and length, varying from a short tail of 11 to 19 residues (ANXA 3, 4, 5, 6, 10, 12, 13), to 33 to 42 residues (ANXA 2 and 1, respectively), to more than 100 residues (ANXA 7 and 11). They harbor binding sites for S100 proteins (ANXA1: S100A11, ANXA2: S100A10, ANXA11: S100A6) and various phosphorylation sites, as in case of ANXA1 and 2, for serine/threonine and tyrosine specific kinases.

Comparative structural analysis suggests that interdomain interactions may play critical roles in the folding of ANXA1, it is a symmetric protein and its sequences homology is represented in figure A.1. However, the structure of ANXA1 can be presented as composed of two modules. One module consists of domains I and IV, and the other domains II and III. Each module has a hydrophobic interface between its constituents. The two modules are assembled with mostly hydrophilic interactions between domains II and IV. It

is tempting to speculate that folding of ANXA1 follows a sequential process with domain I as an autonomous initial folding unit. The folded structure of domain I facilitates the folding of domain IV through the hydrophobic interface. Then, the hydrogen bonds and hydrophobic interactions between domains IV and II help domain II to get rid of the non-native cap and reach the native structure. Domain II, in turn, assists the folding of domain III through many hydrophobic interdomain interactions [438; 439].

Figure 8.1: sequence alignment of the four domains. The hydrophobic core residues are shown in yellow and other conserved residues are in blue [439].

Biochemical studies on the ANXA1-phospholipid interaction have shown that the N-terminal domain is important for the aggregation of vesicles but not for the binding of ANXA1 to negatively charged phospholipids [440; 441].

As reported in figure A.2, the N-terminal ANXA1 peptide contains 41 residues. The residues 33-41 form an unstructured coil that runs along the concave side of the molecule, instead the first 26 amino acid residues of the N-terminal domain form two α-helices. The α-helix formed by residues 18-26 interacts with the surface of repeat IV of the core domain, then, the direction of the chain changes at level of the position 17 and the α-helix formed by residues 2-16 points turns towards the convex face of the molecule. Finally, residues 27-33 can be viewed as an extension of the unstructured strand running toward repeat IV and further on to repeat III [206].
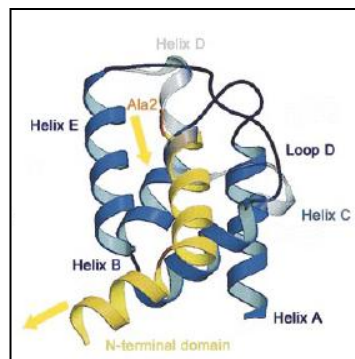
Figure A.2: overlay of the three-dimensional structures of repeat III (bue) of ANXA1 plus residues 2-26 to the N-terminal domain (yellow). The yellow arrow indicates the direction of the α-helices which are connected to the core domain *via* an extended linker [206]

The structure of an ANXA1 N-terminal peptide comprising residues 2-12 in complex with the S100A11 protein, in a specific way, was published [442]. Furthermore, thermodynamics studies of peptide binding, showed not only that this interaction is mediated by calcium ions, but also that it happens in a specific way. Particularly, ANXA1 binds S100A11 and, following more recent works, also S100A6 even if this interaction is not still characterized [443]. Furthermore, the importance of calcium ions was yet described thanks to studies based on X-ray-crystallography: in the presence of $CaCl_2$ 10 mM six calcium ions are found to bind to the truncated ANXAI, two pairs in domains I and IV and one pair in domains II and III [439].

The N-terminal portion of ANXA1 is also responsible of the interaction with another ANXA1 molecule, but, in contrast to the annexin 12 hexamer that can also be interpreted as a trimer of dimmers, the ANXA1 dimer does not show complete face-to-face orientation [444; 445]. The calcium remains important for the dimerization but it can be substituted by a residue of Lys250. The coordination of Lys250 in the binding site of repeat II is mediated by the backbone carbonyl oxygen atoms of Lys128, Gly129 and Gly131 residues in the same loop in the absence of calcium in the full length ANXA1 structure. On the other hand, calcium ion in the type II-binding site of repeat II arranges itself in the middle f the backbone carbonyl oxygen atoms of Met127, Gly129 and Gly131 and Asp171 (two water molecules complete the coordination sphere but are not shown in here). However, it is not known whether the crystallographic dimer represents a physiological dimer [206].

As the results of this PhD project indicate that both intracellular and extracellular ANXA1 is involved in promoting progression and metastatization of PC cells, the protein may represent an attractive target for pharmacological modulation. For this reason, we promoted the construction of peptides that can inhibit the protein effects. This section focuses on the computational design of this molecules and other biochemical experiments have been executed to test the peptide sequence planned and synthesized.

A.2 Methods and results

The approach we used is based on the aspect for which the structure of full length ANXA1 in the absence of calcium represents the inactive form of the protein with its N-terminal domain buried inside to the protein core. Upon calcium-mediated membrane binding, the N-terminal domain is ejected from the hydrophobic pocket formed by repeat III and ends up solvent-accessible on the concave side of the molecule. In this proposed activated conformation, the two α-helices of the N-terminal domain would be free to move around *via* the flexible linker formed by residues 27-41. After this calcium-triggered switch in conformation the previously buried N-terminal domain would be free to interact with new partners. These could include that S100A11 protein or a second ANXA1 molecule can bind the N-terminal domain of ANXA1. However, it is tempting to speculate that each Ca^{2+}/membrane-activated ANXA1 molecule could now bind to a second membrane *via* its exposed N-terminal domain providing a mechanism for membrane aggregation; this model is still not well defined [208; 209; 446].

The modeling study was organized in three section. Firstly, new sequences capable to bind specifically the *N*-terminal portion of ANXA1 have been prepared for an in silico screening. A combinatorial approach, swapping 4 residues (namely 230, 253, 255, and 261) with a small subset of amino acids (polar, apolar, and charged) has been used. Successively, we have checked the stability of the designed peptides and their ability to bind ANXA1. The stability and the conformation of the peptides have been tested by means of molecular dynamics (MD). Finally, the free energy of binding of the dimer ANXA1-inhibitor was calculated by steered molecular dynamics (SMD) method.

A.2.1 Design of new sequences

The design of potential inhibitor of ANXA1 started from the wild type sequence of annexin (uniprot P04083). The three helix surrounding the *N-*

term of ANXA1 with a length of 44 residues, have been considered as a starting point for punctual mutations. To reduce the number of peptides generated by combinatorial approach, we focused mutations on the residues 230, 253, 255, and 261, only. These amino acids have been replaced with Ala (hydrophobic), Ser (polar), Lys (positive), Asp (negative), and Cys, for a total of 625 peptides.

Most of these peptides were suspected to have no secondary structure and a preliminary analysis with the use of HMM analysis (http://toolkit.tuebingen.mpg.de/hhpred) was conducted. The peptides with a plausible secondary structure have been further controlled by MD.

A.2.2 Structure check

Several peptides have been selected for structure check. It was important to determine if a peptide can spontaneously acquire a clear and stable secondary structure, and/or a secondary structure can be observed upon binding with the *N*-terminal portion of ANXA1.

The propensity to acquire spontaneously a secondary structure was checked via *ab initio* folding of the peptides (implicit water MD). The stability of peptides alone and of the complexes were controlled by all atom molecular dynamics, starting from the folding structure obtained by homology. The RMSD of the peptide is followed for 50 ns and calculated respect the initial structure.

Molecular dynamics simulations were performed using the script protein_folding_by_MD.js accessible in Abalone software (http://www.biomolecular-modeling.com/Abalone/), setting AMBER94 force field, temperature to 350 K and implicit water model (Fig. A.3). After force field assigning, we performed structure optimization to avoid overlapping. The simulation time of 50 ns was sufficient to reach the native protein conformation. Also to reduce the computational time and cost we used a grid (GRIMD) to distribute all jobs [447]. Energy minimization was carried out with combined steepest descent and simulated annealing by fixing the backbone atoms of the aligned residues to avoid potential damage to the initial model.
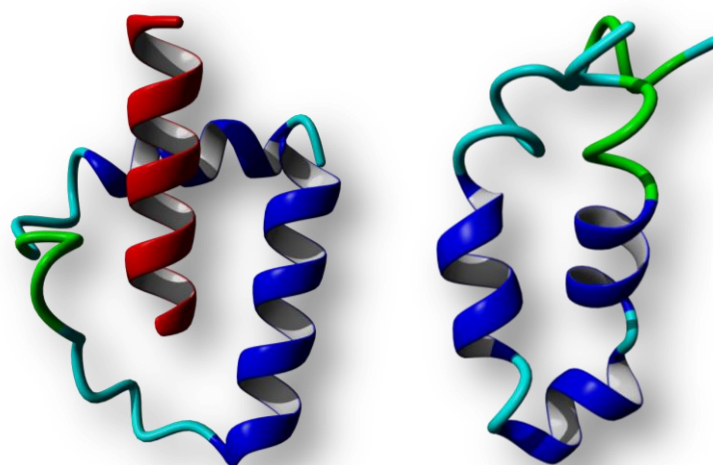
Figure A.3: comparison between 3D-structure of ANXA1 wt and *ab initio* folded inhibitor. On the left is reported the portion of 44 residues of ANXA1 surrounding the *N*-term portion (in red). On the right is shown a designed inhibitor folded by MD. MD technique was able to fold peptides mimicking the 3D-structure of the ANXA1 wild type.

A.2.3 Binding energy calculation

The free energy of binding was then calculated to make an esteem of the affinity of these peptides. The steered molecular dynamics (SMD) technique was chosen.

Each system consisted of a potential inhibitor and the core domain of the ANXA1 portion.

We collected the trajectory traced when the *N*-terminal helix of the ANXA1 is pulled from the inhibitor to the outside. The SMD was carried out using the software YASARA Structure 15.6.21 [448].

The starting structure for the simulations of the ANXA1 was extracted from the X-ray structures from the PDB database (PDB code 1HM6). Other molecules have been removed. A cubic periodic simulation cell of 512000 Å^3 was built around the entire complex.

The charges were assigned at physiological conditions (pH 7.4). The simulation box was filled with water choosing a density of 0.997 g/mL.

The simulation cell was neutralized with NaCl with a final concentration of 0.9%. We minimized the energy of the system using first a steepest descent minimization followed by a simulated annealing

minimization. The pulling acceleration of the ligand was 3 Å/ps^2. The simulation was stopped when the distance between the centers of mass of receptor and ligand was > 30 Å.

Several snapshots were selected from the SMD simulation at regular time intervals (each 500 ps). All simulations were performed with the software YASARA Structure 15.6.21. A simulation cell was centered and dimensions of the box were adapted for each structure to cover the entirety of the system. We used AMBER03 as force field with long-ranged PME potential and a cutoff of 8.0 Å, under periodic boundary conditions. We calculates the binding energy between the *N*-term of ANXA1 and the potential inhibitor according to the current force field. As control we used a scrambled peptide (Fig. A.4).
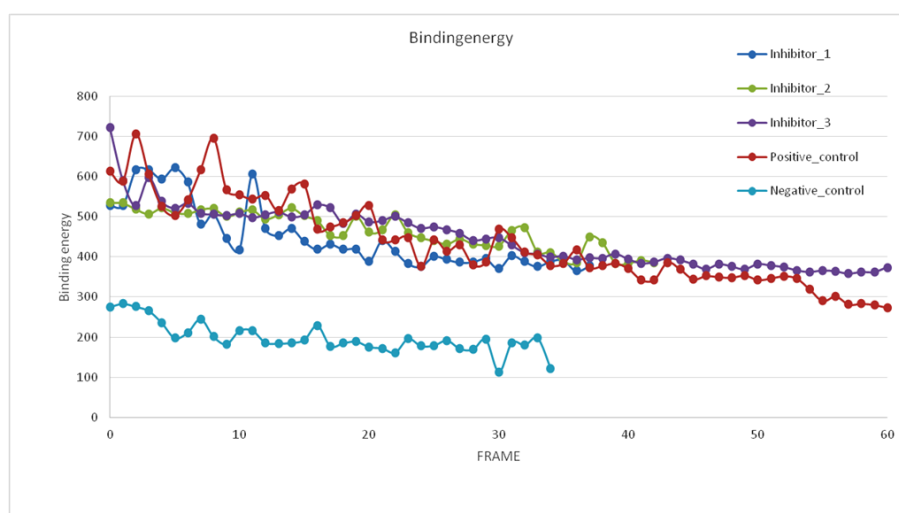
Figure A.4: binding energy evolution evaluated by SMD. The more positive values of the binding energy correspond to better interaction. We used a scrambled peptide as negative control, while the portion of ANXA1 of 44 residues surrounding the N-term portion has been taken as positive control. The scrambled peptide was capable to interact to the N-terminal portion of ANXA1 through unspecific and transient weak interactions. All but the scrambled peptide showed a high and specific interaction suggesting effective binding.

[1] Edlund H. 2001 Developmental biology of the pancreas. *Diabetes* **50(1):**S5-9.

[2] Hepatobiliary and Pancreas Surgery Surgical Options for Biliary Injuries and Pancreas Disease.
http://www.cpmc.org/advanced/liver/patients/topics/PP-hepatobiliary.html

[3] Hruban R.H, Pitman M.B, Klimstra D.S. 2007 *AFIP Atlas of Tumor Pathology, Fourth Series, Fascicle Tumors of the pancreas. American Registry of Pathology, Washington, DC in collaboration with the Armed Forces Institute of Pathology.*

[4] Bockman D.E. 1993 *Anatomy of the Pancreas. The Pancreas: Biology, Pathobiology, and Disease, Second Edition, edited by Go VLW, et al.* Raven Press Ltd.

[5] Daniel S. Longnecker. 2014 Anatomy and Histology of the Pancreas Pancreapedia: Exocrine Pancreas Knowledge Base. 10.3998/panc.2014.3.

[6] Kern H.F. 1993 *Fine Structure of the Human Exocrine Pancreas. The Pancreas: Biology, Pathobiology, and Disease, Second Edition, edited by Go VLW, et al.* Raven Press Ltd.

[7] Valentijn K, Valentijn J.A, Jamieson J.D. 1999 Role of actin in regulated exocytosis and compensatory membrane retrieval: insights from an old acquaintance. *Biochem Biophys Res Commun.* **266(3):** 652-661.

[8] Reichert M, Rustgi AK. 2011 Pancreatic ductal cells in development, regeneration, and neoplasia. *J Clin Invest.* **121(12):**4572-8.

[9] Hellman, B. 1959 Actual distribution of the number and volume of the islets of Langerhans in different size classes in non-diabetic humans of varying ages. *Nature* **184(19):** 1498-1499.

[10] Hellman B. 1959 The frequency distribution of the number and volume of the islets of Langerhans in man. *Acta Soc Med Ups.* **64:** 432-460.

[11] Rahier J, Guiot Y, Goebbels R.M, Sempoux C, Henquin J.C. 2008 Pancreatic beta-cell mass in European subjects with type 2 diabetes. *Diabetes Obes Metab.* **10 (4):** 32-42.

[12] *Wittingen J, Frey C.F.* 1974 Islet concentration in the head, body, tail and uncinate process of the pancreas. *Ann Surg.* **179(4):** 412-414.

[13] Yoon K.H, Ko S.H, Cho J.H, Lee J.M, Ahn Y.B, Song K.H, Yoo S.J, Kang M.I, Cha B.Y, Lee K.W, Son H.Y, Kang S.K, Kim H.S, Lee I.K, Bonner-Weir S. 2003 Selective beta-cell loss and alpha-cell expansion in patients with type 2 diabetes mellitus in Korea. *J Clin Endocrinol Metab.* **88(5):** 2300-2308.

[14] Korc M. *1993 Normal Function of the Endocrine Pancreas. The Pancreas: Biology, Pathobiology, and Disease, Second Edition, edited by Go VLW, et al.* Raven Press Ltd.

[15] Longnecker D.S and Wilson GL. 1991 *Pancreas. Handbook of Toxicologic Pathology,* edited by Haschek-Hock WM and Rousseaux CG. Academic Press Inc.

[16] Goldfine ID, Williams JA 1983 Receptors for insulin and CCK in the acinar pancreas: relationship to hormone action. *Int Rev Cytol.* **85:**1-38.

[17] Bardeesy N, DePinho RA. 2002 Pancreatic cancer biology and genetics. Nat Rev Cancer. **2(12):**897-909.

[18] Jørgensen MC, Ahnfelt-Rønne J, Hald J, Madsen OD, Serup P, Hecksher-Sørensen J. 2007 An illustrated review of early pancreas development in the mouse. *Endocr Rev.* **28(6):**685-705.

[19] Lee P.C and Lebenthal E. 1993 *Prenatal and Postnatal Development of the Human Exocrine Pancreas. The Pancreas: Biology, Pathobiology, and Disease, Second Edition, edited by Go VLW, et al. Raven Press Ltd.*

[20] Reichert M, Rustgi AK. 2011 Pancreatic ductal cells in development, regeneration, and neoplasia. *J Clin Invest.* **121(12):**4572-8.

[21] Polak M., Bouchareb-Banaei L., Scharfmann R., Czernichow P. 2000. Early Pattern of Differentiation in the Human Pancreas. *Diabetes.* **49(2):**225-32.

[22] Wang RN, Klöppel G, Bouwens L. 1995 Duct- to islet-cell differentiation and islet growth in the pancreas of duct-ligated adult rats. *Diabetologia.* **38(12):**1405-11.

[23] Xu X, D'Hoker J, Stangé G, Bonné S, De Leu N, Xiao X, Van de Casteele M, Mellitzer G, Ling Z, Pipeleers D, Bouwens L, Scharfmann R, Gradwohl G, Heimberg H. 2008 Beta cells can be generated from endogenous progenitors in injured adult mouse pancreas. *Cell.* **132(2):**197-207.

[24] Inada A, Nienaber C, Katsuta H, Fujitani Y, Levine J, Morita R, Sharma A, Bonner-Weir S. 2008 Carbonic anhydrase II-positive pancreatic cells are progenitors for both endocrine and exocrine pancreas after birth. *Proc Natl Acad Sci U S A.* **105(50):**19915-9.

[25] Gorelick FS and Jamieson JD, 2006. *Physiology of the gastrointestinal tract.* 5th edition, Elsevier Academic Press.

[26] Lai KC, Cheng CH, Leung PS. 2007 The ghrelin system in acinar cells: localization, expression, and regulation in the exocrine pancreas. *Pancreas.* **35(3):**e1-8.

[27] Zimmermann B. 1952 *Endocrine function of the pancreas.* 114th Edition, Blackwell Scientific publication by The Ryerson press.

[28] Grapin-Botton A. 2005 Ductal cells of the pancreas. *Int J Biochem Cell Biol.* **37(3):**504-10.

[29] Rutter GA, Pullen TJ, Hodson DJ, Martinez-Sanchez A. 2015 Pancreatic β-cell identity, glucose sensing and the control of insulin secretion. *Biochem J.* **466(2):**203-18.

[30] Madeb R, Koniaris LG, Schwartz SI. 2005 The discovery of insulin: the Rochester, New York, connection. *Ann Intern Med.* **143(12):**907-12.

[31] Novak I, 2008 Purinergic receptors in the endocrine and exocrine pancreas, *Purinergic signalling*, **4(3)**, 237-53.

[32] Nussey S, Whitehead S., 2001 *Endocrinology: An Integrated Approach.* BIOS Scientific Publishers.

[33] Brunton L L., Chabner B A., Knollmann B C. 2011 *Goodman & Gilman's The Pharmacological Basis of Therapeutics*, 12th edition.

[34] Siegel RL, Miller KD, Jemal A. 2015 Cancer statistics, 2015. *CA Cancer J Clin.* **65(1):**5-29.

[35] Ferlay J, Soerjomataram I, Dikshit R, Eser S, Mathers C, Rebelo M, Parkin DM, Forman D, Bray F. 2015 Cancer incidence and mortality worldwide: sources, methods and major patterns in GLOBOCAN 2012. *Int J Cancer.* **136(5):**E359-86.

[36] Matsuoka L, Selby R, Genyk Y. 2012 The surgical management of pancreatic cancer. *Gastroenterol Clin North Am.* **41(1):**211-21.

[37] Fuchs CS, Colditz GA, Stampfer MJ, Giovannucci EL, Hunter DJ, Rimm EB, Willett WC, Speizer FE. 1996 A prospective study of cigarette smoking and the risk of pancreatic cancer. *Arch Intern Med.* **156(19):**2255-60.

[38] Pezzilli R, Pagano N. 2013 Is diabetes mellitus a risk factor for pancreatic cancer? *World J Gastroenterol.* **19(30):**4861-6.

[39] Michaud DS, Giovannucci E, Willett WC, Colditz GA, Stampfer MJ, Fuchs CS. 2001 Physical activity, obesity, height, and the risk of pancreatic cancer. *JAMA.* **286(8):**921-9.

[40] Olsen GW, Mandel JS, Gibson RW, Wattenberg LW, Schuman LM. 1989 A case-control study of pancreatic cancer and cigarettes, alcohol, coffee and diet. *Am J Public Health.* **79(8):**1016-9.

[41] 1998 Nutritional aspects of the development of cancer. Report of the Working Group on Diet and Cancer of the Committee on Medical Aspects of Food and Nutrition Policy. *Rep Health Soc Subj (Lond).* **48:**i-xiv, 1-274.

[42] Tersmette AC, Petersen GM, Offerhaus GJ, Falatko FC, Brune KA, Goggins M, Rozenblum E, Wilentz RE, Yeo CJ, Cameron JL, Kern SE, Hruban RH. 2001 Increased risk of incident pancreatic cancer among first-degree relatives of patients with familial pancreatic cancer. *Clin Cancer Res.* **7(3):**738-44.

[43] Weiss FU. 2014 Pancreatic cancer risk in hereditary pancreatitis. *Front Physiol.* **5:**70.

[44] Lynch HT, Smyrk T, Kern SE, Hruban RH, Lightdale CJ, Lemon SJ, Lynch JF, Fusaro LR, Fusaro RM, Ghadirian P. 1996 Familial pancreatic cancer: a review. *Semin Oncol.* **23(2):**251-75.

[45] Hidalgo M. 2010 Pancreatic cancer. *N Engl J Med.* **362(17):**1605-17.

[46] Bond-Smith G, Banga N, Hammond TM, Imber CJ. 2012 Pancreatic adenocarcinoma. *BMJ.* **344:**e2476.

[47] Loc WS, Smith JP, Matters G, Kester M, Adair JH 2014 Novel strategies for managing pancreatic cancer. *World J Gastroenterol.* **20(40):**14717-25.

[48] Reynolds R B, & Folloder J. 2014 Clinical Management of Pancreatic Cancer. J *Adv Pract Oncol.* **5(5):** 356–364.

[49] Strobel O, Dor Y, Alsina J, Stirman A, Lauwers G, Trainor A, Castillo CF, Warshaw AL, Thayer SP. 2007 In vivo lineage tracing defines the role of acinar-to-ductal transdifferentiation in inflammatory ductal metaplasia. *Gastroenterology.* **133(6):**1999-2009.

[50] Means AL, Meszoely IM, Suzuki K, Miyamoto Y, Rustgi AK, Coffey RJ Jr, Wright CV, Stoffers DA, Leach SD. 2005 Pancreatic epithelial plasticity mediated by acinar cell transdifferentiation and generation of nestin-positive intermediates. *Development.* **132(16):**3767-76.

[51] Zhu L, Shi G, Schmidt CM, Hruban RH, Konieczny SF. 2007 Acinar cells contribute to the molecular heterogeneity of pancreatic intraepithelial neoplasia. *Am J Pathol.* **171(1):**263-73.

[52] Miyamoto Y, Maitra A, Ghosh B, Zechner U, Argani P, Iacobuzio-Donahue CA, Sriuranpong V, Iso T, Meszoely IM, Wolfe MS, Hruban RH, Ball DW, Schmid RM, Leach SD. 2003 Notch mediates TGF alpha-induced changes in epithelial differentiation during pancreatic tumorigenesis. *Cancer Cell.* **3(6):**565-76.

[53] Rooman I, Heremans Y, Heimberg H, Bouwens L. 2000 Modulation of rat pancreatic acinoductal transdifferentiation and expression of PDX-1 *in vitro. Diabetologia.* **43(7):**907-14.

[54] Zhu L, Tran T, Rukstalis JM, Sun P, Damsz B, Konieczny SF. 2004 Inhibition of Mist1 homodimer formation induces pancreatic acinar-to-ductal metaplasia. *Mol Cell Biol.* **24(7):**2673-81.

[55] Shields JM, Pruitt K, McFall A, Shaub A, Der CJ. 2000 Understanding Ras: 'it ain't over 'til it's over'. *Trends Cell Biol.* **10(4):**147-54.

[56] Korc M, Chandrasekar B, Yamanaka Y, Friess H, Buchier M, Beger HG. 1992 Overexpression of the epidermal growth factor receptor in human pancreatic cancer is associated with concomitant increases in the levels of epidermal growth factor and transforming growth factor alpha. *J Clin Invest.* **90(4):**1352-60.

[57] Friess H, Berberat P, Schilling M, Kunz J, Korc M, Büchler MW. 1996 Pancreatic cancer: the potential clinical relevance of alterations in growth factors and their receptors. *J Mol Med (Berl).* **74(1):**35-42.

[58] Watanabe M, Nobuta A, Tanaka J, Asaka M. 1996 An effect of K-ras gene mutation on epidermal growth factor receptor signal transduction in PANC-1 pancreatic carcinoma cells. *Int J Cancer.* **67(2):**264-8.

[59] Aguirre AJ, Bardeesy N, Sinha M, Lopez L, Tuveson DA, Horner J, Redston MS, DePinho RA. 2003 Activated Kras and Ink4a/Arf deficiency cooperate to produce metastatic pancreatic ductal adenocarcinoma. *Genes Dev.* **17(24):**3112-26.

[60] Hingorani SR, Petricoin EF, Maitra A, Rajapakse V, King C, Jacobetz MA, Ross S, Conrads TP, Veenstra TD, Hitt BA, Kawaguchi Y, Johann D, Liotta LA, Crawford HC, Putt ME, Jacks T, Wright CV, Hruban RH, Lowy AM, Tuveson DA. 2003 Preinvasive and invasive ductal pancreatic cancer and its early detection in the mouse. *Cancer Cell.* **4(6):**437-50.

[61] Gidekel Friedlander SY, Chu GC, Snyder EL, Girnius N, Dibelius G, Crowley D, Vasile E, DePinho RA, Jacks T. 2009 Context-dependent transformation of adult pancreatic cells by oncogenic K-Ras. *Cancer Cell.* **16(5):**379-89.

[62] Lowenfels AB & Maisonneuve P 2006 Epidemiology and risk factors for pancreatic cancer. *Best Pract Res Clin Gastroenterol.* **20(2):**197-209.

[63] Tuveson DA, Shaw AT, Willis NA, Silver DP, Jackson EL, Chang S, Mercer KL, Grochow R, Hock H, Crowley D, Hingorani SR, Zaks T, King C, Jacobetz MA, Wang L, Bronson RT, Orkin SH, DePinho RA, Jacks T. 2004

Endogenous oncogenic K-ras(G12D) stimulates proliferation and widespread neoplastic and developmental defects. *Cancer Cell.* **5(4):**375-87.

[64] Shen R, Wang Q, Cheng S, Liu T, Jiang H, Zhu J, Wu Y, Wang L. 2013 The biological features of PanIN initiated from oncogenic Kras mutation in genetically engineered mouse models. *Cancer Lett.* **339(1):**135-43.

[65] Kim H. 2008 Cerulein pancreatitis: oxidative stress, inflammation, and apoptosis. *Gut Liver.* **2(2):**74-80.

[66] Carrière C, Young AL, Gunn JR, Longnecker DS, Korc M. 2009 Acute pancreatitis markedly accelerates pancreatic cancer progression in mice expressing oncogenic Kras. *Biochem Biophys Res Commun.* **382(3):**561-5.

[67] Guerra C, Schuhmacher AJ, Cañamero M, Grippo PJ, Verdaguer L, Pérez-Gallego L, Dubus P, Sandgren EP, Barbacid M. 2007 Chronic pancreatitis is essential for induction of pancreatic ductal adenocarcinoma by K-Ras oncogenes in adult mice. *Cancer Cell.* **11(3):**291-302.

[68] Jonkers YM, Ramaekers FC, Speel EJ. 2007 Molecular alterations during insulinoma tumorigenesis. *Biochim Biophys Acta.* **1775(2):**313-32.

[69] Arrington AK, Heinrich EL, Lee W, Duldulao M, Patel S, Sanchez J, Garcia-Aguilar J, Kim J. 2012 Prognostic and predictive roles of KRAS mutation in colorectal cancer. *Int J Mol Sci.* **13(10):**12153-68.

[70] O'Hagan RC, Heyer J. 2011 KRAS Mouse Models: Modeling Cancer Harboring KRAS Mutations. *Genes Cancer.* **2(3):**335-43.

[71] Goldstein AM, Fraser MC, Struewing JP, Hussussian CJ, Ranade K, Zametkin DP, Fontaine LS, Organic SM, Dracopoli NC, Clark WH Jr. 1995 Increased risk of pancreatic cancer in melanoma-prone kindreds with p16INK4 mutations. *N Engl J Med.* **333(15):**970-4.

[72] Lynch HT, Brand RE, Hogg D, Deters CA, Fusaro RM, Lynch JF, Liu L, Knezetic J, Lassam NJ, Goggins M, Kern S. 2002 Phenotypic variation in eight extended CDKN2A germline mutation familial atypical multiple mole melanoma-pancreatic carcinoma-prone families: the familial atypical mole melanoma-pancreatic carcinoma syndrome. *Cancer.* **94(1):**84-96.

VII

[73] Borg A, Sandberg T, Nilsson K, Johannsson O, Klinker M, Måsbäck A, Westerdahl J, Olsson H, Ingvar C. 2000 High frequency of multiple melanomas and breast and pancreas carcinomas in CDKN2A mutation-positive melanoma families. J *Natl Cancer Inst.* **92(15):**1260-6.

[74] Sharpless NE, Bardeesy N, Lee KH, Carrasco D, Castrillon DH, Aguirre AJ, Wu EA, Horner JW, DePinho RA. 2001 Loss of p16Ink4a with retention of p19Arf predisposes mice to tumorigenesis. *Nature.* **413(6851):**86-91.

[75] Serrano M, Lin AW, McCurrach ME, Beach D, Lowe SW. 1997 Oncogenic ras provokes premature cell senescence associated with accumulation of p53 and p16INK4a. *Cell.* **88(5):**593-602.

[76] Schmitt CA, Fridman JS, Yang M, Lee S, Baranov E, Hoffman RM, Lowe SW. 2002 A senescence program controlled by p53 and p16INK4a contributes to the outcome of cancer therapy. *Cell.* **109(3):**335-46.

[77] Lüttges J, Schlehe B, Menke MA, Vogel I, Henne-Bruns D, Klöppel G. 1999 The K-ras mutation pattern in pancreatic ductal adenocarcinoma usually is identical to that in associated normal, hyperplastic, and metaplastic ductal epithelium. *Cancer.* **85(8):**1703-10.

[78] Laghi L, Orbetegli O, Bianchi P, Zerbi A, Di Carlo V, Boland CR, Malesci A. 2002 Common occurrence of multiple K-RAS mutations in pancreatic cancers with associated precursor lesions and in biliary cancers. *Oncogene.* **21(27):**4301-6.

[79] Sharpless NE & DePinho RA. 1999 The INK4A/ARF locus and its two gene products. *Curr Opin Genet Dev.* **9(1):**22-30.

[80] Chin L, Pomerantz J, Polsky D, Jacobson M, Cohen C, Cordon-Cardo C, Horner JW 2nd, DePinho RA. 1997 Cooperative effects of INK4a and ras in melanoma susceptibility in vivo. *Genes Dev.* **11(21):**2822-34.

[81] Rozenblum E, Schutte M, Goggins M, Hahn SA, Panzer S, Zahurak M, Goodman SN, Sohn TA, Hruban RH, Yeo CJ, Kern SE. Tumor-suppressive pathways in pancreatic carcinoma. *Cancer Res.* **57(9):**1731-4.

[82] Hingorani SR, Wang L, Multani AS, Combs C, Deramaudt TB, Hruban RH, Rustgi AK, Chang S, Tuveson DA. 2005 Trp53R172H and KrasG12D cooperate to promote chromosomal instability and widely metastatic pancreatic ductal adenocarcinoma in mice. *Cancer Cell.* **7(5):**469-83.

[83] Gorunova L, Höglund M, Andrén-Sandberg A, Dawiskiba S, Jin Y, Mitelman F, Johansson B. 1998 Cytogenetic analysis of pancreatic carcinomas: intratumor heterogeneity and nonrandom pattern of chromosome aberrations. *Genes Chromosomes Cancer.* **23(2):**81-99.

[84] Maser RS, DePinho RA. 2002 Connecting chromosomes, crisis, and cancer. *Science.* **297(5581):**565-9.

[85] Chin L, Artandi SE, Shen Q, Tam A, Lee SL, Gottlieb GJ, Greider CW, DePinho RA. 1999 p53 deficiency rescues the adverse effects of telomere loss and cooperates with telomere dysfunction to accelerate carcinogenesis. *Cell.* **97(4):**527-38.

[86] Gisselsson D, Pettersson L, Höglund M, Heidenblad M, Gorunova L, Wiegant J, Mertens F, Dal Cin P, Mitelman F, Mandahl N. 2000 Chromosomal breakage-fusion-bridge events cause genetic intratumor heterogeneity. *Proc Natl Acad Sci U S A.* **97(10):**5357-62.

[87] Gisselsson D, Jonson T, Petersén A, Strömbeck B, Dal Cin P, Höglund M, Mitelman F, Mertens F, Mandahl N. 2001 Telomere dysfunction triggers extensive DNA fragmentation and evolution of complex chromosome abnormalities in human malignant tumors. *Proc Natl Acad Sci U S A.* **98(22):**12683-8.

[88] Hahn SA, Schutte M, Hoque AT, Moskaluk CA, da Costa LT, Rozenblum E, Weinstein CL, Fischer A, Yeo CJ, Hruban RH, Kern SE. 1996 DPC4, a candidate tumor suppressor gene at human chromosome 18q21.1. *Science.* **271(5247):**350-3.

[89] Lüttges J, Galehdari H, Bröcker V, Schwarte-Waldhoff I, Henne-Bruns D, Klöppel G, Schmiegel W, Hahn SA. 2001 Allelic loss is often the first hit in the biallelic inactivation of the p53 and DPC4 genes during pancreatic carcinogenesis. *Am J Pathol.* **158(5):**1677-83.

[90] Wilentz RE, Iacobuzio-Donahue CA, Argani P, McCarthy DM, Parsons JL, Yeo CJ, Kern SE, Hruban RH. 2000 Loss of expression of Dpc4 in pancreatic intraepithelial neoplasia: evidence that DPC4 inactivation occurs late in neoplastic progression. *Cancer Res.* **60(7):**2002-6.

[91] Heinmöller E, Dietmaier W, Zirngibl H, Heinmöller P, Scaringe W, Jauch KW, Hofstädter F, Rüschoff J. 2000 Molecular analysis of microdissected tumors and preneoplastic intraductal lesions in pancreatic carcinoma. *Am J Pathol.* **157(1):**83-92.

[92] Maitra A & Hruban RH. 2008 Pancreatic cancer. *Annu Rev Pathol.* **3:**157-88.

[93] Derynck R, Akhurst R J, Balmain A. 2001 ʹTGF-β signaling in tumor suppression and cancer progression *Nature Genetics.* **29**, 117 - 129 (2001).

[94] Reiss M, Barcellos-Hoff MH. 1997 Transforming growth factor-beta in breast cancer: a working hypothesis. *Breast Cancer Res Treat.* **45(1):**81-95.

[95] Peng B, Fleming JB, Breslin T, Grau AM, Fojioka S, Abbruzzese JL, Evans DB, Ayers D, Wathen K, Wu T, Robertson KD, Chiao PJ. 2002 Suppression of tumorigenesis and induction of p15(ink4b) by Smad4/DPC4 in human pancreatic cancer cells. *Clin Cancer Res.* **8(11):**3628-38.

[96] Schwarte-Waldhoff I, Volpert O V, Bouck N P, Sipos B, Hahn S A, Klein-Scory S, Lüttges J, Klöppel G, Graeven U, Eilert-Micus C, Hintelmann A, Schmiegel W. 2000 Smad4/DPC4-mediated tumor suppression through suppression of angiogenesis. *Proc Natl Acad Sci U S A.* **97(17):** 9624–9629.

[97] Jonson T, Albrechtsson E, Axelson J, Heidenblad M, Gorunova L, Johansson B, Höglund M. 2001 Altered expression of TGFB receptors and mitogenic effects of TGFB in pancreatic carcinomas. *Int J Oncol.* **19(1):**71-81.

[98] Dai JL, Schutte M, Bansal RK, Wilentz RE, Sugar AY, Kern SE. 1999 Transforming growth factor-beta responsiveness in DPC4/SMAD4-null cancer cells. *Mol Carcinog.* **26(1)**:37-43.

[99] Giehl K, Seidel B, Gierschik P, Adler G, Menke A. 2000 TGFbeta1 represses proliferation of pancreatic carcinoma cells which correlates with Smad4-independent inhibition of ERK activation. *Oncogene.* **19(39):**4531-41.

X

[100] Rowland-Goldsmith MA, Maruyama H, Kusama T, Ralli S, Korc M. 2001 Soluble type II transforming growth factor-beta (TGF-beta) receptor inhibits TGF-beta signaling in COLO-357 pancreatic cancer cells in vitro and attenuates tumor formation. *Clin Cancer Res.* **7(9):**2931-40.

[101] Klöppel G. 2011 Classification and pathology of gastroenteropancreatic neuroendocrine neoplasms. *Endocr Relat Cancer.* **18 Suppl 1:**S1-16.

[102] Löhr M, Schmidt C, Ringel J, Kluth M, Müller P, Nizze H, Jesnowski R. 2001 Transforming growth factor-beta1 induces desmoplasia in an experimental model of human pancreatic carcinoma. *Cancer Res.* **61(2):**550-5.

[103] Bissell MJ & Radisky D. 2001 Putting tumours in context. *Nat Rev Cancer.* **1(1):**46-54.

[104] Olumi AF, Grossfeld GD, Hayward SW, Carroll PR, Tlsty TD, Cunha GR. 1999 Carcinoma-associated fibroblasts direct tumor progression of initiated human prostatic epithelium. *Cancer Res.* **59(19):**5002-11.

[105] Herreros-Villanueva M, Hijona E, Cosme A, Bujanda L. 2012 Mouse models of pancreatic cancer. *World J Gastroenterol.* **18(12):** 1286–1294.

[106] Hruban RH, Takaori K, Klimstra DS, Adsay NV, Albores-Saavedra J, Biankin AV, Biankin SA, Compton C, Fukushima N, Furukawa T, Goggins M, Kato Y, Klöppel G, Longnecker DS, Lüttges J, Maitra A, Offerhaus GJ, Shimizu M, Yonezawa S. 2004 An illustrated consensus on the classification of pancreatic intraepithelial neoplasia and intraductal papillary mucinous neoplasms. *Am J Surg Pathol.* **28(8):**977-87.

[107] Lennon AM, Wolfgang CL, Canto MI, Klein AP, Herman JM, Goggins M, Fishman EK, Kamel I, Weiss MJ, Diaz LA, Papadopoulos N, Kinzler KW, Vogelstein B, Hruban RH. 2014 The early detection of pancreatic cancer: what will it take to diagnose and treat curable pancreatic neoplasia? *Cancer Res.* **74(13):**3381-9.

[108] Capella C, Albarello L, Capelli P, Sessa F, Zamboni G. 2013 Carcinoma of the exocrine pancreas: histology report. *Pathologica.* **105(1):**28-38.

[109] Murphy SJ, Hart SN, Lima JF, Kipp BR, Klebig M, Winters JL, Szabo C, Zhang L, Eckloff BW, Petersen GM, Scherer SE, Gibbs RA, McWilliams RR, Vasmatzis G, Couch FJ.2013 Genetic alterations associated with progression from pancreatic intraepithelial neoplasia to invasive pancreatic tumor. *Gastroenterology.* **145(5):**1098-1109.e1.

[110] Biankin AV, Waddell N, Kassahn KS, Gingras MC, Muthuswamy LB, Johns AL, Miller DK, Wilson PJ, Patch AM, *et al.* 2012 Pancreatic cancer genomes reveal aberrations in axon guidance pathway genes. *Nature.* **491(7424):**399-405.

[111] Andea A, Sarkar F, Adsay VN. 2003 Clinicopathological correlates of pancreatic intraepithelial neoplasia: a comparative analysis of 82 cases with and 152 cases without pancreatic ductal adenocarcinoma. *Mod Pathol.* **16(10):**996-1006.

[112] Cubilla AL, Fitzgerald PJ. 1976 Morphological lesions associated with human primary invasive nonendocrine pancreas cancer. *Cancer Res.* **36(7 PT 2):**2690-8.

[113] Shi C, Klein AP, Goggins M, Maitra A, Canto M, Ali S, Schulick R, Palmisano E, Hruban RH. 2009 Increased Prevalence of Precursor Lesions in Familial Pancreatic Cancer Patients. *Clin Cancer Res.* **15(24):**7737-7743.

[114] Feldmann G, Beaty R, Hruban RH, Maitra A. 2007 Molecular genetics of pancreatic intraepithelial neoplasia. *J Hepatobiliary Pancreat Surg.* **14(3):**224-32.

[115] Jung K W, Kim M-H, Lee T Y, Kwon S, Oh H-C, Lee S S, Seo D W, Lee S K. 2007 Clinicopathological Aspects of 542 Cases of Pancreatic Cancer: a Special Emphasis on Small Pancreatic Cancer. *J Korean Med Sci.* **22(Suppl):**S79–S85.

[116] Brand RE & Matamoros A. 1998 Imaging techniques in the evaluation of adenocarcinoma of the pancreas. *Dig Dis.* **16(4):**242-52.

[117] K.S. Goonetilleke & A.K. Siriwardena. 2007 Systematic review of carbohydrate antigen (CA 19-9) as a biochemical marker in the diagnosis of pancreatic cancer. *EJSO.* **33(3):**266-270.

[118] Koopmann J, Rosenzweig CN, Zhang Z, Canto MI, Brown DA, Hunter M, Yeo C, Chan DW, Breit SN, Goggins M. 2006 Serum markers in patients with resectable pancreatic adenocarcinoma: macrophage inhibitory cytokine 1 versus CA19-9. *Clin Cancer Res.* **12(2):**442-6.

[119] Faca VM, Song KS, Wang H, Zhang Q, Krasnoselsky AL, Newcomb LF, Plentz RR, Gurumurthy S, Redston MS, et al. 2008 A mouse to human search for plasma proteome changes associated with pancreatic tumor development. *PLoS Med.* **5(6):**e123.

[120] Brand RE, Nolen BM, Zeh HJ, Allen PJ, Eloubeidi MA, Goldberg M, Elton E, Arnoletti JP, Christein JD, Vickers SM, Langmead CJ, Landsittel DP, Whitcomb DC, Grizzle WE, Lokshin AE. 2011 Serum biomarker panels for the detection of pancreatic cancer. *Clin Cancer Res.* **17(4):**805-16.

[121] Sessa F, Furlan D, Zampatti C, Carnevali I, Franzi F, Capella C. 2007 Prognostic factors for ampullary adenocarcinomas: tumor stage, tumor histology, tumor location, immunohistochemistry and microsatellite instability. *Virchows Arch.* **451(3):**649-57.

[122] Chiu J & Yau T. 2012 Metastatic pancreatic cancer: are we making progress in treatment? *Gastroenterol Res Pract.* **2012:**898931.

[123] Colucci G, Labianca R, Di Costanzo F, Gebbia V, Cartenì G, Massidda B, Dapretto E, Manzione L, Piazza E, Sannicolò M, Ciaparrone M, Cavanna L, Giuliani F, Maiello E, Testa A, Pederzoli P, Falconi M, Gallo C, Di Maio M, Perrone F. 2010 Randomized phase III trial of gemcitabine plus cisplatin compared with single-agent gemcitabine as first-line treatment of patients with advanced pancreatic cancer: the GIP-1 study. *J Clin Oncol.* **28(10):**1645-51.

[124] Poplin E, Feng Y, Berlin J, Rothenberg ML, Hochster H, Mitchell E, Alberts S, O'Dwyer P, Haller D, Catalano P, Cella D, Benson AB 3rd. 2009 Phase III, randomized study of gemcitabine and oxaliplatin versus gemcitabine (fixed-dose rate infusion) compared with gemcitabine (30-minute infusion) in patients with pancreatic carcinoma E6201: a trial of the Eastern Cooperative Oncology Group. *J Clin Oncol.* **27(23):**3778-85.

[125] Oettle H, Arnold D, Hempel C, Riess H. 2000 The role of gemcitabine alone and in combination in the treatment of pancreatic cancer. *Anticancer Drugs.* **11(10):**771-86.

[126] Oettle H & Riess H. 2002 Gemcitabine in combination with 5-fluorouracil with or without folinic acid in the treatment of pancreatic cancer. *Cancer.* **95(4 Suppl):**912-22.

[127] Pino SM, Xiong HQ, McConkey D, Abbruzzese J L. 2004 Novel therapies for pancreatic adenocarcinoma. Current Gastroenterology Reports*.* **6(2):**119-125.

[128] Wheatley SP, McNeish IA. 2005 Survivin: a protein with dual roles in mitosis and apoptosis. *Int Rev Cytol.* **247:**35-88.

[129] Schniewind B, Christgen M, Kurdow R, Haye S, Kremer B, Kalthoff H, Ungefroren H. 2004 Resistance of pancreatic cancer to gemcitabine treatment is dependent on mitochondria-mediated apoptosis. *Int J Cancer.* **109(2):**182-8.

[130] Mimeault M, Johansson SL, Senapati S, Momi N, Chakraborty S, Batra SK. 2010 MUC4 down-regulation reverses chemoresistance of pancreatic cancer stem/progenitor cells and their progenies. *Cancer Lett.* **295(1):**69-84.

[131] Bafna S, Kaur S, Momi N, Batra SK. 2009 Pancreatic cancer cells resistance to gemcitabine: the role of MUC4 mucin. *Br J Cancer.* **101(7):**1155-61.

[132] Swartz MJ, Batra SK, Varshney GC, Hollingsworth MA, Yeo CJ, Cameron JL, Wilentz RE, Hruban RH, Argani P. 2002 MUC4 expression increases progressively in pancreatic intraepithelial neoplasia. *Am J Clin Pathol.* **117(5):**791-6.

[133] Park HU, Kim JW, Kim GE, Bae HI, Crawley SC, Yang SC, Gum JR Jr, Batra SK, Rousseau K, Swallow DM, Sleisenger MH, Kim YS. 2003 Aberrant expression of MUC3 and MUC4 membrane-associated mucins and sialyl Le(x) antigen in pancreatic intraepithelial neoplasia. *Pancreas.* **26(3):**e48-54.

[134] Bafna S, Kaur S, Batra SK. 2010 Membrane-bound mucins: the mechanistic basis for alterations in the growth and survival of cancer cells. *Oncogene.* **29(20):**2893-904.

[135] Singh AP, Moniaux N, Chauhan SC, Meza JL, Batra SK. 2004 Inhibition of MUC4 expression suppresses pancreatic tumor cell growth and metastasis. *Cancer Res.* **64(2):**622-30.

[136] Chaturvedi P, Singh AP, Moniaux N, Senapati S, Chakraborty S, Meza JL, Batra SK. 2007 MUC4 mucin potentiates pancreatic tumor cell proliferation, survival, and invasive properties and interferes with its interaction to extracellular matrix proteins. *Mol Cancer Res.* **5(4):**309-20.

[137] Moniaux N, Chaturvedi P, Varshney GC, Meza JL, Rodriguez-Sierra JF, Aubert JP, Batra SK. Human MUC4 mucin induces ultra-structural changes and tumorigenicity in pancreatic cancer cells. *Br J Cancer.* **97(3):**345-57.

[138] Feig C, Gopinathan A, Neesse A, Chan DS, Cook N, Tuveson DA. 2012 The pancreas cancer microenvironment. *Clin Cancer Res.* **18(16):**4266-76.

[139] Neesse A, Frese KK, Bapiro TE, Nakagawa T, Sternlicht MD, Seeley TW, Pilarsky C, Jodrell DI, Spong SM, Tuveson DA. 2013 CTGF antagonism with mAb FG-3019 enhances chemotherapy response without increasing drug delivery in murine ductal pancreas cancer. *Proc Natl Acad Sci U S A.* **110(30):**12325-30.

[140] Provenzano PP, Cuevas C, Chang AE, Goel VK, Von Hoff DD, Hingorani SR. 2012 Enzymatic targeting of the stroma ablates physical barriers to treatment of pancreatic ductal adenocarcinoma. *Cancer Cell.* **21(3):**418-29.

[141] Hidalgo M & Von Hoff DD. 2012 Translational therapeutic opportunities in ductal adenocarcinoma of the pancreas. *Clin Cancer Res.* **18(16):**4249-56.

[142] Fanciullino R, Ciccolini J, Milano G. Challenges, expectations and limits for nanoparticles-based therapeutics in cancer: a focus on nano-albumin-bound drugs. *Crit Rev Oncol Hematol.* **88(3):**504-13.

[143] Felice B, Prabhakaran MP, Rodríguez AP, Ramakrishna S. 2014 Drug delivery vehicles on a nano-engineering perspective. *Mater Sci Eng C Mater Biol Appl.* **41:**178-95.

[144] Guarneri V, Dieci MV, Conte P. 2012 Enhancing intracellular taxane delivery: current role and perspectives of nanoparticle albumin-bound paclitaxel in the treatment of advanced breast cancer. *Expert Opin Pharmacother.* **13(3):**395-406.

[145] Jain RK. 2005 Normalization of tumor vasculature: an emerging concept in antiangiogenic therapy. *Science.* **307(5706):**58-62.

[146] Viúdez A, Ramírez N, Hernández-García I, Carvalho FL, Vera R, Hidalgo M. 2014 Nab-paclitaxel: a flattering facelift. *Crit Rev Oncol Hematol.* **92(3):**166-80.

[147] Yu KH, Ricigliano M, Hidalgo M, Abou-Alfa GK, Lowery MA, Saltz LB, Crotty JF, Gary K, Cooper B, Lapidus R, Sadowska M, O'Reilly EM. 2014 Pharmacogenomic modeling of circulating tumor and invasive cells for prediction of chemotherapy response and resistance in pancreatic cancer. *Clin Cancer Res.* **20(20):**5281-9.

[148] Mani SA, Guo W, Liao MJ, Eaton EN, Ayyanan A, Zhou AY, Brooks M, Reinhard F, Zhang CC, Shipitsin M, Campbell LL, Polyak K, Brisken C, Yang J, Weinberg RA. 2008 The epithelial-mesenchymal transition generates cells with properties of stem cells. *Cell.* **133(4):**704-15.

[149] Hay ED. 1995 An overview of epithelio-mesenchymal transformation. *Acta Anat (Basel).* **154(1):**8-20.

[150] Thiery J P& Sleeman J P.2006 Complex networks orchestrate epithelial–mesenchymal transitions. *Nat Rev Mol Cell Biol.* **7:**131-142.

[151] Kalluri R & Weinberg RA. 2009 The basics of epithelial-mesenchymal transition. *J Clin Invest.* **119(6):**1420-8.

[152] Sauka-Spengler T & Bronner-Fraser M. 2008 A gene regulatory network orchestrates neural crest formation. *Nat Rev Mol Cell Biol.* **9(7):**557-68.

[153] Kalluri R &Neilson EG. 2003 Epithelial-mesenchymal transition and its implications for fibrosis. *J Clin Invest.* **112(12):**1776-84.

XVI

[154] Zeisberg EM, Tarnavski O, Zeisberg M, Dorfman AL, McMullen JR, Gustafsson E, Chandraker A, Yuan X, Pu WT, Roberts AB, Neilson EG, Sayegh MH, Izumo S, Kalluri R. 2007 Endothelial-to-mesenchymal transition contributes to cardiac fibrosis. *Nat Med.* **13(8):**952-61.

[155] Potenta S, Zeisberg E, Kalluri R. 2008 The role of endothelial-to-mesenchymal transition in cancer progression. *Br J Cancer.* **99(9):**1375-9.

[156] Rastaldi MP, Ferrario F, Giardino L, Dell'Antonio G, Grillo C, Grillo P, Strutz F, Müller GA, Colasanti G, D'Amico G. 2002 Epithelial-mesenchymal transition of tubular epithelial cells in human renal biopsies. *Kidney Int.* **62(1):**137-46.

[157] Bataille F, Rohrmeier C, Bates R, Weber A, Rieder F, Brenmoehl J, Strauch U, Farkas S, Fürst A, Hofstädter F, Schölmerich J, Herfarth H, Rogler G 2008 Evidence for a role of epithelial mesenchymal transition during pathogenesis of fistulae in Crohn's disease. *Inflamm Bowel Dis.* **14(11):**1514-27.

[158] Keshamouni VG & Schiemann WP. 2009 Special Focus Content: Epithelial-mesenchymal transition in tumor metastasis: a method to the madness. *Future Oncology.* **5(8):**1109-1111.

[159] Zeisberg M & Neilson EG. 2009 Biomarkers for epithelial-mesenchymal transitions. *J Clin Invest.* **119(6):**1429–1437.

[160] Chao YL, Shepard CR, Wells A. 2010 Breast carcinoma cells re-express E-cadherin during mesenchymal to epithelial reverting transition. *Mol Cancer.* **9:**179.

[161] Olmeda D, Jordá M, Peinado H, Fabra A, Cano A. 2007 Snail silencing effectively suppresses tumour growth and invasiveness. *Oncogene.* **26(13):**1862-74.

[162] Ota I, Li XY, Hu Y, Weiss SJ. 2009 Induction of a MT1-MMP and MT2-MMP-dependent basement membrane transmigration program in cancer cells by Snail1. *Proc Natl Acad Sci U S A.* **106(48):**20318-23.

XVII

[163] Ye X & Weinberg RA. 2015 Epithelial–Mesenchymal Plasticity: A Central Regulator of Cancer Progression. *Trends in Cell Biology.* **25(11):**675-686.

[164] Drake JM, Strohbehn G, Bair TB, Moreland JG, Henry MD. 2009 ZEB1 enhances transendothelial migration and represses the epithelial phenotype of prostate cancer cells. *Mol Biol Cell.* **20(8):**2207-17.

[165] Eckert MA, Lwin TM, Chang AT, Kim J, Danis E, Ohno-Machado L, Yang J. 2011 Twist1-induced invadopodia formation promotes tumor metastasis. *Cancer Cell.* **19(3):**372-86.

[166] Huber MA, Kraut N, Beug H. 2005 Molecular requirements for epithelial-mesenchymal transition during tumor progression. *Curr Opin Cell Biol.* **17(5):**548-58.

[167] Strutz F, Zeisberg M, Ziyadeh FN, Yang CQ, Kalluri R, Müller GA, Neilson EG. 2002 Role of basic fibroblast growth factor-2 in epithelial-mesenchymal transformation. *Kidney Int.* **61(5):**1714-28.

[168] Bates RC, Bellovin DI, Brown C, Maynard E, Wu B, Kawakatsu H, Sheppard D, Oettgen P, Mercurio AM. 2005 Transcriptional activation of integrin beta6 during the epithelial-mesenchymal transition defines a novel prognostic indicator of aggressive colon carcinoma. *J Clin Invest.* **115(2):**339-47.

[169] Qian F, Zhang ZC, Wu XF, Li YP, Xu Q. 2005 Interaction between integrin alpha(5) and fibronectin is required for metastasis of B16F10 melanoma cells. *Biochem Biophys Res Commun.* **333(4):**1269-75.

[170] Vogel W, Gish GD, Alves F, Pawson T. 1997 The discoidin domain receptor tyrosine kinases are activated by collagen. *Mol Cell.* **1(1):**13-23.

[171] Leitinger B & Kwan AP. 2006 The discoidin domain receptor DDR2 is a receptor for type X collagen. *Matrix Biol.* **25(6):**355-64.

[172] Dellagi K, Vainchenker W, Vinci G, Paulin D, Brouet JC. 1983 Alteration of vimentin intermediate filament expression during differentiation of human hemopoietic cells. *EMBO J.* **2(9):**1509-14.

[173] Brabletz T, Jung A, Hermann K, Günther K, Hohenberger W, Kirchner T. Nuclear overexpression of the oncoprotein beta-catenin in colorectal cancer is localized predominantly at the invasion front. *Pathol Res Pract.* **194(10):**701-4.

[174] Klezovitch O & Vasioukhin V. 2015 Cadherin signaling: keeping cells in touch. *F1000Res.* **4:**550.

[175] Monga SP. 2015 β-Catenin Signaling and Roles in Liver Homeostasis, Injury, and Tumorigenesis. *Gastroenterology.* **148(7):**1294-310.

[176] Hynes RO &Yamada KM. 1982 Fibronectins: multifunctional modular glycoproteins. *J Cell Biol.* **95(2 Pt 1):**369-77.

[177] Duband JL & Thiery JP. 1982 Appearance and distribution of fibronectin during chick embryo gastrulation and neurulation. *Dev Biol.* **94(2):**337-50.

[178] Yang Z, Zhang X, Gang H, Li X, Li Z, Wang T, Han J, Luo T, Wen F, Wu X. 2007 Up-regulation of gastric cancer cell invasion by Twist is accompanied by N-cadherin and fibronectin expression. *Biochem Biophys Res Commun.* **358(3):**925-30.

[179] Colognato H & Yurchenco PD. 2000 Form and function: the laminin family of heterotrimers. *Dev Dyn.* **218(2):**213-34.

[180] Sarrió D, Rodriguez-Pinilla SM, Hardisson D, Cano A, Moreno-Bueno G, Palacios J 2008 Epithelial-mesenchymal transition in breast cancer relates to the basal-like phenotype. *Cancer Res.* **68(4):**989-97.

[181] Zeisberg M, Maeshima Y, Mosterman B, Kalluri R. 2002 Renal fibrosis. Extracellular matrix microenvironment regulates migratory behavior of activated tubular epithelial cells. *Am J Pathol.* **160(6):**2001-8.

[182] Carpenter PM, Wang-Rodriguez J, Chan OT, Wilczynski SP. 2008 Laminin 5 expression in metaplastic breast carcinomas. *Am J Surg Pathol.* **32(3):**345-53.

[183] Massagué J, Blain SW, Lo RS. 2000 TGFbeta signaling in growth control, cancer, and heritable disorders. *Cell.* **103(2):**295-309.

[184] Derynck R, Zhang Y, Feng XH. 1998 Smads: transcriptional activators of TGF-beta responses. *Cell.* **95(6):**737-40.

[185] Massagué J. 1998 TGF-beta signal transduction. *Annu Rev Biochem.* **67:**753-91.

[186] Papageorgis P. 2015 TGFβ Signaling in Tumor Initiation, Epithelial-to-Mesenchymal Transition, and Metastasis. *J Oncol.* **2015:**587193.

[187] Ashcroft GS, Yang X, Glick AB, Weinstein M, Letterio JL, Mizel DE, Anzano M, Greenwell-Wild T, Wahl SM, Deng C, Roberts AB. 1999 Mice lacking Smad3 show accelerated wound healing and an impaired local inflammatory response. *Nat Cell Biol.* **1(5):**260-6.

[188] Jang CW, Chen CH, Chen CC, Chen JY, Su YH, Chen RH. 2002 TGF-beta induces apoptosis through Smad-mediated expression of DAP-kinase. *Nat Cell Biol.* **4(1):**51-8.

[189] Riggins GJ, Kinzler KW, Vogelstein B, Thiagalingam S. 1997 Frequency of Smad gene mutations in human cancers. *Cancer Res.* **57(13):**2578-80.

[190] Massagué J. 2008 TGFβ in Cancer. *Cell.* **134(2):**215-230.

[191] Papageorgis P, Lambert AW, Ozturk S, Gao F, Pan H, Manne U, Alekseyev YO, Thiagalingam A, Abdolmaleky HM, Lenburg M, Thiagalingam S. 2010 Smad signaling is required to maintain epigenetic silencing during breast cancer progression. *Cancer Res.* **70(3):**968-78.

[192] Morrison CD, Parvani JG, Schiemann WP. 2013 The relevance of the TGF-β Paradox to EMT-MET programs. *Cancer Lett.* **341(1):**30-40.

[193] Moustakas A & Heldin P. 2014 TGFβ and matrix-regulated epithelial to mesenchymal transition. *Biochimica et Biophysica Acta (BBA).* **1840(8):**2621–2634.

[194] Deng S, Zhu S, Wang B, Li X, Liu Y, Qin Q, Gong Q, Niu Y, Xiang C, Chen J, Yan J, Deng S, Yin T, Yang M, Wu H, Wang C, Zhao G. 2014 Chronic pancreatitis and pancreatic cancer demonstrate active epithelial-mesenchymal transition profile, regulated by miR-217-SIRT1 pathway. *Cancer Lett.* **355(2):**184-91.

[195] Li Y, VandenBoom TG 2nd, Kong D, Wang Z, Ali S, Philip PA, Sarkar FH. 2009 Up-regulation of miR-200 and let-7 by natural agents leads to the reversal of epithelial-to-mesenchymal transition in gemcitabine-resistant pancreatic cancer cells. *Cancer Res.* **69(16):**6704-12.

[196] Arumugam T, Ramachandran V, Fournier KF, Wang H, Marquis L, Abbruzzese JL, Gallick GE, Logsdon CD, McConkey DJ, Choi W. 2009 Epithelial to mesenchymal transition contributes to drug resistance in pancreatic cancer. *Cancer Res.* **69(14):**5820-8.

[197] Javle MM, Gibbs JF, Iwata KK, Pak Y, Rutledge P, Yu J, Black JD, Tan D, Khoury T. 2007 Epithelial-mesenchymal transition (EMT) and activated extracellular signal-regulated kinase (p-Erk) in surgically resected pancreatic cancer. *Ann Surg Oncol.* **14(12):**3527-33.

[198] Karamitopoulou E. 2013 Role of epithelial-mesenchymal transition in pancreatic ductal adenocarcinoma: is tumor budding the missing link? *Front Oncol.* **3:**221.

[199] Kang Y, Ling J, Suzuki R, Roife D, Chopin-Laly X, Truty MJ, Chatterjee D, Wang H, Thomas RM, Katz MH, Chiao PJ, Fleming JB. 2014 SMAD4 regulates cell motility through transcription of N-cadherin in human pancreatic ductal epithelium. *PLoS One.* **9(9):**e107948.

[200] Wang R, Cheng L, Xia J, Wang Z, Wu Q, Wang Z. 2014 Gemcitabine resistance is associated with epithelial-mesenchymal transition and induction of HIF-1α in pancreatic cancer cells. *Curr Cancer Drug Targets.* **14(4):**407-17.

[201] Yamada S, Fuchs BC, Fujii T, Shimoyama Y, Sugimoto H, Nomoto S, Takeda S, Tanabe KK, Kodera Y, Nakao A. 2013 Epithelial-to-mesenchymal transition predicts prognosis of pancreatic cancer. *Surgery.* **154(5):**946-54.

[202] Solito E, de Coupade C, Parente L, Flower RJ, Russo-Marie F. 1998 Human annexin 1 is highly expressed during the differentiation of the epithelial cell line A 549: involvement of nuclear factor interleukin 6 in phorbol ester induction of annexin 1. *Cell Growth Differ.* **9(4):**327-36.

[203] Morgan RO & Fernández MP. 1997 Annexin gene structures and molecular evolutionary genetics. *Cell Mol Life Sci.* **53(6):**508-15.

[204] Morgan RO, Jenkins NA, Gilbert DJ, Copeland NG, Balsara BR, Testa JR, Fernandez MP. 1999 Novel human and mouse annexin A10 are linked to the genome duplications during early chordate evolution. *Genomics.* **60(1):**40-9.

[205] Weng X, Luecke H, Song IS, Kang DS, Kim SH, Huber R. 1993 Crystal structure of human annexin I at 2.5 A resolution. *Protein Sci.* **2(3):**448-58.

[206] Rosengarth A, Gerke V, Luecke H. 2001 X-ray structure of full-length annexin 1 and implications for membrane aggregation. *J Mol Biol.* **306(3):**489-98.

[207] Huber R, Römisch J, Paques EP. 1990 The crystal and molecular structure of human annexin V, an anticoagulant protein that binds to calcium and membranes. *EMBO J.* **9(12):**3867-74.

[208] Seemann J, Weber K, Gerke V. 1996 Structural requirements for annexin I-S100C complex-formation. *Biochem J.* **319 (1):**123-9.

[209] Mailliard WS, Haigler HT, Schlaepfer DD. 1996 Calcium-dependent binding of S100C to the N-terminal domain of annexin I. *J Biol Chem.* **271(2):**719-25.

[210] Gerke V & Moss SE. 2002 Annexins: from structure to function. *Physiol Rev.* **82(2):**331-71.

[211] Wallner BP, Mattaliano RJ, Hession C, Cate RL, Tizard R, Sinclair LK, Foeller C, Chow EP, Browing JL, Ramachandran KL, et al. 1986 Cloning and expression of human lipocortin, a phospholipase A2 inhibitor with potential anti-inflammatory activity. *Nature.* **320(6057):**77-81.

[212] Peers SH, Smillie F, Elderfield AJ, Flower RJ. 1993 Glucocorticoid-and non-glucocorticoid induction of lipocortins (annexins) 1 and 2 in rat peritoneal leucocytes in vivo. *Br J Pharmacol.* **108(1):**66-72.

[213] Flower RJ. 1988 Eleventh Gaddum Memorial Lecture. Lipocortin and the mechanism of action of the glucocorticoids. *Br J Pharmacol.* **94(4):**987-1015.

[214] Flower RJ & Rothwell NJ. 1994 Lipocortin-1: cellular mechanisms and clinical relevance. *Trends Pharmacol Sci.* **15(3):**71-6.

[215] Croxtall JD, Choudhury Q, Flower RJ. Inhibitory effect of peptides derived from the N-terminus of lipocortin 1 on arachidonic acid release and proliferation in the A549 cell line: identification of E-Q-E-Y-V as a crucial component. *Br J Pharmacol.* **123(5):**975-83.

[216] Croxtall JD, Choudhury Q, Flower RJ. 2000 Glucocorticoids act within minutes to inhibit recruitment of signalling factors to activated EGF receptors through a receptor-dependent, transcription-independent mechanism. *Br J Pharmacol.* **130(2):**289-98.

[217] Solito E, de Coupade C, Parente L, Flower RJ, Russo-Marie F. 1998 IL-6 stimulates annexin 1 expression and translocation and suggests a new biological role as class II acute phase protein. *Cytokine.* **10(7):**514-21.

[218] Cirino G, Flower RJ, Browning JL, Sinclair LK, Pepinsky RB. 1987 Recombinant human lipocortin 1 inhibits thromboxane release from guinea-pig isolated perfused lung. *Nature.* **328(6127):**270-2.

[219] Cirino G, Peers SH, Flower RJ, Browning JL, Pepinsky RB. 1989 Human recombinant lipocortin 1 has acute local anti-inflammatory properties in the rat paw edema test. *Proc Natl Acad Sci U S A.* **86(9):**3428-32.

[220] Carey F, Forder R, Edge MD, Greene AR, Horan MA, Strijbos PJ, Rothwell NJ. 1990 Lipocortin 1 fragment modifies pyrogenic actions of cytokines in rats. *Am J Physiol.* **259(2 Pt 2):**R266-9.

[221] Kim SW, Rhee HJ, Ko J, Kim YJ, Kim HG, Yang JM, Choi EC, Na DS. 2001 Inhibition of cytosolic phospholipase A2 by annexin I. Specific interaction model and mapping of the interaction site. *J Biol Chem.* **276(19):**15712-9.

[222] Davidson FF, Dennis EA, Powell M, Glenney JR Jr. 1987 Inhibition of phospholipase A2 by "lipocortins" and calpactins. An effect of binding to substrate phospholipids. *J Biol Chem.* **262(4):**1698-705.

[223] Wu CC, Croxtall JD, Perretti M, Bryant CE, Thiemermann C, Flower RJ, Vane JR. 1995 Lipocortin 1 mediates the inhibition by dexamethasone of the induction by endotoxin of nitric oxide synthase in the rat. *Proc Natl Acad Sci U S A.* **92(8):**3473-7.

[224] Ferlazzo V, D'Agostino P, Milano S, Caruso R, Feo S, Cillari E, Parente L. 2003 Anti-inflammatory effects of annexin-1: stimulation of IL-10 release and inhibition of nitric oxide synthesis. *Int Immunopharmacol.* **3(10-11):**1363-9.

[225] Minghetti L, Nicolini A, Polazzi E, Greco A, Perretti M, Parente L, Levi G. 1999 Down-regulation of microglial cyclo-oxygenase-2 and inducible nitric oxide synthase expression by lipocortin 1. *Br J Pharmacol.* **126(6):**1307-14.

[226] Hannon R, Croxtall JD, Getting SJ, Roviezzo F, Yona S, Paul-Clark MJ, Gavins FN, Perretti M, Morris JF, Buckingham JC, Flower RJ. 2003 Aberrant inflammation and resistance to glucocorticoids in annexin 1-/- mouse. *FASEB J.* **17(2):**253-5.

[227] Yang YH, Morand EF, Getting SJ, Paul-Clark M, Liu DL, Yona S, Hannon R, Buckingham JC, Perretti M, Flower RJ. 2004 Modulation of inflammation and response to dexamethasone by Annexin 1 in antigen-induced arthritis. *Arthritis Rheum.* **50(3):**976-84.

[228] Vishwanath BS, Frey FJ, Bradbury MJ, Dallman MF, Frey BM. 1993 Glucocorticoid deficiency increases phospholipase A2 activity in rats. *J Clin Invest.* **92(4):**1974-80.

[229] Newman SP, Croxtall JD, Choudhury Q, Flower RJ. 1997 The co-ordinate regulation of lipocortin 1, COX 2 and cPLA2 by IL-1 beta in A549 cells. *Adv Exp Med Biol.* **407:**249-53.

[230] Kwon JH, Lee JH, Kim KS, Chung YW, Kim IY. 2012 Regulation of cytosolic phospholipase A2 phosphorylation by proteolytic cleavage of annexin A1 in activated mast cells. *J Immunol.* **188(11):**5665-73.

[231] Francis JW, Balazovich KJ, Smolen JE, Margolis DI, Boxer LA. 1992 Human neutrophil annexin I promotes granule aggregation and modulates Ca(2+)-dependent membrane fusion. *J Clin Invest*. **90(2):**537-44.

[232] Scannell M, Flanagan MB, deStefani A, Wynne KJ, Cagney G, Godson C, Maderna P. 2007 Annexin-1 and peptide derivatives are released by apoptotic cells and stimulate phagocytosis of apoptotic neutrophils by macrophages. *J Immunol.* **178(7):**4595-605.

XXIV

[233] Arur S, Uche UE, Rezaul K, Fong M, Scranton V, Cowan AE, Mohler W, Han DK. 2003 Annexin I is an endogenous ligand that mediates apoptotic cell engulfment. *Dev Cell.* **4(4):**587-98.

[234] Perretti M, Wheller SK, Flower RJ, Wahid S, Pitzalis C. 1999 Modulation of cellular annexin I in human leukocytes infiltrating DTH skin reactions. *J Leukoc Biol.* **65(5):**583-9.

[235] McArthur S, Cristante E, Paterno M, Christian H, Roncaroli F, Gillies GE, Solito E. 2010 Annexin A1: a central player in the anti-inflammatory and neuroprotective role of microglia. *J Immunol.* **185(10):**6317-28.

[236] Parente L & Solito E. 2004 Annexin 1: more than an anti-phospholipase protein. *Inflamm Res.* **53(4):**125-32.

[237] Allcock GH, Allegra M, Flower RJ, Perretti M. 2001 Neutrophil accumulation induced by bacterial lipopolysaccharide: effects of dexamethasone and annexin 1. *Clin Exp Immunol.* **123(1):**62-7.

[238] Cooray SN, Gobbetti T, Montero-Melendez T, McArthur S, Thompson D, Clark AJ, Flower RJ, Perretti M. 2013 Ligand-specific conformational change of the G-protein-coupled receptor ALX/FPR2 determines proresolving functional responses. *Proc Natl Acad Sci U S A.* **110(45):**18232-7.

[239] Pupjalis D, Goetsch J, Kottas DJ, Gerke V, Rescher U. 2011 Annexin A1 released from apoptotic cells acts through formyl peptide receptors to dampen inflammatory monocyte activation via JAK/STAT/SOCS signalling. *EMBO Mol Med.* **3(2):**102-14.

[240] Tang J, Chen X, Tu W, Guo Y, Zhao Z, Xue Q, Lin C, Xiao J, Sun X, Tao T, Gu M, Liu Y. 2011 Propofol inhibits the activation of p38 through up-regulating the expression of annexin A1 to exert its anti-inflammation effect. *PLoS One.* **6(12):**e27890.

[241] Walther A, Riehemann K, Gerke V. A novel ligand of the formyl peptide receptor: annexin I regulates neutrophil extravasation by interacting with the FPR. *Mol Cell.* **5(5):**831-40.

[242] Panaro MA, Acquafredda A, Sisto M, Lisi S, Maffione AB, Mitolo V. 2006 Biological role of the N-formyl peptide receptors. *Immunopharmacol Immunotoxicol.* **28(1):**103-27.

[243] Perretti M, Chiang N, La M, Fierro IM, Marullo S, Getting SJ, Solito E, Serhan CN. 2002 Endogenous lipid- and peptide-derived anti-inflammatory pathways generated with glucocorticoid and aspirin treatment activate the lipoxin A4 receptor. *Nat Med.* **8(11):**1296-302.

[244] Perretti M & D'Acquisto F. 2009 Annexin A1 and glucocorticoids as effectors of the resolution of inflammation. *Nat Rev Immunol.* **9(1):**62-70.

[245] Perretti M & Dalli J. 2009 Exploiting the Annexin A1 pathway for the development of novel anti-inflammatory therapeutics. *Br J Pharmacol.* **158(4):**936-46.

[246] Kamal AM, Smith SF, De Silva Wijayasinghe M, Solito E, Corrigan CJ. 2001 An annexin 1 (ANXA1)-derived peptide inhibits prototype antigen-driven human T cell Th1 and Th2 responses in vitro. *Clin Exp Allergy.* **31(7):**1116-25.

[247] D'Acunto CW, Gbelcova H, Festa M, Ruml T. 2014 The complex understanding of Annexin A1 phosphorylation. *Cell Signal.* **26(1):**173-8.

[248] Futter CE, Felder S, Schlessinger J, Ullrich A, Hopkins CR. 1993 Annexin I is phosphorylated in the multivesicular body during the processing of the epidermal growth factor receptor. *J Cell Biol.* **120(1):**77-83.

[249] Sawyer ST & Cohen S. 1985 Epidermal growth factor stimulates the phosphorylation of the calcium-dependent 35,000-dalton substrate in intact A-431 cells. *J Biol Chem.* **260(14):**8233-6.

[250] Varticovski L, Chahwala SB, Whitman M, Cantley L, Schindler D, Chow EP, Sinclair LK, Pepinsky RB. 1988 Location of sites in human lipocortin I that are phosphorylated by protein tyrosine kinases and protein kinases A and C. *Biochemistry.* **27(10):**3682-90.

[251] Bitto E & Cho W. 1999 Structural determinant of the vesicle aggregation activity of annexin I. *Biochemistry.* **38(42):**14094-100.

XXVI

[252] Wang W & Creutz CE. 1994 Role of the amino-terminal domain in regulating interactions of annexin I with membranes: effects of amino-terminal truncation and mutagenesis of the phosphorylation sites. *Biochemistry.* **33(1):**275-82.

[253] Schlaepfer DD & Haigler HT. 1988 In vitro protein kinase C phosphorylation sites of placental lipocortin. *Biochemistry.* **27(12):**4253-8.

[254] Rothhut B. 1997 Participation of annexins in protein phosphorylation. *Cell Mol Life Sci.* **53(6):**522-6.

[255] Pederzoli-Ribeil M, Maione F, Cooper D, Al-Kashi A, Dalli J, Perretti M, D'Acquisto F. 2010 Design and characterization of a cleavage-resistant Annexin A1 mutant to control inflammation in the microvasculature. *Blood.* **116(20):**4288-96.

[256] Porte F, de Santa Barbara P, Phalipou S, Liautard JP, Widada JS. 1996 Change in the N-terminal domain conformation of annexin I that correlates with liposome aggregation is impaired by Ser-27 to Glu mutation that mimics phosphorylation. *Biochim Biophys Acta.* **1293(2):**177-84.

[257] Solito E, Christian HC, Festa M, Mulla A, Tierney T, Flower RJ, Buckingham JC. 2006 Post-translational modification plays an essential role in the translocation of annexin A1 from the cytoplasm to the cell surface. *FASEB J.* **20(9):**1498-500.

[258] Solito E, Mulla A, Morris JF, Christian HC, Flower RJ, Buckingham JC. 2003 Dexamethasone induces rapid serine-phosphorylation and membrane translocation of annexin 1 in a human folliculostellate cell line via a novel nongenomic mechanism involving the glucocorticoid receptor, protein kinase C, phosphatidylinositol 3-kinase, and mitogen-activated protein kinase. *Endocrinology.* **144(4):**1164-74.

[259] McArthur S, Yazid S, Christian H, Sirha R, Flower R, Buckingham J, Solito E. 2009 Annexin A1 regulates hormone exocytosis through a mechanism involving actin reorganization. *FASEB J.* **23(11):**4000-10.

[260] Alldridge LC, Harris HJ, Plevin R, Hannon R, Bryant CE. 1999 The annexin protein lipocortin 1 regulates the MAPK/ERK pathway. *J Biol Chem.* **274(53):**37620-8.

XXVII

[261] Futter CE & White IJ. 2007 Annexins and endocytosis. *Traffic.* **8(8):**951-8.

[262] Caron D, Maaroufi H, Michaud S, Tanguay RM, Faure RL. 2013 Annexin A1 is regulated by domains cross-talk through post-translational phosphorylation and SUMOYlation. *Cell Signal.* **25(10):**1962-9.

[263] Wang W & Creutz CE. 1994 Role of the amino-terminal domain in regulating interactions of annexin I with membranes: effects of amino-terminal truncation and mutagenesis of the phosphorylation sites. *Biochemistry.* **33(1):**275-82.

[264] Rescher U, Goebeler V, Wilbers A, Gerke V. 2006 Proteolytic cleavage of annexin 1 by human leukocyte elastase. *Biochim Biophys Acta.* **1763(11):**1320-4.

[265] Vong L, D'Acquisto F, Pederzoli-Ribeil M, Lavagno L, Flower RJ, Witko-Sarsat V, Perretti M. 2007 Annexin 1 cleavage in activated neutrophils: a pivotal role for proteinase 3. *J Biol Chem.* **282(41):**29998-30004.

[266] Sakaguchi M, Murata H, Sonegawa H, Sakaguchi Y, Futami J, Kitazoe M, Yamada H, Huh NH. 2007 Truncation of annexin A1 is a regulatory lever for linking epidermal growth factor signaling with cytosolic phospholipase A2 in normal and malignant squamous epithelial cells. *J Biol Chem.* **282(49):**35679-86.

[267] Williams SL, Milne IR, Bagley CJ, Gamble JR, Vadas MA, Pitson SM, Khew-Goodall Y. 2010 A proinflammatory role for proteolytically cleaved annexin A1 in neutrophil transendothelial migration. *J Immunol.* **185(5):**3057-63.

[268] Rescher U, Goebeler V, Wilbers A, Gerke V. 2006 Proteolytic cleavage of annexin 1 by human leukocyte elastase. *Biochim Biophys Acta.* **1763(11):**1320-4.

[269] Mussunoor S & Murray GI. 2008 The role of annexins in tumour development and progression. *J Pathol.* **216(2):**131-40.

[270] Paweletz CP, Ornstein DK, Roth MJ, Bichsel VE, Gillespie JW, Calvert VS, Vocke CD, Hewitt SM, Duray PH, Herring J, Wang QH, Hu N, Linehan WM, Taylor PR, Liotta LA, Emmert-Buck MR, Petricoin EF 3rd. 2000 Loss of annexin 1 correlates with early onset of tumorigenesis in esophageal and prostate carcinoma. *Cancer Res.* **60(22):**6293-7.

[271] Patton KT, Chen HM, Joseph L, Yang XJ. 2005 Decreased annexin I expression in prostatic adenocarcinoma and in high-grade prostatic intraepithelial neoplasia. *Histopathology.* **47(6):**597-601.

[272] Kang JS, Calvo BF, Maygarden SJ, Caskey LS, Mohler JL, Ornstein DK. 2002 Dysregulation of annexin I protein expression in high-grade prostatic intraepithelial neoplasia and prostate cancer. *Clin Cancer Res.* **8(1):**117-23.

[273] Schaeffer EM, Marchionni L, Huang Z, Simons B, Blackman A, Yu W, Parmigiani G, Berman DM. 2008 Androgen-induced programs for prostate epithelial growth and invasion arise in embryogenesis and are reactivated in cancer. *Oncogene.* **27(57):**7180-91.

[274] Inokuchi J, Lau A, Tyson DR, Ornstein DK. 2009 Loss of annexin A1 disrupts normal prostate glandular structure by inducing autocrine IL-6 signaling. *Carcinogenesis.* **30(7):**1082-8.

[275] Milone MR, Pucci B, Bruzzese F, Carbone C, Piro G, Costantini S, Capone F, Leone A, Di Gennaro E, Caraglia M, Budillon A. 2013 Acquired resistance to zoledronic acid and the parallel acquisition of an aggressive phenotype are mediated by p38-MAP kinase activation in prostate cancer cells. *Cell Death Dis.* **4:**e641.

[276] Hsiang CH, Tunoda T, Whang YE, Tyson DR, Ornstein DK. 2006 The impact of altered annexin I protein levels on apoptosis and signal transduction pathways in prostate cancer cells. *Prostate.* **66(13):**1413-24.

[277] Geary LA, Nash KA, Adisetiyo H, Liang M, Liao CP, Jeong JH, Zandi E, Roy-Burman P. 2014 CAF-secreted annexin A1 induces prostate cancer cells to gain stem cell-like features. *Mol Cancer Res.* **12(4):**607-21.

[278] Bizzarro V, Belvedere R, Milone MR, Pucci B, Lombardi R, Bruzzese F, Popolo A, Parente L, Budillon A, Petrella A. 2015 Annexin A1 is involved in the acquisition and maintenance of a stem cell-like/aggressive phenotype in prostate cancer cells with acquired resistance to zoledronic acid. *Oncotarget.* **6(28):**25076-92.

[279] Guzmán-Aránguez A, Olmo N, Turnay J, Lecona E, Pérez-Ramos P, López de Silanes I, Lizarbe MA. 2005 Differentiation of human colon adenocarcinoma cells alters the expression and intracellular localization of annexins A1, A2, and A5. *J Cell Biochem.* **94(1):**178-93.

[280] Duncan R, Carpenter B, Main LC, Telfer C, Murray GI. 2008 Characterisation and protein expression profiling of annexins in colorectal cancer. *Br J Cancer.* **98(2):**426-33.

[281] Liang L, Qu L, Ding Y. 2007 Protein and mRNA characterization in human colorectal carcinoma cell lines with different metastatic potentials. *Cancer Invest.* **25(6):**427-34.

[282] Su N, Xu XY, Chen H, Gao WC, Ruan CP, Wang Q, Sun YP. 2010 Increased expression of annexin A1 is correlated with K-ras mutation in colorectal cancer. *Tohoku J Exp Med.* **222(4):**243-50.

[283] Babbin BA, Lee WY, Parkos CA, Winfree LM, Akyildiz A, Perretti M, Nusrat A. 2006 Annexin I regulates SKCO-15 cell invasion by signaling through formyl peptide receptors. *J Biol Chem.* **281(28):**19588-99.

[284] Biaoxue R, Xiling J, Shuanying Y, Wei Z, Xiguang C, Jinsui W, Min Z. 2012 Upregulation of Hsp90-beta and annexin A1 correlates with poor survival and lymphatic metastasis in lung cancer patients. *J Exp Clin Cancer Res.* **31:**70.

[285] Liu YF, Zhang PF, Li MY, Li QQ, Chen ZC. 2011 Identification of annexin A1 as a proinvasive and prognostic factor for lung adenocarcinoma. *Clin Exp Metastasis.* **28(5):**413-25.

[286] Rong B, Zhao C, Liu H, Ming Z, Cai X, Gao W, Yang S. 2014 Elevated serum annexin A1 as potential diagnostic marker for lung cancer: a retrospective case-control study. *Am J Transl Res.* **6(5):**558-69.

XXX

[287] Wang C, Xiao Q, Li YW, Zhao C, Jia N, Li RL, Cao SS, Cui J, Wang L, Wu Y, Wen AD. 2014 Regulatory mechanisms of annexin-induced chemotherapy resistance in cisplatin resistant lung adenocarcinoma. *Asian Pac J Cancer Prev.* **15(7):**3191-4.

[288] Rondepierre F, Bouchon B, Papon J, Bonnet-Duquennoy M, Kintossou R, Moins N, Maublant J, Madelmont JC, D'Incan M, Degoul F. 2009 Proteomic studies of B16 lines: involvement of annexin A1 in melanoma dissemination. *Biochim Biophys Acta.* **1794(1):**61-9.

[289] Boudhraa Z, Rondepierre F, Ouchchane L, Kintossou R, Trzeciakiewicz A, Franck F, Kanitakis J, Labeille B, Joubert-Zakeyh J, Bouchon B, Perrot JL, Mansard S, Papon J, Dechelotte P, Chezal JM, Miot-Noirault E, Bonnet M, D'Incan M, Degoul F. 2014 Annexin A1 in primary tumors promotes melanoma dissemination. *Clin Exp Metastasis.* **31(7):**749-60.

[290] Boudhraa Z, Merle C, Mazzocut D, Chezal JM, Chambon C, Miot-Noirault E, Theisen M, Bouchon B, Degoul F. 2014 Characterization of pro-invasive mechanisms and N-terminal cleavage of ANXA1 in melanoma. *Arch Dermatol Res.* **306(10):**903-14.

[291] Shen D, Chang HR, Chen Z, He J, Lonsberry V, Elshimali Y, Chia D, Seligson D, Goodglick L, Nelson SF, Gornbein JA. 2005 Loss of annexin A1 expression in human breast cancer detected by multiple high-throughput analyses. *Biochem Biophys Res Commun.* **326(1):**218-27.

[292] Ou K, Yu K, Kesuma D, Hooi M, Huang N, Chen W, Lee SY, Goh XP, Tan LK, Liu J, Soon SY, Bin Abdul Rashid S, Putti TC, Jikuya H, Ichikawa T, Nishimura O, Salto-Tellez M, Tan P. 2008 Novel breast cancer biomarkers identified by integrative proteomic and gene expression mapping. *J Proteome Res.* **7(4):**1518-28.

[293] Ang EZ, Nguyen HT, Sim HL, Putti TC, Lim LH. 2009 Annexin-1 regulates growth arrest induced by high levels of estrogen in MCF-7 breast cancer cells. *Mol Cancer Res.* **7(2):**266-74.

[294] Khau T, Langenbach SY, Schuliga M, Harris T, Johnstone CN, Anderson RL, Stewart AG. 2011 Annexin-1 signals mitogen-stimulated breast tumor cell proliferation by activation of the formyl peptide receptors (FPRs) 1 and 2. *FASEB J.* **25(2):**483-96.

XXXI

[295] Maschler S, Gebeshuber CA, Wiedemann EM, Alacakaptan M, Schreiber M, Custic I, Beug H. 2010 Annexin A1 attenuates EMT and metastatic potential in breast cancer. *EMBO Mol Med.* **2(10):**401-14.

[296] de Graauw M, van Miltenburg MH, Schmidt MK, Pont C, Lalai R, Kartopawiro J, Pardali E, Le Dévédec SE, Smit VT, van der Wal A, Van't Veer LJ, Cleton-Jansen AM, ten Dijke P, van de Water B. 2010 Annexin A1 regulates TGF-beta signaling and promotes metastasis formation of basal-like breast cancer cells. *Proc Natl Acad Sci U S A.* **107(14):**6340-5.

[297] Yom CK, Han W, Kim SW, Kim HS, Shin HC, Chang JN, Koo M, Noh DY, Moon BI. 2011 Clinical significance of annexin A1 expression in breast cancer. *J Breast Cancer.* **14(4):**262-8.

[298] Araujo TG, Marangoni K, Rocha RM, Maia YC, Araujo GR, Alcântar TM, Alves PT, Calábria L, Neves AF, Soares FA, Goulart LR. 2014 Dynamic dialog between cytokeratin 18 and annexin A1 in breast cancer: a transcriptional disequilibrium. *Acta Histochem.* **116(7):**1178-84.

[299] Kang H, Ko J, Jang SW. 2012 The role of annexin A1 in expression of matrix metalloproteinase-9 and invasion of breast cancer cells. *Biochem Biophys Res Commun.* **423(1):**188-94.

[300] Swa HL, Shaik AA, Lim LH, Gunaratne J. 2015 Mass spectrometry based quantitative proteomics and integrative network analysis accentuates modulating roles of annexin-1 in mammary tumorigenesis. *Proteomics.* **15(2-3):**408-18.

[301] Yoshida K, Kuramitsu Y, Murakami K, Ryozawa S, Taba K, Kaino S, Zhang X, Sakaida I, Nakamura K. 2011 Proteomic differential display analysis for TS-1-resistant and -sensitive pancreatic cancer cells using two-dimensional gel electrophoresis and mass spectrometry. *Anticancer Res.* **31(6):**2103-8.

[302] Chen CY, Shen JQ, Wang F, Wan R, Wang XP. 2012 Prognostic significance of annexin A1 expression in pancreatic ductal adenocarcinoma. *Asian Pac J Cancer Prev.* **13(9):**4707-12.

[303] Bai XF, Ni XG, Zhao P, Liu SM, Wang HX, Guo B, Zhou LP, Liu F, Zhang JS, Wang K, Xie YQ, Shao YF, Zhao XH. 2004 Overexpression of annexin 1 in pancreatic cancer and its clinical significance. *World J Gastroenterol.* **10(10):**1466-70.

[304] Gerdes HH. 2008 Membrane traffic in the secretory pathway. Cell Mol Life Sci. 65(18):2779-80.

[305] Wallner BP, Mattaliano RJ, Hession C, Cate RL, Tizard R, Sinclair LK, Foeller C, Chow EP, Browing JL, Ramachandran KL, *et al.* 1986 Cloning and expression of human lipocortin, a phospholipase A2 inhibitor with potential anti-inflammatory activity. *Nature.* **320(6057):**77-81.

[306] Christmas P, Callaway J, Fallon J, Jones J, Haigler HT. 1991 Selective secretion of annexin 1, a protein without a signal sequence, by the human prostate gland. *J Biol Chem.* **266(4):**2499-507.

[307] Aderem AA, Albert KA, Keum MM, Wang JK, Greengard P, Cohn ZA. 1988 Stimulus-dependent myristoylation of a major substrate for protein kinase C. *Nature.* **332(6162):**362-4.

[308] Omer S, Meredith D, Morris JF, Christian HC. 2006 Evidence for the role of adenosine 5'-triphosphate-binding cassette (ABC)-A1 in the externalization of annexin 1 from pituitary folliculostellate cells and ABCA1-transfected cell models. *Endocrinology.* **147(7):**3219-27.

[309] Euzger HS, Flower RJ, Goulding NJ, Perretti M. 1999 Differential modulation of annexin I binding sites on monocytes and neutrophils. *Mediators Inflamm.* **8(1):**53-62.

[310] Dalli J, Norling LV, Renshaw D, Cooper D, Leung KY, Perretti M. 2008 Annexin 1 mediates the rapid anti-inflammatory effects of neutrophil-derived microparticles. *Blood.* **112(6):**2512-9.

[311] Raposo G & Stoorvogel W. 2013 Extracellular vesicles: exosomes, microvesicles, and friends. *J Cell Biol.* **200(4):**373-83.

[312] Prossnitz ER & Ye RD. 1997 The N-formyl peptide receptor: a model for the study of chemoattractant receptor structure and function. *Pharmacol Ther.* **74(1):**73-102.

XXXIII

[313] Ye RD, Boulay F, Wang JM, Dahlgren C, Gerard C, Parmentier M, Serhan CN, Murphy PM. 2009 International Union of Basic and Clinical Pharmacology. LXXIII. Nomenclature for the formyl peptide receptor (FPR) family. *Pharmacol Rev.* **61(2):**119-61.

[314] Bao L, Gerard NP, Eddy RL Jr, Shows TB, Gerard C. 1992 Mapping of genes for the human C5a receptor (C5AR), human FMLP receptor (FPR), and two FMLP receptor homologue orphan receptors (FPRH1, FPRH2) to chromosome 19*. Genomics.* **13(2):**437-40.

[315] Murphy PM, Gallin EK, Tiffany HL, Malech HL. 1990 The formyl peptide chemoattractant receptor is encoded by a 2 kilobase messenger RNA. Expression in Xenopus oocytes. *FEBS Lett.* **261(2):**353-7.

[316] Prossnitz ER, Quehenberger O, Cochrane CG, Ye RD. 1993 Signal transducing properties of the N-formyl peptide receptor expressed in undifferentiated HL60 cells. *J Immunol.* **151(10):**5704-15.

[317] Dorward DA, Lucas CD, Chapman GB, Haslett C, Dhaliwal K, Rossi AG. 2015 The role of formylated peptides and formyl peptide receptor 1 in governing neutrophil function during acute inflammation. *Am J Pathol.* **185(5):**1172-84.

[318] Yang D, Chen Q, Le Y, Wang JM, Oppenheim JJ. 2001 Differential regulation of formyl peptide receptor-like 1 expression during the differentiation of monocytes to dendritic cells and macrophages. *J Immunol.* **166(6):**4092-8.

[319] Yang D, Chen Q, Gertz B, He R, Phulsuksombati M, Ye RD, Oppenheim JJ. 2002 Human dendritic cells express functional formyl peptide receptor-like-2 (FPRL2) throughout maturation. *J Leukoc Biol.* **72(3):**598-607.

[320] Bizzarro V, Petrella A, Parente L. 2012 Annexin A1: novel roles in skeletal muscle biology. *J Cell Physiol.* **227(8):**3007-15.

[321] Hazeldine J, Hampson P, Opoku FA, Foster M, Lord JM. 2015 N-Formyl peptides drive mitochondrial damage associated molecular pattern induced neutrophil activation through ERK1/2 and P38 MAP kinase signalling pathways. *Injury.* **46(6):**975-84.

[322] Li Y, Cai L, Wang H, Wu P, Gu W, Chen Y, Hao H, Tang K, Yi P, Liu M, Miao S, Ye D. 2011 Pleiotropic regulation of macrophage polarization and tumorigenesis by formyl peptide receptor-2. *Oncogene.* **30(36):**3887-99.

[323] Wan M, Godson C, Guiry PJ, Agerberth B, Haeggström JZ. 2011 Leukotriene B4/antimicrobial peptide LL-37 proinflammatory circuits are mediated by BLT1 and FPR2/ALX and are counterregulated by lipoxin A4 and resolvin E1. *FASEB J.* **25(5):**1697-705.

[324] El Kebir D, József L, Khreiss T, Pan W, Petasis NA, Serhan CN, Filep JG. 2007 Aspirin-triggered lipoxins override the apoptosis-delaying action of serum amyloid A in human neutrophils: a novel mechanism for resolution of inflammation. *J Immunol.* **179(1):**616-22.

[325] Devosse T, Guillabert A, D'Haene N, Berton A, De Nadai P, Noel S, Brait M, Franssen JD, Sozzani S, Salmon I, Parmentier M. 2009 Formyl peptide receptor-like 2 is expressed and functional in plasmacytoid dendritic cells, tissue-specific macrophage subpopulations, and eosinophils. *J Immunol.* **182(8):**4974-84.

[326] Kang HK, Lee HY, Kim MK, Park KS, Park YM, Kwak JY, Bae YS. 2005 The synthetic peptide Trp-Lys-Tyr-Met-Val-D-Met inhibits human monocyte-derived dendritic cell maturation via formyl peptide receptor and formyl peptide receptor-like 2. *J Immunol.* **175(2):**685-92.

[327] Harada M, Habata Y, Hosoya M, Nishi K, Fujii R, Kobayashi M, Hinuma S. 2004 N-Formylated humanin activates both formyl peptide receptor-like 1 and 2. *Biochem Biophys Res Commun.* **324(1):**255-61.

[328] Rabiet MJ, Macari L, Dahlgren C, Boulay F. 2011 N-formyl peptide receptor 3 (FPR3) departs from the homologous FPR2/ALX receptor with regard to the major processes governing chemoattractant receptor regulation, expression at the cell surface, and phosphorylation. *J Biol Chem.* **286(30):**26718-31.

[329] Su SB, Gong W, Gao JL, Shen W, Murphy PM, Oppenheim JJ, Wang JM. 1999 A seven-transmembrane, G protein-coupled receptor, FPRL1, mediates the chemotactic activity of serum amyloid A for human phagocytic cells. *J Exp Med.* **189(2):**395-402.

[330] He R, Sang H, Ye RD. 2003 Serum amyloid A induces IL-8 secretion through a G protein-coupled receptor, FPRL1/LXA4R. *Blood.* **101(4):**1572-81.

[331] Le Y, Gong W, Tiffany HL, Tumanov A, Nedospasov S, Shen W, Dunlop NM, Gao JL, Murphy PM, Oppenheim JJ, Wang JM. 2001 Amyloid (beta)42 activates a G-protein-coupled chemoattractant receptor, FPR-like-1. *J Neurosci.* **21(2):**RC123.

[332] Chen K, Iribarren P, Hu J, Chen J, Gong W, Cho EH, Lockett S, Dunlop NM, Wang JM. 2006 Activation of Toll-like receptor 2 on microglia promotes cell uptake of Alzheimer disease-associated amyloid beta peptide. *J Biol Chem.* **281(6):**3651-9.

[333] Betten A, Bylund J, Christophe T, Boulay F, Romero A, Hellstrand K, Dahlgren C. 2001 A proinflammatory peptide from Helicobacter pylori activates monocytes to induce lymphocyte dysfunction and apoptosis. *J Clin Invest.* **108(8):**1221-8.

[334] de Paulis A, Prevete N, Fiorentino I, Walls AF, Curto M, Petraroli A, Castaldo V, Ceppa P, Fiocca R, Marone G. 2004 Basophils infiltrate human gastric mucosa at sites of Helicobacter pylori infection, and exhibit chemotaxis in response to H. pylori-derived peptide Hp(2-20). *J Immunol.* **172(12):**7734-43.

[335] Hartt JK, Liang T, Sahagun-Ruiz A, Wang JM, Gao JL, Murphy PM. 2000 The HIV-1 cell entry inhibitor T-20 potently chemoattracts neutrophils by specifically activating the N-formylpeptide receptor. *Biochem Biophys Res Commun.* **272(3):**699-704.

[336] Bellner L, Thorén F, Nygren E, Liljeqvist JA, Karlsson A, Eriksson K. 2005 A proinflammatory peptide from herpes simplex virus type 2 glycoprotein G affects neutrophil, monocyte, and NK cell functions. *J Immunol.* **174(4):**2235-41.

[337] De Yang, Chen Q, Schmidt AP, Anderson GM, Wang JM, Wooters J, Oppenheim JJ, Chertov O. 2000 LL-37, the neutrophil granule- and epithelial cell-derived cathelicidin, utilizes formyl peptide receptor-like 1 (FPRL1) as a receptor to chemoattract human peripheral blood neutrophils, monocytes, and T cells. *J Exp Med.* **192(7):**1069-74.

[338] Koczulla R, von Degenfeld G, Kupatt C, Krötz F, Zahler S, Gloe T, Issbrücker K, Unterberger P, Zaiou M, et al. 2003 An angiogenic role for the human peptide antibiotic LL-37/hCAP-18. *J Clin Invest.* **111(11):**1665-72.

[339] Migeotte I, Riboldi E, Franssen JD, Grégoire F, Loison C, Wittamer V, Detheux M, *et al.* 2005 Identification and characterization of an endogenous chemotactic ligand specific for FPRL2. *J Exp Med.* **201(1):**83-93.

[340] Serhan CN. 2005 Lipoxins and aspirin-triggered 15-epi-lipoxins are the first lipid mediators of endogenous anti-inflammation and resolution. *Prostaglandins Leukot Essent Fatty Acids.* **73(3-4):**141-62.

[341] Serhan CN. 2007 Resolution phase of inflammation: novel endogenous anti-inflammatory and proresolving lipid mediators and pathways. *Annu Rev Immunol.* **25:**101-37.

[342] Leoni G, Alam A, Neumann PA, Lambeth JD, Cheng G, McCoy J, Hilgarth RS, Kundu K, et al. 2013 Annexin A1, formyl peptide receptor, and NOX1 orchestrate epithelial repair. *J Clin Invest.* **123(1):**443-54.

[343] Buss NA, Gavins FN, Cover PO, Terron A, Buckingham JC. 2015 Targeting the annexin 1-formyl peptide receptor 2/ALX pathway affords protection against bacterial LPS-induced pathologic changes in the murine adrenal cortex. *FASEB J.* **29(7):**2930-42.

[344] Drechsler M, de Jong R, Rossaint J, Viola JR, Leoni G, Wang JM, Grommes J, Hinkel R, Kupatt C, Weber C, Döring Y, Zarbock A, Soehnlein O. 2015 Annexin A1 counteracts chemokine-induced arterial myeloid cell recruitment. *Circ Res.* **116(5):**827-35.

[345] Bizzarro V, Belvedere R, Dal Piaz F, Parente L, Petrella A. 2012 Annexin A1 induces skeletal muscle cell migration acting through formyl peptide receptors. *PLoS One.* **7(10):**e48246.

[346] Bizzarro V, Fontanella B, Carratù A, Belvedere R, Marfella R, Parente L, Petrella A. 2012 Annexin A1 N-terminal derived peptide Ac2-26 stimulates fibroblast migration in high glucose conditions. *PLoS One.* **7(9):**e45639.

XXXVII

[347] Cheng TY, Wu MS, Lin JT, Lin MT, Shun CT, Huang HY, Hua KT, Kuo ML. 2012 Annexin A1 is associated with gastric cancer survival and promotes gastric cancer cell invasiveness through the formyl peptide receptor/extracellular signal-regulated kinase/integrin beta-1-binding protein 1 pathway. *Cancer.* **118(23):**5757-67.

[348] Freer RJ, Day AR, Radding JA, Schiffmann E, Aswanikumar S, Showell HJ, Becker EL. 1980 Further studies on the structural requirements for synthetic peptide chemoattractants. *Biochemistry.* **19(11):**2404-10.

[349] Bae YS, Lee HY, Jo EJ, Kim JI, Kang HK, Ye RD, Kwak JY, Ryu SH. 2004 Identification of peptides that antagonize formyl peptide receptor-like 1-mediated signaling. *J Immunol.* **173(1):**607-14.

[350] Wenzel-Seifert K & Seifert R. 1993 Cyclosporin H is a potent and selective formyl peptide receptor antagonist. Comparison with N-t-butoxycarbonyl-L-phenylalanyl-L-leucyl-L-phenylalanyl-L-leucyl-L-phenylalanine and cyclosporins A, B, C, D, and E. *J Immunol.* **150(10):**4591-9.

[351] Rabiet MJ, Huet E, Boulay F. 2007 The N-formyl peptide receptors and the anaphylatoxin C5a receptors: an overview. *Biochimie.* **89(9):**1089-106.

[352] Prevete N, Liotti F, Marone G, Melillo RM, de Paulis A. 2015 Formyl peptide receptors at the interface of inflammation, angiogenesis and tumor growth. *Pharmacol Res.* **102:**184-91.

[353] Babbin BA, Jesaitis AJ, Ivanov AI, Kelly D, Laukoetter M, Nava P, Parkos CA, Nusrat A. 2007 Formyl peptide receptor-1 activation enhances intestinal epithelial cell restitution through phosphatidylinositol 3-kinase-dependent activation of Rac1 and Cdc42. *J Immunol.* **179(12):**8112-21.

[354] Shao G, Julian MW, Bao S, McCullers MK, Lai JP, Knoell DL, Crouser ED. 2011 Formyl peptide receptor ligands promote wound closure in lung epithelial cells. *Am J Respir Cell Mol Biol.* **44(3):**264-9.

[355] Zhang XG, Hui YN, Huang XF, Du HJ, Zhou J, Ma JX. 2011 Activation of formyl peptide receptor-1 enhances restitution of human retinal pigment epithelial cell monolayer under electric fields. *Invest Ophthalmol Vis Sci.* **52(6):**3160-5.

[356] Liu M, Zhao J, Chen K, Bian X, Wang C, Shi Y, Wang JM. 2012 G protein-coupled receptor FPR1 as a pharmacologic target in inflammation and human glioblastoma. *Int Immunopharmacol.* **14(3):**283-8.

[357] Zhou Y, Bian X, Le Y, Gong W, Hu J, Zhang X, Wang L, Iribarren P, Salcedo R, Howard OM, Farrar W, Wang JM. 2005 Formylpeptide receptor FPR and the rapid growth of malignant human gliomas. *J Natl Cancer Inst.* **97(11):**823-35.

[358] Huang J, Chen K, Chen J, Gong W, Dunlop NM, Howard OM, Gao Y, Bian XW, Wang JM. 2010 The G-protein-coupled formylpeptide receptor FPR confers a more invasive phenotype on human glioblastoma cells. *Br J Cancer.* **102(6):**1052-60.

[359] Chen K, Liu M, Liu Y, Yoshimura T, Shen W, Le Y, Durum S, Gong W, Wang C, Gao JL, Murphy PM, Wang JM. 2013 Formylpeptide receptor-2 contributes to colonic epithelial homeostasis, inflammation, and tumorigenesis. *J Clin Invest.* **123(4):**1694-704.

[360] Otani T, Ikeda S, Lwin H, Arai T, Muramatsu M, Sawabe M. 2011 Polymorphisms of the formylpeptide receptor gene (FPR1) and susceptibility to stomach cancer in 1531 consecutive autopsy cases. *Biochem Biophys Res Commun.* **405(3):**356-61.

[361] Prevete N, Liotti F, Visciano C, Marone G, Melillo RM, de Paulis A. 2015 The formyl peptide receptor 1 exerts a tumor suppressor function in human gastric cancer by inhibiting angiogenesis. *Oncogene.* **34(29):**3826-38.

[362] Cheng TY, Wu MS, Lin JT, Lin MT, Shun CT, Hua KT, Kuo ML. 2014 Formyl Peptide receptor 1 expression is associated with tumor progression and survival in gastric cancer. *Anticancer Res.* **34(5):**2223-9.

[363] Dal Piaz F, Cotugno R, Lepore L, Vassallo A, Malafronte N, Lauro G, Bifulco G, Belisario MA, De Tommasi N. 2013 Chemical proteomics reveals HSP70 1A as a target for the anticancer diterpene oridonin in Jurkat cells. *J Proteomics.* **82:**14-26.

[364] Adesso S, Popolo A, Bianco G, Sorrentino R, Pinto A, Autore G, Marzocco S. 2013 The uremic toxin indoxyl sulphate enhances macrophage response to LPS. *PLoS One.* **8(9):**e76778.

XXXIX

[365] Wade M.2015 High-Throughput Silencing Using the CRISPR-Cas9 System: A Review of the Benefits and Challenges. *J Biomol Screen.* **20(8):**1027-39.

[366] Vidigal JA & Ventura A. 2015 Rapid and efficient one-step generation of paired gRNA CRISPR-Cas9 libraries. *Nat Commun.* **6:**8083.

[367] Ishino Y, Shinagawa H, Makino K, Amemura M, Nakata A. 1987 Nucleotide sequence of the iap gene, responsible for alkaline phosphatase isozyme conversion in Escherichia coli, and identification of the gene product. *J Bacteriol.* **169(12):**5429-33.

[368] Barrangou R, Fremaux C, Deveau H, Richards M, Boyaval P, Moineau S, Romero DA, Horvath P. 2007 CRISPR provides acquired resistance against viruses in prokaryotes. *Science.* **315(5819):**1709-12.

[369] Jinek M, Chylinski K, Fonfara I, Hauer M, Doudna JA, Charpentier E. 2012 A programmable dual-RNA-guided DNA endonuclease in adaptive bacterial immunity. *Science.* **337(6096):**816-21.

[370] Shen B, Zhang W, Zhang J, Zhou J, Wang J, Chen L, Wang L, Hodgkins A, Iyer V, Huang X, Skarnes WC. 2014 Efficient genome modification by CRISPR-Cas9 nickase with minimal off-target effects. *Nat Methods.* **11(4):**399-402.

[371] Sander JD & Joung JK. 2014 CRISPR-Cas systems for editing, regulating and targeting genomes. *Nat Biotechnol.* **32(4):**347-55.

[372] Overballe-Petersen S, Harms K, Orlando LA, Mayar JV, Rasmussen S, Dahl TW, Rosing MT, Poole AM, Sicheritz-Ponten T, Brunak S, Inselmann S, de Vries J, Wackernagel W, Pybus OG, Nielsen R, Johnsen PJ, Nielsen KM, Willerslev E. 2013 Bacterial natural transformation by highly fragmented and damaged DNA. *Proc Natl Acad Sci U S A.* **110(49):**19860-5.

[373] Gong C, Bongiorno P, Martins A, Stephanou NC, Zhu H, Shuman S, Glickman MS. 2005 Mechanism of nonhomologous end-joining in mycobacteria: a low-fidelity repair system driven by Ku, ligase D and ligase C. *Nat Struct Mol Biol.* **12(4):**304-12.

[374] Mali P, Yang L, Esvelt KM, Aach J, Guell M, DiCarlo JE, Norville JE, Church GM. 2013 RNA-guided human genome engineering via Cas9. *Science.* **339(6121):**823-6.

[375] Cong L, Ran FA, Cox D, Lin S, Barretto R, Habib N, Hsu PD, Wu X, Jiang W, Marraffini LA, Zhang F. 2013 Multiplex genome engineering using CRISPR/Cas systems. *Science.* **339(6121):**819-23.

[376] Sánchez-Rivera F J & Jacks T. 2015 Applications of the CRISPR-Cas9 system in cancer biology. *Nat Rev Cancer.* **15(7):** 387–395.

[377] Mussolino C, Morbitzer R, Lütge F, Dannemann N, Lahaye T, Cathomen T. 2011 A novel TALE nuclease scaffold enables high genome editing activity in combination with low toxicity. *Nucleic Acids Res.* **39(21):**9283-93.

[378] Hsu PD, Scott DA, Weinstein JA, Ran FA, Konermann S, Agarwala V, Li Y, Fine EJ, Wu X, Shalem O, Cradick TJ, Marraffini LA, Bao G, Zhang F. 2013 DNA targeting specificity of RNA-guided Cas9 nucleases. *Nat Biotechnol.* **31(9):**827-32.

[379] Pattanayak V, Lin S, Guilinger JP, Ma E, Doudna JA, Liu DR. 2013 High-throughput profiling of off-target DNA cleavage reveals RNA-programmed Cas9 nuclease specificity. *Nat Biotechnol.* **31(9):**839-43.

[380] Ho TT, Zhou N, Huang J, Koirala P, Mu X, Fung R, Wu F, Mo YY. 2014 Targeting non-coding RNAs with the CRISPR/Cas9 system in human cell lines. *Nucl. Acids Res.* **43(3):**e17.

[381] Li W, Xu H, Xiao T, Cong L, Love MI, Zhang F, Irizarry RA, Liu JS, Brown M, Liu XS. 2014 MAGeCK enables robust identification of essential genes from genome-scale CRISPR/Cas9 knockout screens. *Genome Biol.* **15(12):**554.

[382] Kim MP, Evans DB, Wang H, Abbruzzese JL, Fleming JB, Gallick GE. 2009 Generation of orthotopic and heterotopic human pancreatic cancer xenografts in immunodeficient mice. *Nat Protoc.* **4(11):**1670-80.

[383] Deer EL, González-Hernández J, Coursen JD, Shea JE, Ngatia J, Scaife CL, Firpo MA, Mulvihill SJ. 2010 Phenotype and genotype of pancreatic cancer cell lines. *Pancreas.* **39(4):**425-35.

[384] Tan MH, Nowak NJ, Loor R, Ochi H, Sandberg AA, Lopez C, Pickren JW, Berjian R, Douglass HO Jr, Chu TM. 1986 Characterization of a new primary human pancreatic tumor line. *Cancer Invest.* **4(1):**15-23.

[385] Kyriazis AA, Kyriazis AP, Sternberg CN, Sloane NH, Loveless JD. 1986 Morphological, biological, biochemical, and karyotypic characteristics of human pancreatic ductal adenocarcinoma Capan-2 in tissue culture and the nude mouse. *Cancer Res.* **46(11):**5810-5.

[386] Yunis AA, Arimura GK, Russin DJ. 1977 Human pancreatic carcinoma (MIA PaCa-2) in continuous culture: sensitivity to asparaginase. *Int J Cancer.* **19(1):**128-35.

[387] Lieber M, Mazzetta J, Nelson-Rees W, Kaplan M, Todaro G. 1975 Establishment of a continuous tumor-cell line (panc-1) from a human carcinoma of the exocrine pancreas. *Int J Cancer.* **15(5):**741-7.

[388] Thiery JP. 2003 Epithelial-mesenchymal transitions in development and pathologies. *Curr Opin Cell Biol.* **15(6):**740-6.

[389] Salnikov AV, Liu L, Platen M, Gladkich J, Salnikova O, Ryschich E, Mattern J, Moldenhauer G, Werner J, Schemmer P, Büchler MW, Herr I. 2012 Hypoxia induces EMT in low and highly aggressive pancreatic tumor cells but only cells with cancer stem cell characteristics acquire pronounced migratory potential. *PLoS One.* **7(9):**e46391.

[390] Bergman A, Condeelis JS, Gligorijevic B. 2014 Invadopodia in context. *Cell Adh Migr.* **8(3):**273-9.

[391] Li S, Guan JL, Chien S. 2005 Biochemistry and biomechanics of cell motility. *Annu Rev Biomed Eng.* **7:**105-50.

[391] Hullin F, Raynal P, Ragab-Thomas JM, Fauvel J, Chap H. 1989 Effect of dexamethasone on prostaglandin synthesis and on lipocortin status in human endothelial cells. Inhibition of prostaglandin I2 synthesis occurring without alteration of arachidonic acid liberation and of lipocortin synthesis. *J Biol Chem.* **264(6):**3506-13.

[392] Ambrose MP & Hunninghake GW. 1990 Corticosteroids increase lipocortin I in alveolar epithelial cells. *Am J Respir Cell Mol Biol.* **3(4):**349-53.

[393] Croxtall JD, Choudhury Q, Newman S, Flower RJ. 1996 Lipocortin 1 and the control of cPLA2 activity in A549 cells. Glucocorticoids block EGF stimulation of cPLA2 phosphorylation. *Biochem Pharmacol.* **52(2):**351-6.

[394] Perretti M, Croxtall JD, Wheller SK, Goulding NJ, Hannon R, Flower RJ. 1996 Mobilizing lipocortin 1 in adherent human leukocytes downregulates their transmigration. *Nat Med.* **2(11):**1259-62.

[395] Rhee HJ, Kim GY, Huh JW, Kim SW, Na DS. 2000 Annexin I is a stress protein induced by heat, oxidative stress and a sulfhydryl-reactive agent. *Eur J Biochem.* **267(11):**3220-5.

[396] Sampey AV, Hutchinson P, Morand EF. 2000 Annexin I surface binding sites and their regulation on human fibroblast-like synoviocytes*. Arthritis Rheum.* **43(11):**2537-42.

[397] Yang Y, Liu Y, Yao X, Ping Y, Jiang T, Liu Q, Xu S, Huang J, Mou H, Gong W, Chen K, Bian X, Wang JM. 2011 Annexin 1 released by necrotic human glioblastoma cells stimulates tumor cell growth through the formyl peptide receptor 1. *Am J Pathol.* **179:**1504-1512.

[398] Dalli J, Montero-Melendez T, McArthur S, Perretti M. 2012 Annexin A1 N-terminal derived Peptide ac2-26 exerts chemokinetic effects on human neutrophils. *Front Pharmacol.* **3:**28.

[399] Bauer DE, Canver MC, Orkin SH. 2014 Generation of genomic deletions in mammalian cell lines via CRISPR/Cas9. *J Vis Exp.* (95).

[400] Dittmer TA & Misteli T. 2011 The lamin protein family. *Genome Biol.* **12(5):**222.

[401] Sugahara KN, Hirata T, Hayasaka H, Stern R, Murai T, Miyasaka M. 2006 Tumor cells enhance their own CD44 cleavage and motility by generating hyaluronan fragments. *J Biol Chem.* **281(9):**5861-8.

[402] Sugahara KN, Murai T, Nishinakamura H, Kawashima H, Saya H, Miyasaka M. 2003 Hyaluronan oligosaccharides induce CD44 cleavage and promote cell migration in CD44-expressing tumor cells. *J Biol Chem.* **278(34):**32259-65.

[403] Nagano O & Saya H. 2004 Mechanism and biological significance of CD44 cleavage. *Cancer Sci.* **95(12):**930-5.

[404] Lau AT & Chiu JF. 2007 The possible role of cytokeratin 8 in cadmium-induced adaptation and carcinogenesis. *Cancer Res.* **67(5):**2107-13.

[405] Ku NO & Omary MB. 2006 A disease- and phosphorylation-related nonmechanical function for keratin 8. *J Cell Biol.* **174(1):**115-25.

[406] Linder S, Havelka AM, Ueno T, Shoshan MC. 2004 Determining tumor apoptosis and necrosis in patient serum using cytokeratin 18 as a biomarker. *Cancer Lett.* **214(1):**1-9.

[407] Stricker J, Falzone T, Gardel ML. 2010 Mechanics of the F-actin cytoskeleton. *J Biomech.* **43(1):**9-14.

[408] Yam CH, Fung TK, Poon RY. 2002 Cyclin A in cell cycle control and cancer. *Cell Mol Life Sci.* **59(8):**1317-26.

[409] Brocker C, Lassen N, Estey T, Pappa A, Cantore M, Orlova VV, Chavakis T, Kavanagh KL, Oppermann U, Vasiliou V. 2010 Aldehyde dehydrogenase 7A1 (ALDH7A1) is a novel enzyme involved in cellular defense against hyperosmotic stress. *J Biol Chem.* **285(24):**18452-63.

[410] Chan CL, Wong JW, Wong CP, Chan MK, Fong WP. 2011 Human antiquitin: structural and functional studies. *Chem Biol Interact.* **191(1-3):**165-70.

[411] Zhang W & Liu HT. 2002 MAPK signal pathways in the regulation of cell proliferation in mammalian cells. *Cell Res.* **12(1):**9-18.

[412] Mebratu Y & Tesfaigzi Y. 2009 How ERK1/2 activation controls cell proliferation and cell death: Is subcellular localization the answer? *Cell Cycle.* **8(8):**1168-75.

[413] Huynh AS, Abrahams DF, Torres MS, Baldwin MK, Gillies RJ, Morse DL. 2011 Development of an orthotopic human pancreatic cancer xenograft model using ultrasound guided injection of cells. *PLoS One.* **6(5):**e20330.

[414] Lim LH & Pervaiz S. 2007 Annexin 1: the new face of an old molecule. *FASEB J.* **21(4):**968-75.

[415] Sato Y, Kumamoto K, Saito K, Okayama H, Hayase S, Kofunato Y, Miyamoto K, Nakamura I, Ohki S, Koyama Y, Takenoshita S. 2011 Up-regulated Annexin A1 expression in gastrointestinal cancer is associated with cancer invasion and lymph node metastasis. *Exp Ther Med.* **2(2):**239-243.

[416] Liu K, Qin CK, Wang ZY, Liu SX, Cui XP, Zhang DY. 2012 Expression of tumor necrosis factor-alpha-induced protein 8 in pancreas tissues and its correlation with epithelial growth factor receptor levels. *Asian Pac J Cancer Prev.* **13(3):**847-50.

[417] Bizzarro V, Fontanella B, Franceschelli S, Pirozzi M, Christian H, Parente L, Petrella A. Role of Annexin A1 in mouse myoblast cell differentiation. *J Cell Physiol.* **224(3):**757-65.

[418] Prevarskaya N, Skryma R, Shuba Y. 2011 Calcium in tumour metastasis: new roles for known actors. *Nat Rev Cancer.* **11(8):**609-18.

[419] Rescher U, Danielczyk A, Markoff A, Gerke V. 2002 Functional activation of the formyl peptide receptor by a new endogenous ligand in human lung A549 cells. *J Immunol.* **169(3):**1500-4.

[420] Côté MC, Lavoie JR, Houle F, Poirier A, Rousseau S, Huot J. 2010 Regulation of vascular endothelial growth factor-induced endothelial cell migration by LIM kinase 1-mediated phosphorylation of annexin 1. *J Biol Chem.* **285(11):**8013-21.

[421] Pepinsky RB & Sinclair LK. 1986 Epidermal growth factor-dependent phosphorylation of lipocortin. *Nature.* **321(6065):**81-4.

[422] Wu W, Tang X, Hu W, Lotan R, Hong WK, Mao L. 2002 Identification and validation of metastasis-associated proteins in head and neck cancer cell lines by two-dimensional electrophoresis and mass spectrometry. *Clin Exp Metastasis.* **19(4):**319-26.

[423] Takada M, Nakamura Y, Koizumi T, Toyama H, Kamigaki T, Suzuki Y, Takeyama Y, Kuroda Y. 2002 Suppression of human pancreatic carcinoma cell growth and invasion by epigallocatechin-3-gallate. *Pancreas.* **25(1):**45-8.

[424] Ellenrieder V, Hendler SF, Ruhland C, Boeck W, Adler G, Gress TM 2001 TGF-beta-induced invasiveness of pancreatic cancer cells is mediated by matrix metalloproteinase-2 and the urokinase plasminogen activator system. *Int J Cancer.* **93(2):**204-11.

[425] Belvedere R, Bizzarro V, Popolo A, Dal Piaz F, Vasaturo M, Picardi P, Parente L, Petrella A. 2014 Role of intracellular and extracellular annexin A1 in migration and invasion of human pancreatic carcinoma cells. *BMC Cancer.* **14:**961.

[426] Vallenius T. 2013 Actin stress fibre subtypes in mesenchymal-migrating cells. *Open Biol.* **3(6):**130001.

[427] Fischer KR, Durrans A, Lee S, Sheng J, Li F, Wong ST, Choi H, El Rayes T, Ryu S, Troeger J, Schwabe RF, Vahdat LT, Altorki NK, Mittal V, Gao D. 2015 Epithelial-to-mesenchymal transition is not required for lung metastasis but contributes to chemoresistance. *Nature.* **527(7579):**472-6.

[428] Zheng X, Carstens JL, Kim J, Scheible M, Kaye J, Sugimoto H, Wu CC, LeBleu VS, Kalluri R. 2015 Epithelial-to-mesenchymal transition is dispensable for metastasis but induces chemoresistance in pancreatic cancer. *Nature.* **527(7579):**525-30.

[429] Van Eyken P & Desmet VJ. 1993 Cytokeratins and the liver. *Liver international.* **13(3):**113-122.

[430] Bouwens L. 1998 Cytokeratins and cell differentiation in the pancreas. *J Pathol.* **184(3):**234-9.

[431] Robinson EJ, Neal DE, Collins AT. 1998 Basal cells are progenitors of luminal cells in primary cultures of differentiating human prostatic epithelium. *Prostate.* **37(3):**149-60.

[432] Peñafiel-Verdu C, Buendia AJ, Navarro JA, Ramirez GA, Vilafranca M, Altimira J, Sanchez J. 2012 Reduced expression of E-cadherin and β-catenin and high expression of basal cytokeratins in feline mammary carcinomas with regional metastasis. *Vet Pathol.* **49(6):**979-87.

[433] Yoon MK, Park SH, Won HS, Na DS, Lee BJ. 2000 Solution structure and membrane-binding property of the N-terminal tail domain of human annexin I. *FEBS Lett.* **484(3):**241-5.

[434] Rosengarth A, Wintergalen A, Galla HJ, Hinz HJ, Gerke V. 1998 Ca^{2+}-independent interaction of annexin I with phospholipid monolayers. *FEBS Lett.* **438(3):**279-84.

[435] Hoekstra D, Buist-Arkema R, Klappe K, Reutelingsperger CP. 1993 Interaction of annexins with membranes: the N-terminus as a governing parameter as revealed with a chimeric annexin. *Biochemistry.* **32(51):**14194-202.

[436] Chuah SY & Pallen CJ. 1989 Calcium-dependent and phosphorylation-stimulated proteolysis of lipocortin I by an endogenous A431 cell membrane protease. *J Biol Chem.* **264(35):**21160-6.

[437] Wang W & Creutz CE. 1994 Role of the amino-terminal domain in regulating interactions of annexin I with membranes: effects of amino-terminal truncation and mutagenesis of the phosphorylation sites. *Biochemistry.* **33(1):**275-82.

[438] Cordier-Ochsenbein F, Guerois R, Baleux F, Huynh-Dinh T, Lirsac PN, Russo-Marie F, Neumann JM, Sanson A. 1998 Exploring the folding pathways of annexin I, a multidomain protein. I. non-native structures stabilize the partially folded state of the isolated domain 2 of annexin I. *J Mol Biol.* **279(5):**1163-75.

[439] Gao J, Li Y, Yan H. 1999 NMR solution structure of domain 1 of human annexin I shows an autonomous folding unit. *J Biol Chem.* **274(5):**2971-7.

[440] Wang W & Creutz CE. 1994 Role of the amino-terminal domain in regulating interactions of annexin I with membranes: effects of amino-terminal truncation and mutagenesis of the phosphorylation sites. Biochemistry. 33(1):275-82.

[441] de la Fuente M & Parra AV. 1995 Vesicle aggregation by annexin I: role of a secondary membrane binding site. *Biochemistry.* **34(33):**10393-9.

[442] Réty S, Osterloh D, Arié JP, Tabaries S, Seeman J, Russo-Marie F, Gerke V, Lewit-Bentley A. 2000 Structural basis of the Ca(2+)-dependent association between S100C (S100A11) and its target, the N-terminal part of annexin I. *Structure.* **8(2):**175-84.

[443] Streicher WW, Lopez MM, Makhatadze GI. 2009 Annexin I and annexin II N-terminal peptides binding to S100 protein family members: specificity and thermodynamic characterization. *Biochemistry.* **48(12):**2788-98.

[444] Luecke H, Chang BT, Mailliard WS, Schlaepfer DD, Haigler HT. 1995 Crystal structure of the annexin XII hexamer and implications for bilayer insertion. *Nature.* **378(6556):**512-5.

[445] Cartailler JP, Haigler HT, Luecke H. 2000 Annexin XII E105K crystal structure: identification of a pH-dependent switch for mutant hexamerization. *Biochemistry.* **39(10):**2475-83.

[446] Lambert O, Gerke V, Bader MF, Porte F, Brisson A. 1997 Structural analysis of junctions formed between lipid membranes and several annexins by cryo-electron microscopy. *J Mol Biol.* **272(1):**42-55.

[447] Piotto S, Biasi LD, Concilio S, Castiglione A, Cattaneo G. 2014 GRIMD: distributed computing for chemists and biologists. *Bioinformation.* **10(1):**43-7.

[448] Krieger E & Vriend G. 2015 New ways to boost molecular dynamics simulations. *J Comput Chem.* **36(13):**996-1007.

XLVII